Structure functions in the three nucleon system

François René Pierre Bissey

Thesis submitted for the degree of
Doctor of Philosophy
at
The University of Adelaide
(Department of Physics and Mathematical Physics)

13th September 2002

Résumé

Le principal objectif de cette thèse est l'étude des fonctions de structure, polarisées et non-polarisées, des nucléons à partir des fonctions de structure du système à trois nucléons. Un premier aspect de cette étude est consacré à l'extraction des fonctions de structures des nucléons libres, et plus particulièrement du neutron (pour lequel il n'existe pas de cible pure), à partir de celle du système à trois nucléons. Un second point d'intérêt est l'étude des modifications des propriétés des nucléons dans la matière nucléaire légère.

Nous avons commencé ce travail par le calcul de la fonction d'onde non-relativiste du système à trois nucléons. Pour effectuer ce calcul nous avons utilisé les équations de Faddeev. Pour simplifier le problème, nous avons considéré que le système est invariant par symétrie d'isospin et donc composé de particules identiques. Pour simplifier encore plus notre problème, nous avons décomposé la fonction d'onde en ondes partielles et fait appel à un potentiel séparable.

Nous posons ensuite les bases du formalisme de convolution. Ce formalisme permet d'obtenir les fonctions de structure de noyaux complexes à partir de celles de leurs constituants. Nous avons alors montré comment calculer les distributions d'impulsion sur le cône de lumière des différents nucléons à l'aide de la fonction d'onde du système à trois nucléons que nous avions précédemment calculée.

Nous sommes alors passés à l'étude des fonctions de structure non-polarisées des noyaux d'hélium 3 et de tritium. Dans un premier temps nous présentons notre prédiction pour l'effet EMC dans ces deux noyaux . Nous avons ensuite étudié les prédictions de notre modèle pour la règle de somme de Gottfried. Enfin, nous avons terminé cette partie par la présentation d'une nouvelle façon d'accéder à la fonction de structure F_2 du neutron libre à partir des mesures de cette quantité pour les noyaux d'hélium 3 et de tritium.

Après avoir étudié les fonctions de structure non-polarisées du système à trois nucléons nous sommes passés au cas polarisé. On sait depuis longtemps que la fonction de structure g_1 de l'hélium 3 constitue une bonne approximation de cette même fonction pour le neutron libre. Nous avons donc étudié les diverses corrections qu'il est nécessaire d'inclure pour avoir la meilleure extraction possible de cette fonction pour le neutron libre à partir des données de l'hélium 3.

Pour finir, nous présentons nos conclusions et les extensions possibles de ce travail dans deux directions : l'étude de la fonction g_2 du neutron et du système à trois nucléons ; les fonctions de structure du noyau de lithium 6 considéré comme un cœur d'hélium et de deux nucléons. L'étude du lithium 6 pourrait compléter les données provenant de l'hélium et du tritium.

Abstract

In this thesis, we study the structure functions, both polarised and unpolarised, of the three nucleon system and how they can give us information on two aspects of nuclear physics. First, we examine how to extract information on the free neutron structure functions and second we ask how does the nucleon's structure change in nuclei. Starting from a non-relativistic wave function for the three nucleon system, we use the standard convolution formalism to produce both polarised and unpolarised structure functions of ^{3}He and ^{3}H. In the unpolarised case we demonstrate a new way of extracting the unpolarised structure function F_2 of the neutron from the measurement of the EMC effects in both ^{3}He and ^{3}H. In the polarised case we discuss how close an approximation $g_1^{^3\mathrm{He}}$ is to g_1^n. We also study the different corrections which must be included to obtain the best possible estimate for g_1^n. In this case we study the nuclear effects included in the convolution formalism, the contribution of the Δ-resonance and novel off-shell corrections to the free structure functions inside ^{3}He computed in QMC (Quark Meson Coupling model). With respect to the effects of the nuclear medium on nucleons, this thesis presents estimates of the EMC effect in both ^{3}He and ^{3}H and of the nuclear medium on the Gottfried sum rule. Finally, we present a clear signature of off-shell effects on the proton inside ^{3}H. In this case off-shell corrections from QMC have been used but the results show that a variety of off-shell effects are, in fact, enhanced by the convolution formalism and consequently, can be similarly identified.

Contents

Résumé (French summary) **i**

Abstract **iii**

Contents **v**

List of Figures **vii**

List of Tables **ix**

Acknowledgements **xi**

1 Introduction **1**

2 The three nucleon wave function **7**
2.1 Introduction 8
2.2 Notation 8
2.3 The partial wave expansion 10
2.4 Separable potential 10
2.5 The three-nucleon wave function 11
2.6 Numerical results 15

3 Structure functions and convolution formalism **19**
3.1 The electromagnetic cross section 20
3.2 Particularly interesting cross sections 23
3.2.1 Unpolarised scattering 23
3.2.2 Polarised scattering 23
3.3 The convolution formalism 24
3.3.1 The partial wave impulse approximation 24
3.3.2 Convolution of the structure functions 29

4 Spectral functions and light-cone momentum distributions of the three nucleon system **33**
4.1 The spectral function 34
4.2 The case of ^{3}He 36
4.2.1 Neutron in ^{3}He 36
4.2.2 Proton in ^{3}He 39
4.3 Results 40

5 Unpolarised structure functions of the three nucleon system **45**
5.1 Parton model 46
5.2 EMC effect 47
5.3 Gottfried sum rule 50
5.4 The neutron structure function F_2^n 52

6 Polarised structure functions of the three nucleon system **59**
6.1 Parton model 60
6.2 Off-shell corrections 61
6.3 Non-nucleonic degrees of freedom 62
6.4 The neutron in ^{3}He 65
6.5 The proton in tritium 70

7 Conclusions **73**

A The kernel of the homogeneous Faddeev equation **79**

B The permutation term **85**

Bibliography **89**

List of Publications **97**

List of Figures

2.1 A graphical representation of Eq. (2.1). 9
2.2 Angular momentum and momentum in the three body system. 9

3.1 Scattering of a lepton l on a nucleus A, with one photon exchange. 20
3.2 In PWIA, only one nucleon of the nucleus is struck by the photon. 25
3.3 Handbag diagram. 27
3.4 Cross term diagram. 28
3.5 Higher twist diagram neglected using assumption (3). 28

4.1 Neutron light-cone momentum distribution in ^{3}He for various potentials. 38
4.2 Neutron polarised light-cone momentum distribution in ^{3}He for various potentials. 38
4.3 Proton light-cone momentum distribution in ^{3}He for various potentials. 41
4.4 Proton polarised light-cone momentum distribution in ^{3}He for various potentials. 41

5.1 The ratio R_3, given in Eq.(5.9), for ^{3}He, at $Q^2 = 10$ GeV^2, calculated for various potentials using the CTEQ5 quark distributions. 49
5.2 The ratio R_3, given in Eq.(5.9), for ^{3}H, at $Q^2 = 10$ GeV^2, calculated for various potentials using the CTEQ5 quark distributions. 49
5.3 The ratio R_3, given in Eq.(5.9), for ^{3}He, at $Q^2 = 10$ GeV^2, calculated for the PEST potential, using various quark distributions for the nucleons. 50
5.4 The difference $F_2^{\mathrm{A}}(x) - F_2^{\mathrm{A}'}(x)$ for both the tri-nucleon system and the free nucleon, at $Q^2 = 10$ GeV^2, using the CTEQ5 quark distributions. 53

5.5 The difference $(F_2^{\rm A}(x) - F_2^{\rm A'}(x))/x$ for both the tri-nucleon system and the free nucleon, at $Q^2 = 10$ GeV^2, using the CTEQ5 quark distributions. 53
5.6 The ratio of ratios, Eq. (5.19), for various potentials, using the CTEQ5 parametrisation at $Q^2 = 10$ GeV^2. 55
5.7 The ratio of ratios, Eq. (5.19), using the CTEQ5 quark parametrisation at $Q^2 = 10$ GeV^2, for isospin symmetric and non isospin symmetric three-nucleon wave functions. 56
5.8 The ratio of ratios, Eq. (5.19), for various quark distributions, using the PEST potential. 56

6.1 Comparison of several calculations of $xg_1(x)$ for ^{3}He and the free neutron at $Q^2 = 4$ GeV^2. 66
6.2 Δ_g, $\Delta_g^{'}$ and g_1^n at $Q^2 = 4$ GeV^2. 68
6.3 Δ_g, $\Delta_g^{'}$ and g_1^n, without off-shell corrections, at $Q^2 = 4$ GeV^2. 68
6.4 Corrections to g_1^n data from E154. White circles represent the original data. Black circles are corrected for binding energy and nuclear effects. Diamonds have all corrections from the black circles as well as off-shell corrections. Squares have all the corrections from the diamonds as well as Δ isobar corrections. The error bars are statistical errors. 69
6.5 Corrections to g_1^n data from HERMES. White circles represent the original data. Black circles are corrected for binding energy and nuclear effects. Diamonds have all corrections from the black circles as well as off-shell corrections. Square have all the corrections from the diamond as well as Δ isobar corrections. The error bars are statistical errors. 69
6.6 The ratio R_g and R_g' of Eqs. (6.22) and (6.23) at 4 GeV^2, without any off-shell corrections. 72
6.7 The ratio R_g' of Eq. (6.23) at 4 GeV^2. The dotted line is without off-shell corrections. The dashed line is with off-shell corrections and the solid line include both off-shell corrections and Δ isobar corrections. 72

List of Tables

2.1 Binding energy for a given potential and components of the wave function. 16

4.1 Effective polarisation of the nucleons in ^{3}He for various potentials. 42

4.2 Effective polarisation of the nucleons in ^{3}He and ^{3}H, with two-body interaction adjusted to produce the experimental binding energies. 42

Acknowledgements

First of all, I would like to thanks both of my supervisors, Professor Tony Thomas in Adelaide and Jean-François Mathiot in Clermont-Ferrand, for undertaking all the paper work that made my coming to Australia and the completion of this thesis possible.

I must also thanks all the people that contributed to my understanding of physics. Among those people I especially would like to thank: Iraj Afnan, Wally Melnitchouk, Koichi Saito, Kazuo Tsushima, Csaba Boros, Andreas Schrebeir, Vadim Guzey, G. G. Petratos, A. T. Katramatou, Hélène Fonvielle, Vladimir Karmanov, Jean-Jacques Dugne and M. Strickman. A good part of the work presented here, came from collaborations with one or several people mentioned here. A special mention has to given to Iraj Afnan and Wally Melnitchouck who, beside Tony Thomas, gave me a lot of support, made me part of larger efforts and pushed me towards new frontiers.

I also would like to thank all the members and the staff of the CSSM as well as the physics department of the University of Adelaide for the hospitality and friendship they extended to me during my stay in Adelaide. I also have to thank the members and staff of the Laboratoire de Physique Corpusculaire in Clermont-Ferrand for coping with my special situation as a particular breed of exchange student and the support of the "Conseil général de la région Auvergne".

I also would like to thank my familly for their ongoing support during the whole lenght of my thesis. I also have to thank my wife Caroline for being able to stand me and the support gave me when she entered my life. I want to give a special mention for my maternal grand father, Pierre Buillit (1909-1999), who was like a father to me, always supportive, very proud of my accomplishments and who died during the course of this thesis.

Chapter 1

Introduction

One the main issue of today's physics, is the understanding of nuclear matter from its most fundamental description – Quantum Chromo-Dynamics (QCD). For years, physicists have been able to describe, with some success, many nuclear phenomenon in terms of hadronic degrees of freedom, that is in terms of baryons and mesons. However, a full understanding of nuclear matter can only be reached by a description in terms of quarks and gluons in interaction.

After the discovery of the nucleus, by E. Rutherford and his students in 1909 [83], what physicists wanted to know was: what, exactly, is a nucleus? Slowly, we learned that the nucleus is a composite object. The first indication of the compositeness of the nucleus came in 1919, when Rutherford discovered the proton. Not long after, in 1921, J. Chadwick and E. S. Bieler concluded that some "strong force" must be holding the nucleus together. Then in 1931, Chadwick discovered the neutron. The central question of nuclear physics then definitely moved to: what is holding these particles, neutrons and protons together in such a compact object? The first theory of this strong interaction, came from H. Yukawa in 1933. It not only explained some features of the interaction, but also made the prediction that there should exist a particle with a mass of about 200 MeV. Such a particle, called pion, was eventually discovered in 1947[1], giving a lot of credibility to Yukawa's theory. Subsequently during the 1950s and 1960s, a wide variety of particles were found, first in cosmic rays and then in ever more powerful accelerators.

This proliferation of particles leads physicists to search for ways to put some order into their bestiary. First, in 1961, they came with a mathematical classification based on the group $SU(3)$ [86]. Then in 1964, M. Gell-Mann and G. Zweig [85] came up with the idea that all hadrons could be made up of smaller particles which would be later be universally known as quarks. This idea was treated more as mathematical scheme to put some order in the increasing number of hadrons rather than a physical reality. This, because of the facts that nobody ever observed a quark and that quarks have fractionary electric charge never found in nature before. In 1965, O. W. Greenberg [97], M. Y. Han and Y. Nambu [87] added the property of colour charge to quarks in order to be able to describe the Δ^{++} particle in terms of quarks. All observed hadrons are colour neutral. In 1968 and 1969, at SLAC in an experiment in which electrons are scattered off protons [88], the electrons appeared to be bouncing off small hard core inside the proton. J. Bjorken and R. P. Feynman [89] suggested that these data reflect the existence of constituent particles inside the proton. This was the first evidence for quarks.

[1] In 1937, there was indication of a particle of similar mass. However it was later identified as being a heavy charged lepton: the muon.

Finally, in 1973, QCD was formulated as a gauge theory by H. Fritzsch, M. Gell-Mann and H. Leutwyller [98]. In this theory, quarks exchange colour via new particles called gluons which are similar to the photon of Quantum Electro-Dynamics (QED). It was soon found that QCD has a number of unique features, like "asymptotic freedom" [90]. This means that the effective coupling constant of the strong interaction becomes small at short distances, so that one can make use of perturbation theory to describe short-distance processes – or equivalently, processes involving large momentum transfer. This property is responsible for the fact that one cannot observe quarks directly outside a hadron. Perturbative QCD, which deals with the behaviour of QCD at high energy and small distance is quite reliable. However, tools that would be able to unveil the secrets of QCD in "normal" nuclear matter, like lattice QCD, are still in their infancy and need further development and ever more computing power.

To help us build an understanding of nuclear matter we need to have a good knowledge of its properties and of its behaviour. There are several aspects to the study of the properties of nuclear matter. First, one can study the properties of the fundamental building blocks of the nucleus, that is the proton and neutron. Then one can also study the properties of more complex nuclear matter like light, or even heavy. One can also probe a nuclear target with different probes or under different physical conditions (unpolarised or polarised scattering for example).

If we had a complete understanding of QCD, we could precisely predict the cross-section of a probe of any kind on a nuclear target. While we are not able to make such predictions, we know, from first principles, how to write such a cross-section as a function of unknown quantities. These quantities could be computed from QCD, if we had a complete understanding of it. While we cannot compute them, they can be measured experimentally. These quantities called either form factors, in elastic scattering (at low energy transfer), or structure functions, in deep inelastic scattering (at high energy transfer), contain all the information one can extract from the target with a given probe. In the electromagnetic scattering of a lepton off a nuclear target of spin 1/2, that is a nucleon or ^{3}He and ^{3}H for example, the behaviour of the target is completely described by four structure functions called F_1, F_2, g_1 and g_2 [59, 60, 18][2]. Nuclear targets with higher spin have more structure functions, however the four mentioned above are the dominant ones.

A point-like target does not have any form factors (structure functions), its behaviour is entirely determined by kinematic variables. The observation

[2]Or equivalently by four form factors: W_1, W_2, G_1 and G_2 or by some combinations of the above.

of a form factor is a proof of the fact that the target has a complex structure and is not point-like. From 1953 to 1957, various experiments of electron scattering off of nuclei [84] revealed that both proton and neutron have a "charge density", that is they do have form factors. At that time it was not interpreted as a sign that the nucleons were composite objects, but rather that nucleons were surrounded by a cloud of pions or other mesons constantly in interaction with the nucleon. This interpretation in terms of hadronic degrees of freedom can explain the existence of nucleon form factors and can give a somewhat accurate description of the hadronic system at low energy. However, at high momentum transfer, the picture is different. In this regime, experiments at SLAC in 1968 and 1969 [88] showed that the measured structure functions of the nucleon exhibit scaling and are become almost independent of the momentum transfer. This phenomenon is the clear signature of the presence of smaller elementary objects inside the nucleon, the quarks. In deep inelastic scattering, one probes directly the quarks inside nuclear matter, as if they were quasi-free. Thus, deep inelastic scattering, offers a clear picture of the quark structure of nuclear matter.

Since then, experimentalist have continued to probe nuclear matter under different conditions. The properties of the proton are still studied to this day. As there is no such thing as a pure neutron target, it is not possible to access to the properties of the neutron directly. To study the neutron one has to make experiment on a nucleus and extract the neutron information from the nucleus data. The target of choice to study the structure functions of the neutron in unpolarised has for a long time been the deuteron. This nucleus, made of only one proton and one neutron weakly bound, was usually thought to be very simple and the extraction of the neutron straightforward. However, recent analysis has cast a new light on the extraction of neutron information from deuterium data in some kinematic regions [66]. Experiments have also been performed on heavier targets, leading to the discovery in 1983, to what is now known as the "EMC effect" by the Electron Muon Collaboration [42]. It was followed by the discovery of two other effects known as "shadowing" and "anti-shadowing". These effects show that the the properties of the neutron and proton inside a nucleus are changed in a non trivial way and that some physical phenomenon have more importance than was previously thought. Several models have been put forward to explain these effects. The EMC effect in particular, may be dealt with using convolution formalism, see Ref. [17] for a review of the various experiment and of some models.

In their investigation of proton and neutron, physicists have, for a long time, focused on unpolarised (or "spin averaged") experiments (at least in electromagnetic scattering). In these kind of experiments F_1 and F_2 are the only structure functions contributing to the cross-section. F_1 and F_2 are for

this reason called the unpolarised, or spin averaged, structure functions while on the other hand g_1 and g_2 are called polarised, or spin, structure functions. To access g_1 and g_2, one needs to devise an experiment where both the target and the probe are polarised [18, 19]. The first experiment of this kind took place at SLAC in 1976 and was, of course, probing the proton [91]. Several experiments followed after that throughout the 1980s and lead to at least two unexpected results. First, the strange quark from the "sea" are polarised and contribute to the spin of the proton [92]. The other unexpected result, is the fact that the quark contribute little to the total spin of the proton [92, 99].

Like we already said, there is no such thing as a pure neutron target. To extract the polarised structure functions of the neutron, experimentalists have to use more complex nuclear target. Like for the unpolarised case, one can extract the information from the deuteron. However, for the measurement of polarised structure functions of the neutron we have a better target: ^{3}He. The nucleus of ^{3}He is made up of one neutron and two protons and in first approximation the spin of the nucleus is entirely carried by the neutron while the two protons must have opposite spin. Of course, this is only an approximation, but a very good one as the neutron polarisation is about 87% while the polarisation of the protons is about -2.5%. The first experiment measuring the structure function g_1 of the neutron were conducted 1992 [93] using a ^{3}He target. These results were then combined with the previous results from the proton to get a new estimate of the fraction of nucleon spin carried by the quarks [51]. Since then, several new experiments have measured the structure functions of ^{3}He to extract information on the neutron, among those we can mention HERMES at DESY, E154 and E155 at SLAC.

This thesis has several goal. First we want to show how it is possible to extract information on the neutron from ^{3}He and even, in one occurrence, from ^{3}He and its mirror nucleus, ^{3}H. The other aim of this thesis, which is closely related to the first one, is to try to understand how the properties of nucleons change in light nuclear matter. This thesis has five main parts:

- First we will show how to compute the wave function of ^{3}He with the help of Faddeev equations and of separable potentials. Since we will use isospin symmetry to simplify the problem, we will really compute wave functions for the three nucleon system and our results will be applicable to ^{3}H. We will compute wave functions for four different potentials in order to isolate any model dependence from the potential.

- Then we will turn on the definition of the structure functions for a spin 1/2 target and to the derivation of the convolution formalism. The convolution formalism will enable us to link structure functions of the free nucleons to structure functions of more complex nuclei. We

will also discuss the domain of applicability and the limitations of this formalism.

- In the next part, we will show how one can extract the fundamental ingredient of the convolution formalism from the three nucleon wave function we computed in the first part. The fundamental quantity needed in the convolution formalism is the light-cone momentum distribution. We will examine the dependence of this quantity to the kind of potential used to compute the wave function.

- In this fourth part we will apply our knowledge of the convolution formalism and of the light-cone momentum distribution to study unpolarised structure functions of the three nucleon system and of the nucleon themselves. First we will show our prediction for the EMC effects in both ^{3}He and ^{3}H and its dependence to various parameters like the potential and the parton distributions used to compute the free nucleons structure functions. We will also apply our results to the computation of the Gottfried sum rule in the ^{3}He-^{3}H system. Finally, we will how one can extract unpolarised neutron structure functions from measurements of both ^{3}He and ^{3}H structure functions.

- Lastly, we will study the polarised structure functions of the three nucleon system and their relationship with free nucleon structure functions. Since one usually wants to extract neutron information from ^{3}He, we will study very carefully different kinds of corrections that must included in such a computation. We will then study the effects of our corrections to experimental results. Finally, ^{3}H is a perfect target to study the effect of nuclear medium on the polarised structure functions of the proton. So we will investigate how to single out such effects.

Finally, we will summarise and make some concluding remarks.

Chapter 2

The three nucleon wave function

2.1 Introduction

For the three-nucleon problem we can determine the non-relativistic wave function by solving the Faddeev equations exactly for any realistic two-body interaction. However, to simplify the computational aspects of the problem, with no sacrifice in the quality of the wave function, we turn to separable expansions that have been extensively tested [7, 8]. This will result in a three-nucleon wave function that can be used to calculate the spectral function and the light-cone momentum distribution. In the present chapter we detail the three-nucleon formalism required to evaluate the wave functions for ^{3}He and ^{3}H.

2.2 Notation

With the extensive literature on the Faddeev equations [12] and their use in the three-nucleon system, we restrict ourselves here to a summary of the notation used in the present analysis. The Faddeev decomposition of the three-nucleon wave function is given by

$$|\Psi\rangle = |\varphi_1\rangle + |\varphi_2\rangle + |\varphi_3\rangle = \{e + (123) + (132)\}\,|\varphi_3\rangle\,. \tag{2.1}$$

Here "e", "(123)" and "(132)" are members of the permutation group of three objects, with e being the unit element (*i.e.* $e\,|\varphi_\alpha\rangle = |\varphi_\alpha\rangle$) and the other two being cyclic permutations of $\{1, 2, 3\}$. The second equality results from the requirement that we have identical particles, the wave function is then invariant under any cyclic permutation of our particles. Since we have a system of identical fermions, the total wave function must also be antisymmetric under the exchange of any two particles in the system. This requirement leads to following conditions

$$\begin{aligned} (\alpha\beta)\,|\varphi_\alpha\rangle &= -\,|\varphi_\beta\rangle\,, \\ (\alpha\beta)\,|\varphi_\beta\rangle &= -\,|\varphi_\alpha\rangle\,, \\ (\alpha\beta)\,|\varphi_\gamma\rangle &= -\,|\varphi_\gamma\rangle\,. \end{aligned} \tag{2.2}$$

In the above equations α, β and γ are indices running from 1 to 3, and always different from each other, and $(\alpha\beta)$ is again a member of the permutation group of three objects which exchange particles α and β leaving the third one unchanged. Since we are dealing with a three-body problem, there will be only two independent momenta in the centre of mass frame. All the particles have spin and isospin $\frac{1}{2}$ and one must account for their orbital angular momentum. We briefly summarise the quantum numbers and momenta used throughout this chapter:

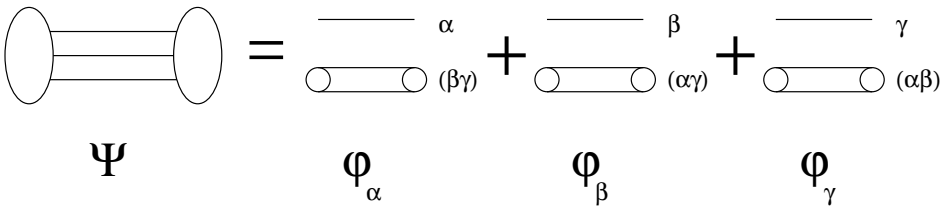

Figure 2.1: A graphical representation of Eq. (2.1).

- N_α is a set of quantum numbers describing a three body channel from the point of view of the particle α, which is the spectator; the set is unique for each channel.
- $\vec{\ell}_\alpha$ is the orbital angular momentum between particles β and γ (see Fig. 2.2).
- $\vec{L}_\alpha$ is the orbital angular momentum between particle α and the centre of mass of the system consisting of particles β and γ (see Fig. 2.2).
- $\vec{j}_\alpha$, $\vec{j}_\beta$, $\vec{j}_\gamma$ are the spins of each particle.
- $\vec{\imath}_\alpha$, $\vec{\imath}_\beta$, $\vec{\imath}_\gamma$ are the isospins of each particle.
- $\vec{p}_\alpha$ is the momentum of particle α in the centre of mass frame.
- $\vec{q}_\alpha$ is the relative momentum of the pair of particles β and γ, defined as $\vec{q}_\alpha = (\vec{p}_\gamma - \vec{p}_\beta)/2$.
- $\vec{I}$ and $\vec{J}$ are respectively the total isospin and total angular momentum of the system.

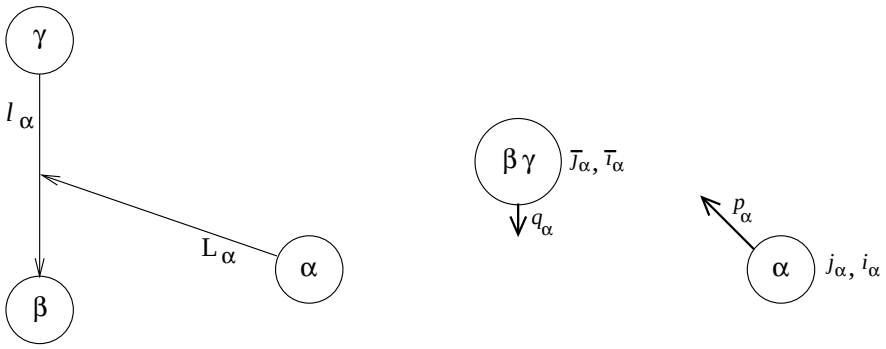

Figure 2.2: Angular momentum and momentum in the three body system.

2.3 The partial wave expansion

We now turn to the partial wave expansion of our wave function. To minimise the number of coupled Faddeev equations, having truncated the interaction to a set of partial waves, we have used the following coupling scheme:

$$\begin{aligned} &\vec{\jmath}_\beta + \vec{\jmath}_\gamma = \vec{s}_\alpha, \quad \vec{\ell}_\alpha + \vec{s}_\alpha = \vec{\jmath}_\alpha, \quad \vec{\jmath}_\alpha + \vec{\jmath}_\alpha = \vec{S}_\alpha, \; \vec{L}_\alpha + \vec{S}_\alpha = \vec{J}, \\ &\vec{\imath}_\beta + \vec{\imath}_\gamma = \vec{\imath}_\alpha, \quad \vec{\imath}_\alpha + \vec{\imath}_\alpha = \vec{I}, \end{aligned}$$

which is known as the channel coupling scheme. With this coupling scheme the complete set of quantum numbers N_α describing a three body channel is; $N_\alpha = \{\bar{\imath}_\alpha, s_\alpha, \bar{\jmath}_\alpha, S_\alpha, L_\alpha\}$. A subset of these quantum numbers that describes the two-body channels is; $n_\alpha = \{\bar{\imath}_\alpha, s_\alpha, \bar{\jmath}_\alpha\}$, and therefore $N_\alpha = \{n_\alpha, S_\alpha, L_\alpha\}$. We have not included ℓ_α in the set of quantum numbers since the tensor force mixes values of ℓ_α. This allows us to define the angular momentum and isospin basis as

$$\left|\Omega^{JI}_{\ell_\alpha N_\alpha}\right\rangle = |\{L_\alpha,\, [(\ell_\alpha,\, (\,\jmath_\beta,\, \jmath_\gamma)\, s_\alpha)\, \bar{\jmath}_\alpha,\, \jmath_\alpha]\, S_\alpha\}\, J\rangle \;\; |[(\,\imath_\beta,\, \imath_\gamma)\, \bar{\imath}_\alpha,\, \imath_\alpha]\, I\rangle\,, \qquad (2.3)$$

These basis states satisfy the following orthogonality relation $\left\langle\Omega^{JI}_{\ell_\alpha N_\alpha}\middle|\Omega^{JI}_{\ell_\beta N_\beta}\right\rangle = \delta_{\ell_\alpha,\ell_\beta}\,\delta_{N_\alpha,N_\beta}$.

We are now in a position to write the partial wave expansion of the total three-nucleon wave function as

$$|\Psi\rangle = \sum_{\ell_\alpha N_\alpha} \left|\Omega^{JI}_{\ell_\alpha N_\alpha}\right\rangle \;\left|\mathcal{U}^{IJ}_{\ell_\alpha N_\alpha}\right\rangle, \qquad (2.4)$$

where $\left|\mathcal{U}^{IJ}_{\ell_\alpha N_\alpha}\right\rangle$ is defined as the radial part of the wave function corresponding to the partial wave $\{\ell_\alpha, N_\alpha\}$.

2.4 Separable potential

To reduce the dimensionality of the Faddeev integral equations (after partial wave expansion) from two to one, and in this way simplify the three-body wave function, we have employed a separable expansion of the nucleon-nucleon interaction. Our potential for the interaction of particles β and γ in a given partial wave is of the form [9]

$$V^{n_\alpha}_{\ell_\alpha,\ell'_\alpha} = \left|g^{n_\alpha}_{\ell_\alpha}\right\rangle \lambda^{n_\alpha}_{\ell_\alpha\ell'_\alpha} \left\langle g^{n_\alpha}_{\ell'_\alpha}\right|, \qquad (2.5)$$

where $\left|g^{n_\alpha}_{\ell_\alpha}\right\rangle$ is a "form factor" and $\lambda^{n_\alpha}_{\ell_\alpha\ell'_\alpha}$ is the strength of the potential in that partial wave. By taking $\ell_\alpha \neq \ell'_\alpha$ we can accommodate a tensor interaction,

as in the case of the $^3S_1$-$^3D_1$ nucleon-nucleon channel. The above expression for the potential is for a rank one potential. To incorporate higher rank potentials, we turn the strength $\lambda^{n_\alpha}_{\ell_\alpha \ell'_\alpha}$ into a matrix and as a result $\left| g^{n_\alpha}_{\ell_\alpha} \right\rangle$ is a row matrix. In resorting to separable expansions, we have taken the view that the expansion is a numerical procedure analogous to the use of quadratures. The main problem with the use of a separable expansion is that the resulting potential is non-local. However, the use of a low order expansion, such as the UPA (Unitary Pole Approximation [9, 95, 13]) or of a separable potential, is justified on the grounds that it generates the same analytic structure in the amplitude (*i.e.*, bound or anti-bound state poles) as a corresponding realistic potential [13]. Thus, we can assume it is safe to use a separable expansion. The use of a separable potential gives rise to a separable t-matrix that satisfies the Lippmann-Schwinger (LS) equation;

$$t_\alpha(E) = V_\alpha + V_\alpha \, G_0(E) \, t_\alpha(E) = (1 - G_0(E) \, V_\alpha)^{-1} \, V_\alpha, \tag{2.6}$$

with $G_0(E) = (E - H_0)^{-1}$ the two-body Green's function. It is simple to show that the separable t-matrix in a given partial wave, resulting from a solution of the LS equation, is of the form

$$t^{n_\alpha}_{\ell_\alpha, \ell'_\alpha}(E) = \left| g^{n_\alpha}_{\ell_\alpha} \right\rangle \tau^{n_\alpha}_{\ell_\alpha \ell'_\alpha}(E) \left\langle g^{n_\alpha}_{\ell'_\alpha} \right|, \tag{2.7}$$

where the form factor $\left| g^{n_\alpha}_{\ell_\alpha} \right\rangle$ is identical to that used in the separable potential. The function $\tau^{n_\alpha}_{\ell_\alpha \ell'_\alpha}(E)$, in a given channel, can be a written in matrix form as

$$[\tau^{n_\alpha}(E)]^{-1} = [\lambda^{n_\alpha}]^{-1} - \langle g^{n_\alpha} \, | \, G_0(E) \, | \, g^{n_\alpha} \rangle \, . \tag{2.8}$$

This separability of the t-matrix will allow us to reduce the dimensionality of the Faddeev integral equations from two to one after the partial wave expansion described in Eq. (2.4).

2.5 The three-nucleon wave function

Having determined the structure of the two-body amplitude, we now turn to the wave function for the three-nucleon system. The Schrödinger equation for this system is

$$(E - H_0) \, |\Psi\rangle = V \, |\Psi\rangle = \sum_{\alpha=1}^{3} V_\alpha \, |\Psi\rangle \, . \tag{2.9}$$

This can be rewritten in a form that suggests the Faddeev decomposition stated in Eq. (2.1), *i.e.*,

$$|\Psi\rangle = G_0(E)\, V\, |\Psi\rangle = \sum_{\alpha=1}^{3} G_0(E)\, V_\alpha\, |\Psi\rangle = \sum_{\alpha=1}^{3} |\varphi_\alpha\rangle\,. \tag{2.10}$$

Here, $G_0(E) = (E - H_0)^{-1}$ is the three-body Green's function. We now can write an equation for the Faddeev components of the wave function as

$$|\varphi_\alpha\rangle = G_0(E)\, V_\alpha\, |\Psi\rangle = G_0(E)\, V_\alpha\, |\varphi_\alpha\rangle + \sum_{\gamma\neq\alpha} G_0(E)\, V_\alpha\, |\varphi_\gamma\rangle\,. \tag{2.11}$$

With the help of Eq. (2.6), the set of coupled integral equations for the Faddeev components of the wave function, $|\varphi_\alpha\rangle$, becomes

$$|\varphi_\alpha\rangle = G_0(E)\, T_\alpha(E)\, (|\varphi_\beta\rangle + |\varphi_\gamma\rangle)\,. \tag{2.12}$$

Here $T_\alpha(E)$ is the t-matrix for particles β and γ in the three-particle Hilbert space, which is related to the two-body amplitude considered in the last section by

$$T_\alpha(E) = t_\alpha(E - \epsilon_\alpha), \tag{2.13}$$

where ϵ_α is the energy of the spectator particle α in the three-body centre of mass.[1]

Eq. (2.12) is in fact a set of three coupled integral equations, known as the Faddeev equations, for the three-body bound state. In their most general form one can write in a matrix form

$$\begin{bmatrix} \varphi_\alpha \\ \varphi_\beta \\ \varphi_\gamma \end{bmatrix} = G_0(E) \begin{bmatrix} 0 & T_\alpha(E) & T_\alpha(E) \\ T_\beta(E) & 0 & T_\beta(E) \\ T_\gamma(E) & T_\gamma(E) & 0 \end{bmatrix} \begin{bmatrix} \varphi_\alpha \\ \varphi_\beta \\ \varphi_\gamma \end{bmatrix}. \tag{2.14}$$

Eq. (2.11) tells us that the component φ_α describes the three body system when the particles β and γ are interacting together with α as a spectator. The Faddeev equation, Eq. (2.12) and Eq. (2.14), tell us how the Faddeev components are linked together. It tells how to exchange a spectator particle with an interacting one in the system. For the three-nucleon system, where we have identical Fermions, we can take advantage of the anti-symmetry, as given in Eq. (2.2), and the fact that $(\beta\gamma)T_\alpha = T_\alpha(\beta\gamma) = -T_\alpha$, to reduce the Faddeev equations to

$$|\varphi_\alpha\rangle = G_0(E)\, T_\alpha(E)\, (1 - (\beta\gamma))\, |\varphi_\beta\rangle = 2\, G_0(E)\, T_\alpha(E)\, |\varphi_\beta\rangle\,, \tag{2.15}$$

[1] For the three-nucleon system in a non-relativistic formulation, $\epsilon_\alpha = \frac{3}{4m} p_\alpha^2$, where m is the nucleon mass.

with $\alpha \neq \beta$. To recast this equation into a form that will admit numerical solutions, we need to first partial wave decompose the Faddeev equations and take into consideration the separability of the two-body amplitudes. This can all be achieved by partial wave expanding the two-body amplitude in three-body Hilbert space in terms of the angular momentum states defined in Eq. (2.3) [14]

$$\begin{aligned} T_\alpha(E) &= \sum_{\substack{\ell_\alpha \ell'_\alpha \\ N_\alpha JI}} \int_0^\infty dp_\alpha \, p_\alpha^2 \left| \Omega^{JI}_{\ell_\alpha N_\alpha}; p_\alpha \right\rangle t^{n_\alpha}_{\ell_\alpha \ell'_\alpha}(E - \epsilon_\alpha) \left\langle p_\alpha; \Omega^{JI}_{\ell'_\alpha N_\alpha} \right| \\ &= \sum_{\substack{\ell_\alpha \ell'_\alpha \\ N_\alpha JI}} \int_0^\infty dp_\alpha \, p_\alpha^2 \left| \Omega^{JI}_{\ell_\alpha N_\alpha}; g^{n_\alpha}_{\ell_\alpha} \right\rangle \tau^{n_\alpha}_{\ell_\alpha \ell'_\alpha}(E - \epsilon_\alpha) \left\langle g^{n_\alpha}_{\ell'_\alpha}; \Omega^{JI}_{\ell'_\alpha N_\alpha} \right| \end{aligned} \tag{2.16}$$

where $\epsilon_\alpha = \frac{3}{4m} p_\alpha^2$ and

$$\left| \Omega^{JI}_{\ell_\alpha N_\alpha}; g^{n_\alpha}_{\ell_\alpha} \right\rangle \; = \left| \Omega^{JI}_{\ell_\alpha N_\alpha} \right\rangle \left| g^{n_\alpha}_{\ell_\alpha}; p_\alpha \right\rangle . \tag{2.17}$$

We now can write Eq. (2.15) as

$$\begin{aligned} |\varphi_\alpha\rangle &= 2\, G_0(E) \sum_{\substack{\ell_\alpha \ell'_\alpha \\ N_\alpha JI}} \int_0^\infty dp_\alpha \, p_\alpha^2 \big| \Omega^{JI}_{\ell_\alpha N_\alpha}; g^{n_\alpha}_{\ell_\alpha} \big\rangle \tau^{n_\alpha}_{\ell_\alpha \ell'_\alpha}(E - \epsilon_\alpha) \big\langle g^{n_\alpha}_{\ell'_\alpha}; \Omega^{JI}_{\ell'_\alpha N_\alpha} \big| \varphi_\beta \big\rangle \\ &\equiv 2\, G_0(E) \sum_{\substack{\ell_\alpha \ell'_\alpha \\ N_\alpha JI}} \int_0^\infty dp_\alpha \, p_\alpha^2 \big| \Omega^{JI}_{\ell_\alpha N_\alpha}; g^{n_\alpha}_{\ell_\alpha} \big\rangle \tau^{n_\alpha}_{\ell_\alpha \ell'_\alpha}(E - \epsilon_\alpha) X^{JI}_{N_\alpha \ell'_\alpha}(p_\alpha), \end{aligned} \tag{2.18}$$

with the spectator function, $X^{JI}_{N_\alpha \ell_\alpha}(p_\alpha)$, satisfying the equation

$$\begin{aligned} X^{JI}_{N_\alpha \ell_\alpha}(p_\alpha) &\equiv \big\langle g^{n_\alpha}_{\ell_\alpha}; \Omega^{JI}_{\ell_\alpha N_\alpha} \big| \varphi_\beta \big\rangle \\ &= 2 \sum_{\substack{\ell_\beta \ell'_\beta \\ N_\beta}} \int_0^\infty dp_\beta \, p_\beta^2 Z^{JI}_{\ell_\alpha N_\alpha; \ell_\beta N_\beta}(p_\alpha, p_\beta; E) \tau^{n_\beta}_{\ell_\beta \ell'_\beta}(E - \epsilon_\beta) X^{JI}_{N_\beta \ell'_\beta}(p_\beta), \end{aligned} \tag{2.19}$$

where

$$Z^{JI}_{\ell_\alpha N_\alpha; \ell_\beta N_\beta}(p_\alpha, p_\beta; E) \equiv \big\langle g^{n_\alpha}_{\ell_\alpha}; \Omega^{JI}_{\ell_\alpha N_\alpha} \big| \, G_0(E) \big| \Omega^{JI}_{\ell_\beta N_\beta}; g^{n_\beta}_{\ell_\beta} \big\rangle, \tag{2.20}$$

with $\alpha \neq \beta$. We give a succinct derivation of $Z^{JI}_{\ell_\alpha N_\alpha;\ell_\beta N_\beta}$ for the coupling scheme used in the present analysis in appendix A [12, 14]. In Eq. (2.19) we have a set of coupled, homogeneous, integral equations for the spectator wave function, $X^{JI}_{N_\alpha \ell_\alpha}(p_\alpha)$, which we can use to construct the total wave function. Here, we note that the spectator wave function is only a function of the momentum of the spectator particle and the energy of the system, which is the binding energy of ^{3}He or ^{3}H. We now turn to the total wave function for the three-nucleon system. Making use of the orthogonality of the angular functions, $\left|\Omega^{JI}_{\ell_\alpha N_\alpha}\right\rangle$, we can write the total radial wave function, defined in Eq. (2.4), as

$$\begin{aligned}\left|\mathcal{U}^{JI}_{N_\alpha \ell_\alpha}\right\rangle &= \left\langle \Omega^{JI}_{\ell_\alpha N_\alpha}\middle|\Psi\right\rangle \\ &= \left\langle \Omega^{JI}_{\ell_\alpha, N_\alpha}\middle|\varphi_\alpha\right\rangle + \left\langle \Omega^{JI}_{\ell_\alpha N_\alpha}\middle|\varphi_\beta + \varphi_\gamma\right\rangle \\ &= \left|\eta^{JI1}_{\ell_\alpha N_\alpha}\right\rangle + \left|\eta^{JI2}_{\ell_\alpha N_\alpha}\right\rangle,\end{aligned} \tag{2.21}$$

where

$$\begin{aligned}\eta^{JI1}_{\ell_\alpha N_\alpha}(p_\alpha, q_\alpha) &\equiv \left\langle p_\alpha q_\alpha\middle|\eta^{JI1}_{\ell_\alpha N_\alpha}\right\rangle \\ &= \left\langle p_\alpha q_\alpha; \Omega^{JI}_{\ell_\alpha N_\alpha}\middle|\varphi_\alpha\right\rangle \\ &= 2G_0(q_\alpha, p_\alpha; E)\, g^{n_\alpha}_{\ell_\alpha}(q_\alpha) \sum_{\ell'_\alpha} \tau^{n_\alpha}_{\ell_\alpha \ell'_\alpha}(E - \epsilon_\alpha) X^{JI}_{N_\alpha \ell'_\alpha}(p_\alpha),\end{aligned} \tag{2.22}$$

with $G_0(q_\alpha, p_\alpha; E) = \left[E - \frac{1}{m}\left(q^2_\alpha + \frac{3}{4}p^2_\alpha\right)\right]^{-1}$. The second component of the radial wave function in Eq. (2.21) is given by

$$\begin{aligned}\eta^{JI2}_{\ell_\alpha N_\alpha}(p_\alpha, q_\alpha) &\equiv \left\langle p_\alpha q_\alpha\middle|\eta^{JI2}_{\ell_\alpha N_\alpha}\right\rangle, \\ &= \left\langle p_\alpha q_\alpha; \Omega^{JI}_{\ell_\alpha N_\alpha}\middle|\varphi_\beta + \varphi_\gamma\right\rangle, \\ &= \left\langle p_\alpha q_\alpha; \Omega^{JI}_{\ell_\alpha N_\alpha}\right| \{1 - (\beta\gamma)\} \left|\Omega^{JI}_{\ell_\beta N_\beta}\right\rangle \left|\eta^{JI1}_{\ell_\beta N_\beta}\right\rangle, \\ &= 2 \sum_{\ell_\beta N_\beta} \left\langle p_\alpha q_\alpha; \Omega^{JI}_{\ell_\alpha N_\alpha}\middle|\Omega^{JI}_{\ell_\beta N_\beta}\right\rangle \left|\eta^{JI1}_{\ell_\beta N_\beta}\right\rangle.\end{aligned} \tag{2.23}$$

The exact form of this equation, which we call the permutation term, will be the object of section B. We can write the last line because we have $(\beta\delta)|\Omega^{JI}_{\ell_\alpha N_\alpha}\rangle = -|\Omega^{JI}_{\ell_\alpha N_\alpha}\rangle$ from Eq. (2.2), since the permutation operator acts through the angular part of $|\varphi_\alpha\rangle$. The normalisation of the total wave function is then given by

$$\begin{aligned}\langle\Psi|\Psi\rangle &= 3\langle\varphi_\alpha|\varphi_\alpha\rangle + 6\langle\varphi_\alpha|\varphi_\beta\rangle \\ &= 3 \sum_{\ell_\alpha N_\alpha} \left[\left\langle \eta^{JI1}_{\ell_\alpha N_\alpha}\middle|\eta^{JI1}_{\ell_\alpha N_\alpha}\right\rangle + 2\left\langle \eta^{JI1}_{\ell_\alpha N_\alpha}\middle|\eta^{JI2}_{\ell_\alpha N_\alpha}\right\rangle\right].\end{aligned} \tag{2.24}$$

Here the sum is restricted by the two-body partial waves included in the Faddeev equations. Since the partial wave expansion of the total wave function involves an infinite sum, we need to truncate this sum such that the normalisation evaluated by the truncated sum, that is:

$$\langle \Psi | \Psi \rangle = \sum_{\ell_\alpha N_\alpha} \left\langle \mathcal{U}^{JI}_{N_\alpha \ell_\alpha} \middle| \mathcal{U}^{JI}_{N_\alpha \ell_\alpha} \right\rangle , \tag{2.25}$$

agrees with the result of Eq. (2.24). In this way we ensure that our total wave function includes all the partial waves dictated by the two-body interaction.

2.6 Numerical results

As a first step in the determination of our wave function, we calculate the binding energy of the three-nucleon system for the class of potentials being considered. For the UPA to the Reid Soft core (RSC)[10] and the Yamaguchi (YAM) potentials [11] the interaction is restricted to the $^1S_0$ and $^3S_1$-$^3D_1$ channels. This reduces the homogeneous Faddeev equations to five coupled integral equations for the spectator wave function. For the PEST (a multi-rank separable expansion of the Paris potential)[5, 6] potentials the number of coupled channels depends on the rank of the interaction in a given channel and the number of partial waves included. To get the optimal representation of the Paris potential we need to have achieved convergence in the rank. This varies from channel to channel. In all cases the rank has been chosen in such a way that the binding energy for a given number of channels has converged and is in agreement with the results of calculations using the Paris potential directly [8].

In Table 2.1 we present the result for the binding energy for the three classes of potentials. The experimental binding energy of ^{3}He is -7.72 MeV while the binding energy of ^{3}H is -8.48 MeV. The difference in binding energy between the two nucleus is caused by isospin symmetry breaking and Coulomb forces. Since we did not include any of those our results should be compared to the binding energy of ^{3}H. For the PEST potentials we have taken the 5, 10, and 18 channel potentials. The 18 channel calculation corresponds to including all nucleon-nucleon channels with $J \leq 2$. This will allow us to examine the contribution to the spectral function from higher partial waves. We observe that the Yamaguchi potentials over-bind the three-nucleon system, while the UPA and PEST potentials under-bind. Since the binding energy determines the long range part of the wave function, this difference allows us to examine the sensitivity of the structure functions to the binding energy and therefore to the tail of the wave function.

Table 2.1: Binding energy for a given potential and components of the wave function.

Potential	number of channels	binding energy (MeV)	$P(S)$ %	$P(S')$ %	$P(D)$ %
RSC	5	-7.15	88.37%	1.88%	8.89%
YAM4	5	-9.12	93.08%	1.58%	4.97%
YAM7	5	-8.05	89.1%	1.59%	8.71%
PEST	5	-7.27	89.3%	1.88%	8.11%
PEST	10	-7.10	89.72%	1.71%	7.85%
PEST	18	-7.32	89.56%	1.66%	8.07%
PARIS	–	-7.31	89.88%	1.62%	8.43%
PEST (^{3}He)	5	-7.72	89.52%	1.6%	8.11%
PEST (^{3}H)	5	-8.48	89.95%	1.23%	8.1%

A comparison of the PEST five channel and the UPA suggests that the difference between these two models is minimal. In fact, that is the case for most realistic potentials that do not include energy dependence. The higher partial waves in the PEST potential seem to have a small but significant contribution to the binding energy. Here again, this potential, in common with all realistic potentials, tends to under-bind the three nucleon system. As we can see from Table 2.1 the result from PEST and RSC potential are more than 1 MeV short (more than 10%). This is also the case of the PARIS potential we give as comparison to PEST and also other potential. A review of the triton binding energy given by recent potentials can be found in Ref. [96]. In [96], the value of the binding energy for potential from the Nijmegen group (Nijm-I and Nijm-II) and the Argonne group (V_{18}) are between -7.6 and 7.7 MeV. The solution to this under-binding problem may involve the short-range, velocity dependence of the two-nucleon force [15], as well as a genuine three-body force [16].

Table 2.1 also gives the contribution of the three dominant kind of partial waves (S, S' and D waves) to the wave function. The fundamental distinction between the different kind of waves is based on the total angular momentum of the system $\vec{\mathcal{L}} = \vec{L} + \vec{\ell}$ which can only have the following value $\mathcal{L} =$ 0, 1 or 2 (S, P or D wave)[2]. Further distinction between S and S' wave are based on other properties of symmetry of the different waves, a complete and accurate description of the classification of the different kind of waves

[2]The spin of the three nucleons add up to either $\frac{1}{2}$ or $\frac{3}{2}$. The total angular momentum of the tri-nucleon system is $\frac{1}{2}$, this requirement limits $\mathcal{L}$ to the above values.

in the tri-nucleon system can be found in [80]. The figures for the different kind of waves are similar for all potential, with the exception of YAM4 which presents an excess of S waves and a depletion of D waves.

Since we have neglected the Coulomb contribution to the energy of ^{3}He, and our more realistic potentials under-bind the three nucleon system, we have chosen to adjust the strength of the $^1S_0$ interaction to reproduce the experimental binding energy of both ^{3}He and ^{3}H. This procedure does not affect the deuteron wave function, but could have some influence on the continuum wave function in the $^1S_0$. In this way, we may estimate the error in neglecting the Coulomb energy for ^{3}He, and the possible error in the tail of the wave function due to under-binding of the three nucleon system. The contribution of this correction will be discussed when considering the spectral functions and light-cone momentum distributions.

Chapter 3

Structure functions and convolution formalism

3.1 The electromagnetic cross section

The cross section for the scattering of a charged lepton with a nucleus, assuming we exchange only one photon, as in Fig. 3.1, is proportional to the product of the leptonic tensor $L_{\mu\nu}$ with the hadronic tensor $W_{\mu\nu}$. In the following we consider a lepton of mass m, initial (final) four momentum k (k') and s (s') its covariant polarisation vector, such that $s{\cdot}k = 0$ ($s'{\cdot}k' = 0$) and $s{\cdot}s = -1$ ($s'{\cdot}s' = -1$). The hadronic system will have a mass M and four momentum and polarisation P and S. In the laboratory frame we consider that $P = (M, \vec{0})$, $k = (E, \vec{k})$ and $k' = (E', \vec{k'})$. Then the differential cross section for detecting a final lepton in a solid angle $d\Omega$ and in the energy range $(E', E' + dE')$ is

$$\frac{d^2\sigma}{d\Omega dE'} = \frac{\alpha^2}{q^4}\frac{E'}{E}L_{\mu\nu}W^{\mu\nu}, \tag{3.1}$$

where $q = k - k'$ is the momentum of the exchanged photon and α is the fine structure constant. The leptonic tensor has the following form in the case of

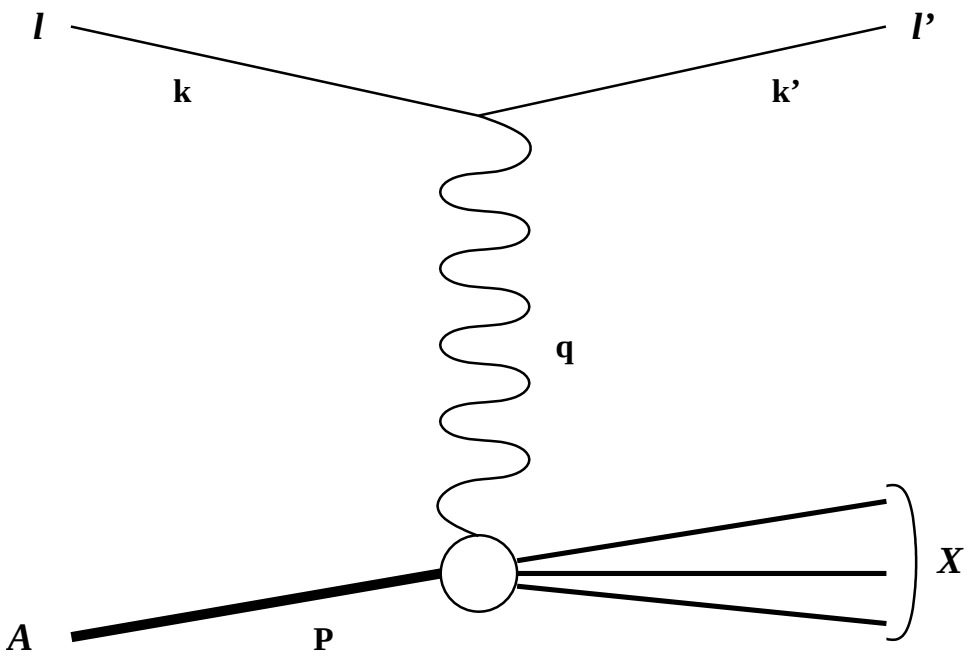

Figure 3.1: Scattering of a lepton l on a nucleus A, with one photon exchange.

an electromagnetic current

$$\begin{aligned} L_{\mu\nu}(k,s;k',s') &= \left[\bar{u}(k',s')\gamma_\mu u(k,s)\right]^\dagger \left[\bar{u}(k',s')\gamma_\nu u(k,s)\right] \\ &= L^{(S)}_{\mu\nu}(k;k')+L^{(A)}_{\mu\nu}(k,s;k')+L'^{(S)}_{\mu\nu}(k,s;k',s')+L'^{(A)}_{\mu\nu}(k;k',s'). \end{aligned} \tag{3.2}$$

Here the leptonic tensor is a sum of four parts because we consider the possibility of a different polarisation for the final state of the lepton. In practice, the measurement of the polarisation of the final lepton is difficult and never done. So one sums over the polarisation of the final lepton, s', and the leptonic tensor is reduced to a sum of two terms: $2L^{(S)}_{\mu\nu}(k;k') + 2L^{(A)}_{\mu\nu}(k,s;k')$. Finally if we average over initial polarisation, to consider the use of an unpolarised lepton probe, the leptonic tensor is reduced to only one, symmetric, component: $L^{(S)}_{\mu\nu}(k;k')$. We have

$$L^{(S)}_{\mu\nu}(k;k') = k_\mu k'_\nu + k'_\mu k_\nu + g_{\mu\nu}(k\cdot k' - m^2) \tag{3.3}$$

$$L^{(A)}_{\mu\nu}(k,s;k') = im\epsilon_{\mu\nu\alpha\beta}s^\alpha(k-k')^\beta \tag{3.4}$$

$$\begin{aligned} L'^{(S)}_{\mu\nu}(k,s;k',s') = {} & k\cdot s'\left(k'_\mu s_\nu + s_\mu k'_\nu - g_{\mu\nu}s\cdot k'\right) \\ & -\left(k\cdot k' - m^2\right)\left(s_\mu s'_\nu + s'_\mu s_\nu - g_{\mu\nu}s\cdot s'\right) \\ & +k'\cdot s\left(s'_\mu k_\nu + k_\mu s'_\nu\right) - s\cdot s'\left(k_\mu k'_\nu + k'_\mu k_\nu\right) \end{aligned} \tag{3.5}$$

$$L'^{(A)}_{\mu\nu}(k;k',s') = im\epsilon_{\mu\nu\alpha\beta}s'^\alpha(k-k')^\beta. \tag{3.6}$$

Since leptons are point like objects, the leptonic tensor is very simple and depends only on the kinematics. The hadronic tensor, on the other hand, represents a composite object. It depends on how the composite object is made, and how it is bound. However, from general principles one can write the general form of the electromagnetic current for the hadronic system. For an hadronic system of spin $\frac{1}{2}$ (*i.e.* free nucleon, ^{3}He, ^{3}H etc.) the hadronic tensor has the following form [17, 18, 19]

$$\begin{aligned} \mathcal{W}_{\mu\nu}(q;P,S) &= \int d^4\xi e^{iq\xi}\left\langle PS\left|J_\mu(\xi)J_\nu(0)\right|PS\right\rangle \\ &= \mathcal{W}^{(S)}_{\mu\nu}(q;P) + \mathcal{W}^{(A)}_{\mu\nu}(q;P,S), \end{aligned} \tag{3.7}$$

where J^μ is the electromagnetic current. Here we have separated the hadronic tensor into symmetric and antisymmetric parts. As in the case of the leptonic tensor, if one averages over the initial polarisation only the symmetric component, $\mathcal{W}^{(S)}_{\mu\nu}$, remains. Each of these components depends on two form

factors:

$$\begin{aligned}\mathcal{W}^{(S)}_{\mu\nu}(q;P) = &\left(-g_{\mu\nu}+\frac{q_\mu q_\nu}{q^2}\right) W_1(P\cdot q, q^2) \\ &+\left(P_\mu-\frac{P\cdot q}{q^2}q_\mu\right)\left(P_\nu-\frac{P\cdot q}{q^2}q_\nu\right)\frac{W_2(P\cdot q,q^2)}{M^2},\end{aligned} \tag{3.8}$$

and

$$\begin{aligned}\mathcal{W}^{(A)}_{\mu\nu}(q;P,S) =& i\epsilon_{\mu\nu\alpha\beta}q^\alpha\Bigg[MS^\beta G_1(P\cdot q,q^2) \\ &+\left[(P\cdot q)\,S^\beta-(S\cdot q)\,P^\beta\right]\frac{G_2(P\cdot q,q^2)}{M}\Bigg],\end{aligned} \tag{3.9}$$

where W_1, W_2, G_1 and G_2 are the form factors of the hadronic system. All the dependence of the cross section on the internal structure of the hadronic system is included in the form factors. Therefore these form factors may be used as a probe of the structure of the hadronic system. The deep inelastic scattering (DIS) or Bjorken limit is given by the following conditions, in the rest frame of the target

$$-q^2 = Q^2 \to \infty, \quad \nu = E-E' \to \infty \quad \text{and} \quad x = \frac{Q^2}{2P\cdot q} = \frac{Q^2}{2M\nu}\,, \text{ fixed.} \tag{3.10}$$

Note that Q^2 and x are defined covariantly while ν is defined in the laboratory frame. In the deep inelastic (Bjorken) regime, one prefers to use the strucutre functions which are known to approximately scale as functions of x (to logarithmic corrections in Q^2):

$$\begin{aligned}\lim_{Bj} MW_1(P\cdot q,Q^2) &= F_1(x), \\ \lim_{Bj} \nu W_2(P\cdot q,Q^2) &= F_2(x), \\ \lim_{Bj} \frac{(P\cdot q)^2}{\nu} G_1(P\cdot q,Q^2) &= g_1(x), \\ \lim_{Bj} \nu(P\cdot q) G_2(P\cdot q,Q^2) &= g_2(x).\end{aligned} \tag{3.11}$$

3.2 Particularly interesting cross sections

3.2.1 Unpolarised scattering

In unpolarised scattering one has to sum over the final polarisations and average over the initial polarisations. The cross section becomes

$$\begin{aligned}\frac{d^2\sigma^{unp}}{d\Omega dE'} &= \frac{1}{4}\frac{\alpha^2}{q^4}\frac{E'}{E}\sum_{s,s',S} L_{\mu\nu}\mathcal{W}^{\mu\nu}, \\ &= \frac{\alpha^2}{q^4}\frac{E'}{E} 2L^{(S)}_{\mu\nu}\mathcal{W}^{\mu\nu(S)}, \\ &= \frac{4\alpha^2 E'^2}{q^4}\left[2W_1\sin^2\frac{\theta}{2} + W_2\cos^2\frac{\theta}{2}\right],\end{aligned} \tag{3.12}$$

or

$$\frac{d^2\sigma^{unp}}{dxdQ^2} = \frac{4\pi\alpha^2 E'^2}{xQ^4}\frac{E'}{E}\left[F_2\cos^2\frac{\theta}{2} + 2\frac{\nu}{M}F_1\sin^2\frac{\theta}{2}\right], \tag{3.13}$$

where θ is the scattering angle of the lepton. So in unpolarised scattering the cross section depends only on the two first form factors, or in DIS the two first structure functions F_1 and F_2. This is why they are often called unpolarised form factors (structure functions).

3.2.2 Polarised scattering

To measure the polarised structure function g_1 and g_2 one needs not only a polarised target but also a polarised probe as one can tell by the structure of the hadronic and leptonic tensors. To access precisely the two polarised structure functions one forms the difference of the cross sections between a polarised probe and two targets of opposite polarisation. That is

$$\begin{aligned}\frac{d^2\sigma^{s,S}}{d\Omega dE'} - \frac{d^2\sigma^{s,-S}}{d\Omega dE'} &= \frac{\alpha^2}{q^4}\frac{E'}{E}\sum_{s'} L_{\mu\nu}(k,s;k',s')\left[\mathcal{W}^{\mu\nu}(q;P,S) - \mathcal{W}^{\mu\nu}(q;P,-S)\right] \\ &= \frac{\alpha^2}{q^4}\frac{E'}{E} 4L^{(A)}_{\mu\nu}(k,s;k')\mathcal{W}^{\mu\nu(A)}(q;P,S) \\ &= \frac{8m\alpha^2 E'}{q^4 E}\Big\{\left[(q\cdot S)(q\cdot s) + Q^2(s\cdot S)\right]MG_1 \\ &\quad + Q^2\left[(s\cdot S)(P\cdot q) - (q\cdot S)(P\cdot s)\right]\frac{G_2}{M}\Big\}.\end{aligned} \tag{3.14}$$

In particular, if we polarise the probe longitudinally ($\rightarrow$) and then polarise the target, first in the same direction as the probe ($\Rightarrow$), then in the opposite direction ($\Leftarrow$), we have (to the first order in m/E)

$$\frac{d^2\sigma^{\vec{\Rightarrow}}}{d\Omega dE'} - \frac{d^2\sigma^{\vec{\Leftarrow}}}{d\Omega dE'} = -\frac{4\alpha^2}{Q^2}\frac{E'^2}{E}\left[(E + E'\cos\theta)MG_1 - Q^2G_2\right]. \tag{3.15}$$

The structure of Eq. (3.15) is such that it is mainly sensitive to G_1. Another set up, which is important if one wishes to measure the polarised G_2 structure function, is to polarise the hadronic target transversely ($\Uparrow$ or $\Downarrow$) while the probe is polarised longitudinally ($\rightarrow$). In this case Eq. (3.14) leads to

$$\frac{d^2\sigma^{\rightarrow\Uparrow}}{d\Omega dE'} - \frac{d^2\sigma^{\rightarrow\Downarrow}}{d\Omega dE'} = -\frac{4\alpha^2}{Q^2}\frac{E'^2}{E}\sin\theta\cos\phi\left(MG_1 + 2EG_2\right), \tag{3.16}$$

where ϕ is the angle between the scattering plane, $(\vec{k}, \vec{k}')$, and the polarisation plane, $(\vec{k}, \vec{S})$.

3.3 The convolution formalism

3.3.1 The partial wave impulse approximation

As we have said the hadronic tensor has the same form for both the nucleon and tri-nucleon system. What we are looking at now is how one can relate the free nucleon structure functions to the structure functions of a nucleus. We will use the plane wave impulse approximation (PWIA) to derive a relation between the hadronic tensor of nucleus and its constituent nucleons . The PWIA involves the following assumptions:

1. Only the sum of single-nucleon currents contributes to the inclusive cross section.

2. Interference between different constituent nucleons does not contribute.

3. The effect of final-state interactions between the products of the struck nucleon and the residual hadronic state is neglected.

Assumption (1) implies that we will neglect multiple rescattering. It is justified by the fact that at high Q^2 we expect to be in the perturbative regime of QCD. Consequently, the contribution from multiple scattering should be low. However, this does not apply at small Bjorken-x. x is a measure of the

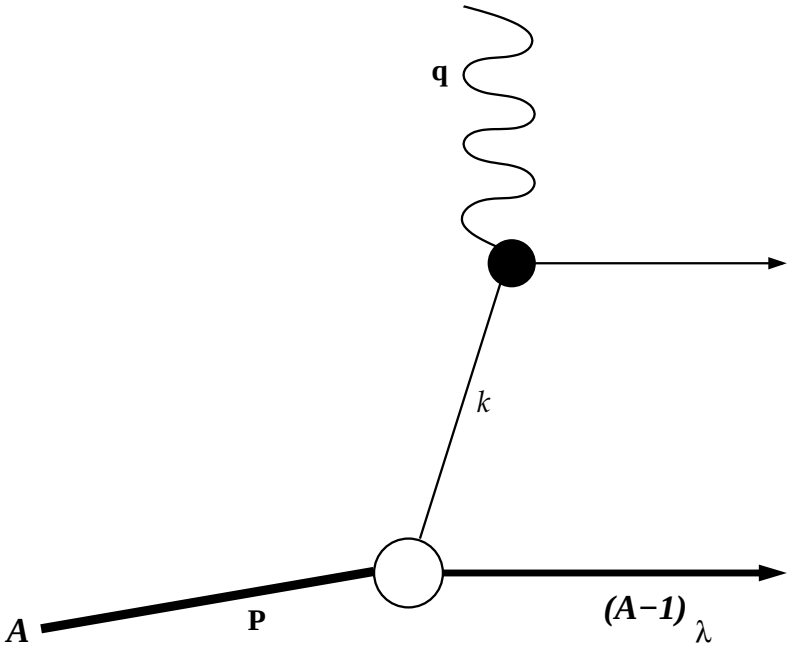

Figure 3.2: In PWIA, only one nucleon of the nucleus is struck by the photon.

momentum of the struck nucleon along the impulsion of the photon. A low value of x means that the interaction between the photon and the nucleus occurs at a low energy scale, outside the perturbative regime.

(2) implies that the nucleon constituents are quasi-free, which is expected in DIS as the energy of interaction is far greater than the binding energy of the constituent. So from the point of view of the probe, the constituent nucleons are quasi-free.

Finally (3) means that we consider the final state as the product of a wave function describing the products of the struck nucleon with an independent wave function describing the spectators. This supposes that the products of the collision will not interact or that the contribution of such interaction will be very small. We checked the validity of this assumption for the neutron in ^{3}He and we found that indeed the contribution of this interaction was very small in this case.

Using (1) we can write the electromagnetic current of the nucleus as the sum of the individual particle currents, so in the three nucleon system

$$J^\mu = \sum_{\alpha=1}^{3} j_\alpha^\mu \,, \tag{3.17}$$

where j^μ_α is the electromagnetic current of the nucleon α in the nucleus. Note that in the previous equation we assumed that the nucleus did not have any other constituents beside the nucleons. However, one can easily extend the derivation of the convolution formalism to include other components of the nucleus if needed. So now we can write the hadronic tensor for the three nucleon system as

$$\mathcal{W}^{\mu\nu}(q;P_A,S_A)=\sum_{\alpha=1}^{3}\int d^4\xi e^{iq\xi}\left\langle P_AS_A\left|j^\mu_\alpha(\xi)j^\nu_\alpha(0)\right|P_AS_A\right\rangle, \tag{3.18}$$

note that here we used (2) to get rid of the possibility of cross terms of the kind $j^\mu_\alpha(\xi)j^\nu_\beta(0)$. This hadronic tensor arises from the reaction depicted in Fig. 3.3, cross terms would arise from a diagram of the form of Fig. 3.4. Assumption (3) also gets rid of the diagram represented in Fig. 3.5, thanks to this assumption we can write the final state as a product $|p_\alpha s_\alpha\rangle|P_{A-1}S_{A-1}f\rangle$, where f is an index over all $A-1$ states having same P_{A-1} and S_{A-1}. We can then write the hadronic tensor as

$$\begin{aligned}\mathcal{W}^{\mu\nu}(q;P_A,S_A)=&\\ &\sum_{\alpha=1}^{3}\sum_{\substack{\text{final}\\ \text{states}}}\int d^4\xi e^{iq\xi}\left\langle P_AS_A|p_\alpha s_\alpha\right\rangle|P_{A-1}S_{A-1}f\rangle\,\delta^4(P_A-(p_\alpha+P_{A-1}))\\ &\qquad\times\left\langle P_{A-1}S_{A-1}f\right|\left\langle p_\alpha s_\alpha\right|j^\mu_\alpha(\xi)j^\nu_\alpha(0)\left|p'_\alpha s'_\alpha\right\rangle\left|P'_{A-1}S'_{A-1}f'\right\rangle\\ &\qquad\qquad\times\left\langle P'_{A-1}S'_{A-1}f'\right|\left\langle p'_\alpha s'_\alpha|P_AS_A\right\rangle\delta^4\big(P_A-(p'_\alpha-P'_{A-1})\big).\end{aligned} \tag{3.19}$$

In Eq. (3.19) the sum over all final states refers to both $|p_\alpha s_\alpha\rangle|P_{A-1}S_{A-1}f\rangle$ and $|p'_\alpha s'_\alpha\rangle|P'_{A-1}S'_{A-1}f'\rangle$, and where it is needed an integral over 4-momentum as well. If the set of $A-1$ states is complete then we have

$$\left\langle P_{A-1}S_{A-1}f|P'_{A-1}S'_{A-1}f'\right\rangle=\delta^4(P_{A-1}-P'_{A-1})\delta(S_{A-1}-S'_{A-1})\delta_{f,f'}\,. \tag{3.20}$$

Since the current operators in Eq. (3.19) act only on the particle labeled α leaving the $A-1$ state untouched we can use Eq. (3.20) to simplify Eq. (3.19)

$$\begin{aligned}\mathcal{W}^{\mu\nu}(q;P_A,S_A)=\sum_{\alpha=1}^{3}\sum_{\substack{\text{final}\\ \text{states}}}\int d^4\xi e^{iq\xi}\left\langle p_\alpha s_\alpha\right|j^\mu_\alpha(\xi)j^\nu_\alpha(0)\left|p_\alpha s_\alpha\right\rangle&\\ \times\left\langle P_AS_A|p_\alpha s_\alpha\right\rangle|P_{A-1}S_{A-1}f\rangle\,\delta^4(P_A-(p_\alpha+P_{A-1}))&\\ \times\left\langle P_{A-1}S_{A-1}f\right|\left\langle p_\alpha s_\alpha|P_AS_A\right\rangle.&\end{aligned} \tag{3.21}$$

In the previous equation we can easily spot the nucleon hadronic tensor times a term defined as the spectral function for the nucleon α. This term is

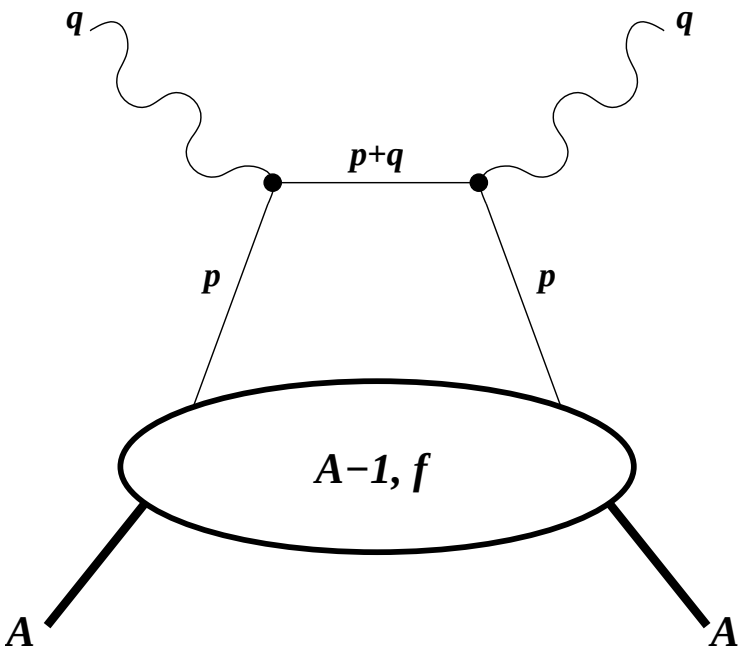

Figure 3.3: Handbag diagram.

interpreted as being the number density of the given nucleon α, with given momentum p and polarisation s, while the remaining system is in a state f with momentum P_{A-1} and polarisation S_{A-1} multiplied by a delta-function:

$$S_f^\alpha(p,s,P_A,S_A) = \sum_{\substack{P_{A-1}\\S_{A-1}}} |\langle P_A S_A|ps\rangle|P_{A-1}S_{A-1}f\rangle|^2\,\delta^4(P_A-(p+P_{A-1}))\ . \tag{3.22}$$

In instant form dynamic the sum over the state of momentum P_{A-1} is an integral over $\vec{P}_{A-1}$. We can split the delta-function of Eq. (3.22) in two parts: $\delta^4(P_A-(p+P_{A-1})) = \delta(P_A^0-(p^0+P_{A-1}^0))\delta^3(\vec{P}_A-(\vec{p}+\vec{P}_{A-1}))$, using the spatial part of this delta-function one can integrate the integral over $\vec{P}_{A-1}$ in Eq. (3.22). Since from assumption (2) we consider the constituent nucleons to be quasi-free, we will consider that the struck nucleon can be described by a plane wave. Therefore, we can replace $|ps\rangle$ by $a_s^\dagger(\vec{p})|0\rangle$, where $a_s^\dagger(\vec{p})$ is the creation operator of the nucleon of spin s and momentum $\vec{p}$. We can now rewrite Eq. (3.22) as:

$$\begin{aligned} S_f^\alpha(p,s,P_A,S_A) = &\sum_{S_{A-1}} \langle P_A S_A|a_{s,\alpha}^\dagger(\vec{p})|0\rangle|P_{A-1}S_{A-1}f\rangle \\ &\times \langle P_{A-1}S_{A-1}f|\langle 0|a_{s,\alpha}(\vec{p})|P_A S_A\rangle\delta\big(P_A^0-p^0-P_{A-1}^0\big)\,, \end{aligned} \tag{3.23}$$

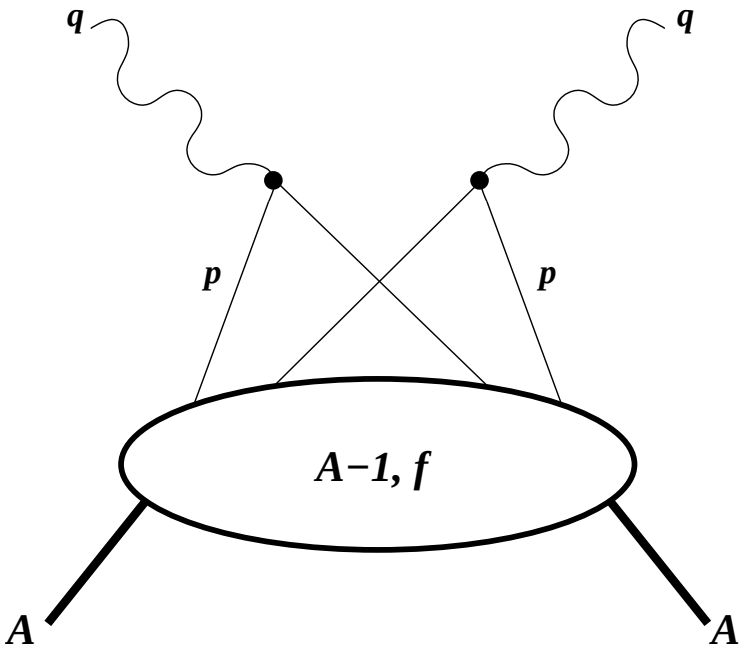

Figure 3.4: Cross term diagram.

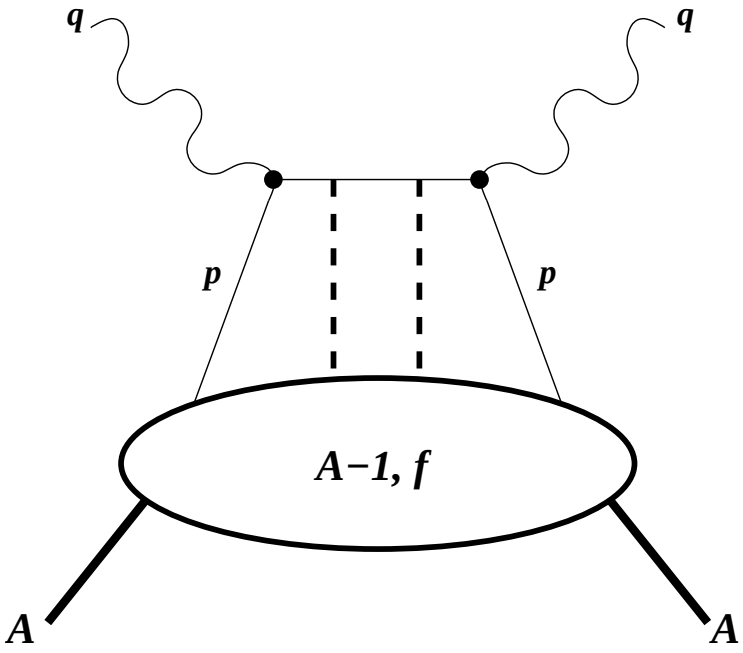

Figure 3.5: Higher twist diagram neglected using assumption (3).

with $\vec{P}_{A-1} = \vec{P}_A - \vec{p}$. In the previous equation, the index α in the creation and destruction operators indicates that we act on the nucleon labelled α inside the nucleus. If we suppose that for a given value of P_{A-1} and label f, the set of state $|P_{A-1}S_{A-1}f\rangle$ is complete, we can replace the sum over those states by the identity. In the end the spectral function is expressed by:

$$S_f^\alpha(p,s,P_A,S_A) = \langle P_A S_A | a^\dagger_{s,\alpha}(\vec{p}) a_{s,\alpha}(\vec{p}) | P_A S_A \rangle \delta\big(p^0 - (P_A^0 - P_{A-1}^0)\big) \ . \quad (3.24)$$

Alternatively the energy p^0 of the nucleon in Eq. (3.24) can also be expressed phenomenologically [17] as the sum of the nucleon mass, m, plus the separation energy of this nucleon, ϵ_f[1], and minus the recoil kinetic energy, Tr_f, of the remaining $A-1$ state. In this case we have $p^0 = m + \epsilon_f - Tr_f$. As we will see later, one can find ϵ_f and Tr_f in terms of P_A and P_{A-1}. So one can write Eq. (3.24) in the following way:

$$S_f^\alpha(p,s,P_A,S_A) = \langle P_A S_A | a^\dagger_{s,\alpha}(\vec{p}) a_{s,\alpha}(\vec{p}) | P_A S_A \rangle \delta\big(p^0 - (m + \epsilon_f - Tr_f)\big) \ . \quad (3.25)$$

It is easier to express the spectral function as well as the nucleon electromagnetic tensor in terms of protons and neutrons rather than particle α. In the following we will introduce an isospin index t for the spectral function and the nucleon electromagnetic tensor. So we have:

$$\mathcal{W}_{\mu\nu}(q;P_A,S_A) = \sum_{t=-\frac{1}{2}}^{\frac{1}{2}} \sum_{s,f} \int d^4p S_f^t(p,s,P_A,S_A) \mathcal{W}^t_{\mu\nu}(q;p,s) \, . \quad (3.26)$$

Of course, because of momentum conservation, the electromagnetic tensor of the nucleon actually involves an off-shell particle. We only have measurements and parametrisations of structure functions for on-shell nucleons. There are several ways to deal with this problem. One is to develop the convolution formalism on the light front, where particles are always on-shell – the drawback being that the hadronic system has to be described as a sum of Fock-states. We have also to be careful of the fact that the electromagnetic tensor of the nucleus is defined in terms of q, P_A and S_A, while the nucleon one is defined in terms of q, p and s. In the following we extend the hadronic tensor off-shell by assuming that the off-shell structure functions of the nucleons are equal to the on-shell ones.

3.3.2 Convolution of the structure functions

With Eq. (3.24) and Eq. (3.26), we have all the necessary ingredients for the convolution formalism for the hadronic tensor. However we are ultimately

[1] ϵ_f is defined as $\epsilon_f = M_A - M_f - m$ where M_f is the mass of the remaining $A-1$ remaining hadronic system in the state f.

interested in observable quantities like the structure functions. So, now that we have a convolution formula for the hadronic tensor we will derive convolution formulas for the structure functions. There are several ways to access individual structure functions from the hadronic tensor, see for example Refs. [24, 20]. Before proceeding we will introduce some new notation and some definitions. First the Bjorken variable x, as defined in Eq. (3.10), is not always very convenient, so from now on we will use a new definition for x:

$$x = \frac{Q^2}{2P_A{\cdot}q}\frac{M_A}{M_N} = \frac{Q^2}{2M_N\nu}, \tag{3.27}$$

where M_A is the mass of the target and M_N is the nucleon mass. For the nucleon both definitions of x give the same results. The Bjorken limit is defined in the same way for both definitions and gives the same physics. In our system we want to know the nuclear structure functions, which are given as functions of $x = Q^2/(2M_N\nu)$ and Q^2, as a combination of nucleon structure functions given in terms of $\tilde{x} = Q^2/(2p\cdot q)$ and Q^2. For the convolution formula to be useful we also need to know how to link x and $\tilde{x}$.

In the nuclear rest frame we define the z-axis as being along the direction of the virtual photon. In this frame we have the nuclear momentum $P_A = (M_A, 0, 0, 0)$, and the virtual photon momentum, $q = (\nu, 0, 0, -\sqrt{\nu^2 + Q^2})$. In the Bjorken limit we have $q \to (\nu, 0, 0, -\nu - M_N x)$. We will now move to light-cone coordinates which we define as $a^{\pm} = (a^0 \pm a^3)/\sqrt{2}$, a^1 and a^2 being unchanged and denoted as $\vec{a}_\perp$. In this coordinate system we have $a{\cdot}b = a^+b^- + a^-b^+ - \vec{a}_\perp{\cdot}\vec{b}_\perp$. Finally we have $P_A^+ = P_A^- = M_A/\sqrt{2}$, $q^+ = -M_N x/\sqrt{2}$ and $q^- = (2\nu + M_N x)/\sqrt{2}$. In the Bjorken limit we have $q^- \to \sqrt{2}\nu$ which is infinite. So in the Bjorken limit Eq. (3.27) becomes $x \to M_A Q^2/(2M_N P_A^+ q^-)$ and is dominated by q^-. We now define the quantity y by:

$$y = \frac{p^+}{P_A^+}\frac{M_A}{M_N} = \frac{\sqrt{2}p^+}{M_N}. \tag{3.28}$$

Thus y is the fraction of the momentum of the nucleus carried by the struck nucleon, defined so it runs from 0 to approximately $A(\approx M_A/M_N)$, like x. With this definition, we can now express both p^+ and p^- in terms of y:

$$p^+ = yP_A^+\frac{M_N}{M_A} = \frac{yM_N}{\sqrt{2}}, \tag{3.29}$$

$$p^- = \frac{M_N^2 - \vec{p}_\perp^{\,2}}{2p^+} = \frac{M_N^2 - \vec{p}_\perp^{\,2}}{\sqrt{2}yM_N}. \tag{3.30}$$

If we suppose that the transverse momentum of the struck nucleon cannot become very big, then p^- will remain finite and the dot-product $p{\cdot}q$ will be

dominated by the term p^+q^- which goes to infinity in the Bjorken limit while p^-q^+ stays finite. Consequently we have $p\cdot q \approx p^+q^- = yP_A^+q^-M_N/M_A \approx yP_A\cdot qM_N/M_A$, and the argument of the structure function needed in the nuclear calculation, $\tilde{x} = Q^2/(2p\cdot q)$, is:

$$\tilde{x} = \frac{x}{y}. \tag{3.31}$$

We now can express the convolution formula for the various structure functions, in the Bjorken limit:

$$F_1^A(x,Q^2) = \sum_{t=-\frac{1}{2}}^{\frac{1}{2}} \sum_{s,f} \int d^4p S_f^t(p,s,P_A,S_A) \frac{M_A}{M_N} F_1^t\Big(\frac{x}{y},Q^2\Big), \tag{3.32}$$

$$F_2^A(x,Q^2) = \sum_{t=-\frac{1}{2}}^{\frac{1}{2}} \sum_{s,f} \int d^4p S_f^t(p,s,P_A,S_A) y F_2^t\Big(\frac{x}{y},Q^2\Big), \tag{3.33}$$

$$g_1^A(x,Q^2) = \sum_{t=-\frac{1}{2}}^{\frac{1}{2}} \sum_{s,f} \int d^4p S_f^t(p,s,P_A,S_A) \frac{M_A(q\cdot s)}{yM_N(q\cdot S_A)} g_1^t\Big(\frac{x}{y},Q^2\Big). \tag{3.34}$$

The ratio of masses in Eq. (3.32) comes from the fact that $W_1 = F_1/M$. In Eq. (3.33) this ratio is in fact included in the definition of y. We did not include a convolution formula for g_2 as it is quite complex compared to the other structure functions and we will not study it in the following. As one can notice the structure function of the nucleon on the right hand side depends only on y, which is in fact a measure of p^+. Consequently we can simplify the integrals in the Eqs. (3.32) to (3.34) to the form:

$$F_1^A(x,Q^2) = \sum_{t=-\frac{1}{2}}^{\frac{1}{2}} N_t \int dy \frac{f^t(y)}{y} F_1^t\Big(\frac{x}{y},Q^2\Big), \tag{3.35}$$

$$F_2^A(x,Q^2) = \sum_{t=-\frac{1}{2}}^{\frac{1}{2}} N_t \int dy f^t(y) F_2^t\Big(\frac{x}{y},Q^2\Big), \tag{3.36}$$

$$g_1^A(x,Q^2) = \sum_{t=-\frac{1}{2}}^{\frac{1}{2}} N_t \int dy \frac{\Delta f^t(y)}{y} g_1^t\big(\frac{x}{y},Q^2\big). \tag{3.37}$$

In those equations N_t is the number of particles of isospin t in the nucleus and we have:

$$f^t(y) = \frac{1}{N_t} \sum_{s,f} \int d^4p S_f^t(p,s,P_A,S_A) \frac{p^0+p^3}{p^0} \delta\Big(y - \frac{p^0+p^3}{M_N}\Big). \tag{3.38}$$

$f^t(y)$ is called the (unpolarised) light-cone momentum distribution for the nucleon of isospin t. It is in fact the probability of finding a nucleon of isospin t and fraction of momentum y in the nucleus. The division by N_t is necessary because the spectral function is not a probability but a number density. For the definition of Δf^t we have to remember that a spin 1/2 particle only has two possible spin projections along any given axis, we will call them "+" and "−". We also have the choice of the polarisation S_A, which we will take as being positive (+), so:

$$\Delta f^t(y) = \frac{1}{N_t} \sum_f \int d^4p \left(S_f^t(p, +, P_A, +) - S_f^t(p, -, P_A, +) \right) \times \frac{p^0 + p^3}{p^0} \delta\left(y - \frac{p^0 + p^3}{M_N} \right). \quad (3.39)$$

$\Delta f^t(y)$ is known as the polarised light-cone momentum distribution of the nucleon of isospin t. It is interpreted as the probability of finding a nucleon of given isospin t with the same spin projection as the nucleus along the z-axis, minus the probability of finding the same nucleon with opposite spin projection to that of the nucleus along the z-axis.

Chapter 4

Spectral functions and light-cone momentum distributions of the three nucleon system

4.1 The spectral function

As we saw in the last chapter, to compute the nuclear structure functions, we ultimately need to know the light-cone momentum distributions of the various nucleons. To determine these light-cone momentum distributions we need to know how to compute the spectral function. As we have seen previously in section 3.3.1, the spectral function is proportional to a number density. As one can see in Eqs. (3.38) and (3.39) the light-cone momentum distributions depend on combinations of spectral functions. Those combinations of spectral functions are not dependent on the nuclear polarisation, S_A (up to a sign in the case of Δf). So one can replace the combination of spectral functions in Eqs. (3.38) and (3.39) by spectral functions that have been "averaged" over polarisation. That is:

$$f^t(y) = \frac{1}{N_t}\sum_f \int d^4p \bar{S}_f^t(p,P_A)\frac{p^0+p^3}{p^0}\delta\left(y-\frac{p^0+p^3}{M_N}\right) , \quad (4.1)$$

$$\Delta f^t(y) = \frac{1}{N_t}\sum_f \int d^4p \Delta\bar{S}_f^t(p,P_A)\frac{p^0+p^3}{p^0}\delta\left(y-\frac{p^0+p^3}{M_N}\right) , \quad (4.2)$$

with:

$$\bar{S}_f^t(p,P_A) = \frac{1}{2J_A+1}\sum_{s,S_A} S_f^t(p,s,P_A,S_A) , \quad (4.3)$$

$$\Delta\bar{S}_f^t(p,P_A) = \frac{1}{2J_A+1}\sum_{\pm} \left(S_f^t(p,\pm,P_A,\pm)-S_f^t(p,\mp,P_A,\pm)\right) . \quad (4.4)$$

The quantity $\bar{S}_f^t(p,P_A)$, called the "diagonal spectral function" in Refs. [30, 31], can be interpreted as the number density of particles of isospin t inside the nucleus (while the remaining hadronic system is in a state f). On the other hand, $\Delta\bar{S}_f^t(p,P_A)$ is interpreted as the number density of particles of isospin t, with spin aligned with the spin of the nucleus, minus the number density of the same particles, with spin anti-aligned with the spin of the nucleus (while the remaining hadronic system is in a state f). Since we are summing over all polarisations, we can replace sums over polarisation by sums over spin states, which is easier to use. Note also, that those spectral functions are sometimes defined in terms of E and $\vec{k}$ rather than the four vector k (see for example Refs. [28, 29]). Then E is the energy of the state λ, that is, what has been called P^0_{A-1} in Eqs. (3.24) and (3.25). E and k^0 are, of course, related by energy conservation.

One can define two extra polarised spectral functions, $\bar{S}_f^{t,+}$ and $\bar{S}_f^{t,-}$. $\bar{S}_f^{t,+}$ ($\bar{S}_f^{t,-}$) is the number density of particle of isospin t, with spin aligned (anti-

aligned) with the spin of the nucleus, while the remaining hadronic system is in a state f. They are defined by:

$$\bar{S}_f^{t,+}(p,P_A) = \frac{1}{2J_A+1}\sum_{\pm} S_f^t(p,\pm,P_A,\pm) \ , \tag{4.5}$$

$$\bar{S}_f^{t,-}(p,P_A) = \frac{1}{2J_A+1}\sum_{\pm} S_f^t(p,\mp,P_A,\pm) \ . \tag{4.6}$$

We can also define the corresponding light-cone momentum distributions $f^{t,+}$ and $f^{t,-}$ with equations similar to Eqs. (4.1) and (4.2). We have the following relations between the various spectral functions defined by Eqs. (4.3) through (4.6): $\bar{S}_f^t = \bar{S}_f^{t,+} + \bar{S}_f^{t,-}$ and $\Delta\bar{S}_f^t = \bar{S}_f^{t,+} - \bar{S}_f^{t,-}$.

In the following we will denote the product $a^\dagger_{\sigma,N}(\vec{k})\, a_{\sigma,N}(\vec{k})$ – where σ is a spin index – as the familiar number density operator $\rho_{\sigma,N}(\vec{k})$ and we will define it in a way similar to Ref. [33]. For example, the density of protons with spin $+\frac{1}{2}$ along the z–axis and momentum $\vec{k}$, $\langle\rho_p^+(\vec{k})\rangle$, in a tri-nucleon with wave function $|\Psi\rangle$ and spin projection σ, is defined by

$$\begin{aligned}\langle\rho_p^+(\vec{k})\rangle &= \frac{1}{2}\sum_\sigma \left\langle \Psi^\sigma \middle| \rho_p^+(\vec{k}) \middle| \Psi^\sigma \right\rangle \\ &= \frac{1}{2}\sum_\sigma \sum_{i=1}^{3} \int d^3\vec{p}\, d^3\vec{q} \left\langle \Psi^\sigma\left(\vec{p},\vec{q}\right) \left|\rho_{p,i}^+\right| \Psi^\sigma\left(\vec{p},\vec{q}\right)\right\rangle \delta^3\Big(\vec{p}_i - \vec{k}\Big) \ ,\end{aligned} \tag{4.7}$$

with

$$\rho_{p,i}^+ = \frac{(1+\tau_{3,i})}{2}\frac{(1+\sigma_{z,i})}{2} \ . \tag{4.8}$$

In Eq. (4.8), $\tau_{3,i}$ is the projection operator of the particle i on the third axis in the isospin space, likewise $\sigma_{z,i}$ is the spin projection operator for the same particle on the z-axis. $\vec{p}_i$ is the momentum of the particle i in the nucleus, by default $\vec{p}$ and $\vec{q}$ are understood as being $\vec{p}_1$ and $\vec{q}_1$. In Eq. (4.8) one can recognise the number density, in the sense of Ref. [33]. The other density operators which we may use are

$$\rho_{p,i}^- = \frac{(1+\tau_{3,i})}{2}\frac{(1-\sigma_{z,i})}{2} \ , \tag{4.9}$$

$$\rho_{n,i}^+ = \frac{(1-\tau_{3,i})}{2}\frac{(1+\sigma_{z,i})}{2} \ , \tag{4.10}$$

$$\rho_{n,i}^- = \frac{(1-\tau_{3,i})}{2}\frac{(1-\sigma_{z,i})}{2} \ . \tag{4.11}$$

Using the notation of section 2, and more specifically Eq. (2.4), we can rewrite Eq. (4.7) in a slightly different way, showing explicitly how the calculation is

performed with our three body wave function

$$\langle \rho_p^+(\vec{k})\rangle = \frac{1}{2}\sum_{\substack{\ell_1,N_1\\ \ell_{1'},N_{1'}}}\sum_{i,\sigma}\int d^3\vec{p}_1\, d^3\vec{q}_1 \langle \Omega^{JI}_{\ell_1 N_1}, \sigma(\hat{p}_1,\hat{q}_1)\big|\rho^+_{p,i}\big|\Omega^{JI}_{\ell_{1'}N_{1'}}, \sigma(\hat{p}_1,\hat{q}_1)\rangle \times \langle \mathcal{U}^{IJ}_{\ell_1 N_1}(p_1,q_1)\big|\mathcal{U}^{IJ}_{\ell_{1'}N_{1'}}(p_1,q_1)\rangle \delta^3\left(\vec{p}_i - \vec{k}\right) \quad . \quad (4.12)$$

Since this definition of the number density is averaged over the nuclear spin, it may be used to compute the spectral functions defined in Eqs. (4.3) to (4.6).

4.2 The case of ^{3}He

^{3}He is one of simplest nuclei, along with ^{3}H and deuterium. It consists of 2 protons and 1 neutron. If we compute the light-cone momentum distribution of the neutron, the remaining two protons can only be in a scattering state, since there is no bound state of two protons. On the other hand, if we compute the light-cone momentum distribution of the proton, the remaining two nucleons are a proton and a neutron, which can be in either a bound state, the deuteron, or a scattering state. We will therefore study first the simpler case of the neutron momentum distribution and then turn to the more difficult proton momentum distribution. In the following equations ρ_N will mean the following $\sum_{i,\pm}\rho^{\pm}_{N,i}$. Whenever we omit the index i it means that we implicitly sum over all three particles.

4.2.1 Neutron in ^{3}He

In this case, the remaining two-body system is made up of two protons in a scattering state. The scattering state is characterised by a specific energy distribution. The two scattering protons are on-shell and consequently the neutron is off-shell. As a result the neutron does not satisfy the on-mass-shell relation $E^2 = \vec{p}^2 + m^2$. Since we are using a non-relativistic wave function for ^{3}He we will use a non-relativistic approximation for the relation between the energy and the momentum. We then define the binding energy of the nucleus, E, by the relation $M = 3m + E$, where m is the mass of a nucleon. Since we are working with a non-relativistic wave function, we make use of the approximation $p^0 \approx m + \vec{p}^2/(2m)$. Since we are working in the frame of

the centre of mass of the nucleus we have the following

$$\begin{aligned} M &= p_\alpha^0 + p_\beta^0 + p_\gamma^0, \\ p_\alpha^0 &= M - p_\beta^0 - p_\gamma^0, \\ p_\alpha^0 &= m + E - \frac{\vec{p}_\beta^{\,2}}{2m} - \frac{\vec{p}_\gamma^{\,2}}{2m}, \\ p_\alpha^0 &= m + E - \frac{\vec{p}_\alpha^{\,2}}{2\mu} - \frac{\vec{q}_\alpha^{\,2}}{2\nu} \ , \end{aligned}$$

where ν is the reduced of the mass of the interacting pair and μ is their total mass[1]. If we compare this result with the expression given in Eq. (3.25), then the recoil energy Tr is $\vec{p}_\alpha^{\,2}/(2\mu)$, while the separation energy, ϵ, is $E - \vec{q}_\alpha^{\,2}/(2\nu)$. So the unpolarised spectral function for the neutron in ^{3}He is given by

$$\bar{S}^n(k) = \frac{1}{2}\sum_\sigma \sum_i \int d^3\vec{p}\, d^3\vec{q}\, \langle \Psi^\sigma(\vec{p},\vec{q})|\rho_{n,i}|\, \Psi^\sigma(\vec{p},\vec{q})\rangle \\ \times \delta^3\Big(\vec{k}-\vec{p}_i\Big)\, \delta\bigg(k^0 - \bigg(m + E - \frac{\vec{p}_i^{\,2}}{2\mu} - \frac{\vec{q}_i^{\,2}}{2\nu}\bigg)\bigg) \ . \quad (4.13)$$

We stress that Eqs. (3.23) and (3.24) are equivalent and should give the same results. In order to demonstrate this we computed the light-cone momentum distribution:

$$f_n(y) = \int d^4k \left(1 + \frac{k^3}{k^0}\right) \delta\left(y - \frac{k^0 + k^3}{m}\right) \bar{S}^n(k) \ , \quad (4.14)$$

with the two equations . To compute the light-cone momentum distribution with Eq. (3.23), the final state $|P_{A-1}S_{A-1}\rangle$ was taken to be a plane wave plus a pair of protons interacting in the $^1S_0$ channel. This is by far the most important channel for the final state interaction. We found that the light-cone momentum distributions computed with Eqs. (3.23) and (3.24) were identical, within numerical precision.

For the polarised case we have:

$$\Delta\bar{S}^n(k) = \frac{1}{2}\sum_\pm \sum_i \int d^3\vec{p}\, d^3\vec{q}\, \big\langle \Psi^\pm(\vec{p},\vec{q})\big|\big(\rho_{n,i}^\pm - \rho_{n,i}^\mp\big)\big|\, \Psi^\pm(\vec{p},\vec{q})\big\rangle \\ \times \delta\Big(\vec{k}-\vec{p}_i\Big)\, \delta\bigg(k^0 - \bigg(m + E - \frac{\vec{p}_i^{\,2}}{2\mu} - \frac{\vec{q}_i^{\,2}}{2\nu}\bigg)\bigg) \ . \quad (4.15)$$

This spectral function can then be used in Eq. (4.2) to compute the polarised light-cone momentum distribution.

[1]Note that here, in the case of two identical particles we have $\nu = m/2$ and $\mu = 2m$.

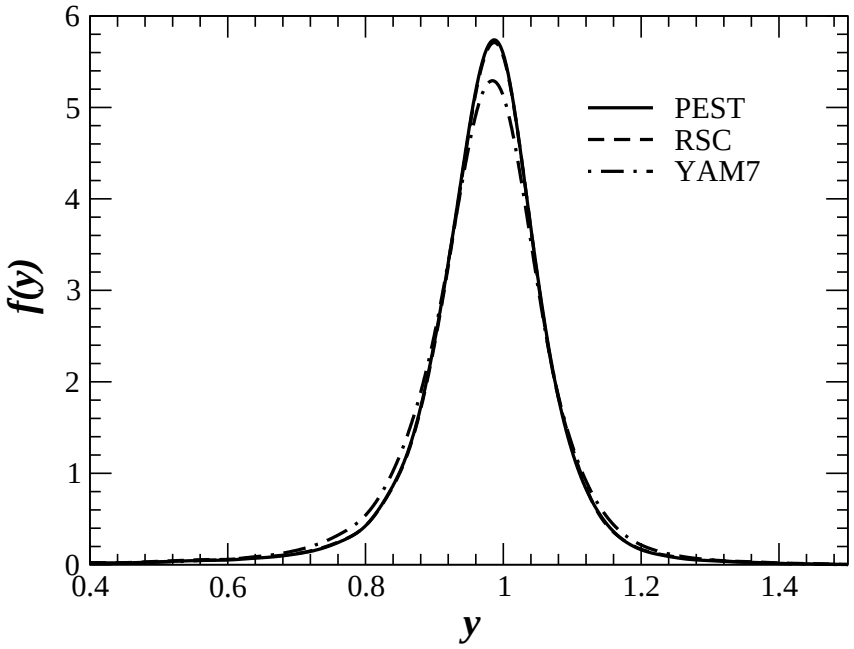

Figure 4.1: Neutron light-cone momentum distribution in ^{3}He for various potentials.

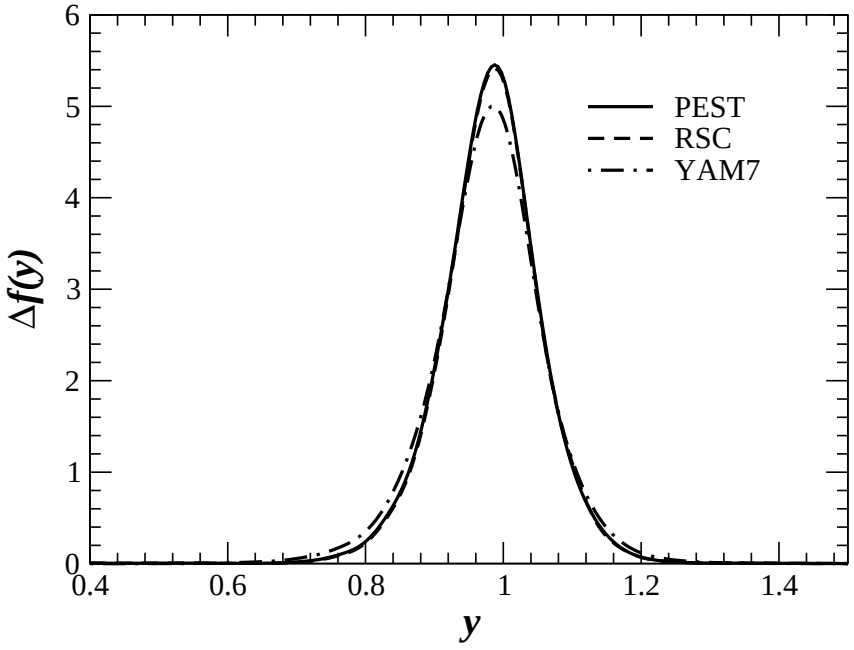

Figure 4.2: Neutron polarised light-cone momentum distribution in ^{3}He for various potentials.

4.2.2 Proton in ^{3}He

In the case of the proton we have two possibilities for the final state, so we also have two spectral functions to compute for each light-cone momentum distribution. The first state is a scattering state similar to the final state encountered in the neutron case, with which it shares the formula for p^0. The second possible final state is made of a scattered proton and a deuteron. We can find the form of the proton energy in the same way we did for the scattering state, only it is now much more simple as we have only two particles in the final state and not three. With the same non relativistic approximation as before, one easily finds that in this case: $p^0_\alpha = M - M_d - \vec{p}^{\,2}_\alpha/(2M_d)$, where M_d is the deuteron mass. Defining the binding energy of the deuteron, E_d, in same way we did for the tri-nucleon we have $M_d = 2m + E_d$ and finally, $p^0_\alpha = m + E - E_d - \vec{p}^{\,2}_\alpha/(2M_d)$.

Because there are two states, it is more practical to use the formulation of Eq. (3.23). To use Eq. (3.23), we have to separate the contributions to each final state by taking the projections of the tri-nucleon wave function over the two-body wave function of the corresponding final state. Here, we can separate the tri-nucleon wave function in two orthogonal parts, one in which the system is a proton plus a deuteron, and one in which the system is a proton plus a proton and a neutron in a scattering state. That is:

$$|\Psi^\pm\rangle = |\Psi^\pm_{p,(pn)}\rangle + |\Psi^\pm_{p,d}\rangle \ , \tag{4.16}$$

where we have:

$$|\Psi^\pm_{p,d}\rangle = \sum_{\sigma=-1}^{+1} |\Phi^\sigma_d\rangle\langle\Phi^\sigma_d|\Psi^\pm\rangle \ . \tag{4.17}$$

In Eq. (4.17), $|\Phi^\sigma_d\rangle$ is the wave function of the deuteron with spin projection σ on the z-axis. The deuteron has a spin equal to 1, so σ can run from -1 to $+1$. One can access $|\Psi^\pm_{p,(pn)}\rangle$ by subtracting $|\Psi^\pm_{p,d}\rangle$ from the total wave function. That is: $|\Psi^\pm_{p,(pn)}\rangle = |\Psi^\pm\rangle - |\Psi^\pm_{p,d}\rangle$. In momentum space Eq. (4:17) becomes:

$$|\Psi^\pm_{p,d}(\vec{p}_i,\vec{q}_i)\rangle = \sum_{\sigma=-1}^{+1} |\Phi^\sigma_d(\vec{q}_i)\rangle \int d^3\vec{p}\,'_1 d^3\vec{q}\,'_1 \langle\Phi^\sigma_d(\vec{q}\,'_i)|\Psi^\pm(\vec{p}\,'_1,\vec{q}\,'_1)\rangle \delta^3\big(\vec{p}_i - \vec{p}\,'_i\big) \ . \tag{4.18}$$

We can now write the two spectral functions for the unpolarised case:

$$\bar{S}^p_d(k) = \frac{1}{2}\sum_\pm \sum_i \int d^3\vec{p}_i\, d^3\vec{q}_i \left\langle \Psi^\pm_{p,d}(\vec{p}_i,\vec{q}_i)|\rho_{p,i}|\,\Psi^\pm_{p,d}(\vec{p}_i,\vec{q}_i)\right\rangle \times \delta^3\Big(\vec{k}-\vec{p}_i\Big)\,\delta\left(k^0 - \left(m+E-E_d-\frac{\vec{p}_i^{\,2}}{2M_d}\right)\right) \ , \tag{4.19}$$

$$\bar{S}_s^p(k) = \frac{1}{2}\sum_{\pm}\sum_i \int d^3\vec{p}_i\, d^3\vec{q}_i \left\langle \Psi^{\pm}_{p,(pn)}(\vec{p}_i,\vec{q}_i)\right| \rho_{p,i} \left|\Psi^{\pm}_{p,(pn)}(\vec{p}_i,\vec{q}_i)\right\rangle \times \delta^3\Big(\vec{k}-\vec{p}_i\Big)\,\delta\left(k^0-\left(m+E-\frac{\vec{p}_i^{\,2}}{2\mu}-\frac{\vec{q}_i^{\,2}}{2\nu}\right)\right) \quad . \quad (4.20)$$

In term of these spectral functions we can write the light-cone momentum distribution of the proton

$$f_p(y) = \frac{1}{2}\int d^4k \left(1+\frac{k^3}{k^0}\right)\delta\left(y-\frac{k^0+k^3}{m}\right)\left(\bar{S}_s^p(k)+\bar{S}_d^p(k)\right) \quad . \quad (4.21)$$

In the preceding equation we introduced factor one-half because there are two protons in a ^{3}He nucleus. This is the coefficient N_t, ensuring the normalisation of the light-cone momentum distribution, we introduced in Eqs. (3.35) to (3.37).

One can easily compute the various polarised spectral functions by substituting the appropriate combination of number densities in Eqs. (4.19) and (4.20). It is then possible to compute the corresponding polarised light-cone momentum distributions, following the procedure outlined in Eq. (4.21).

4.3 Results

Using the formalism presented above, we have computed light-cone momentum distributions for some of our three nucleon wave functions. For all those distributions we used only the first 42 three body channels. This is because the computation of the polarised distributions involves some complicated matrix elements. However, for all these wave functions the 42 first channels add up to more than 99% of the total normalisation, so one can safely assume that the contribution of the remaining channels is negligible. For the unpolarised distribution the matrix elements are quite simple, so one can easily check, in this case, that the contribution from higher channels is indeed small. We compared the light-cone momentum distribution for a proton and a neutron in ^{3}He for respectively 42 and 130 channels and found that for all purposes they were indistinguishable. For the PEST potential we also compared wave functions including 5 and 18 three-body channels and found that they were also indistinguishable.

In Figs. 4.1 and 4.2 we show the proton and neutron light-cone momentum distributions for our potentials (PEST, RSC and YAM7). The light-cone momentum distributions given by the RSC and PEST potentials are almost indistinguishable and they cannot be separated on these figures. The YAM7 potential, however, shows some differences, probably because this potential

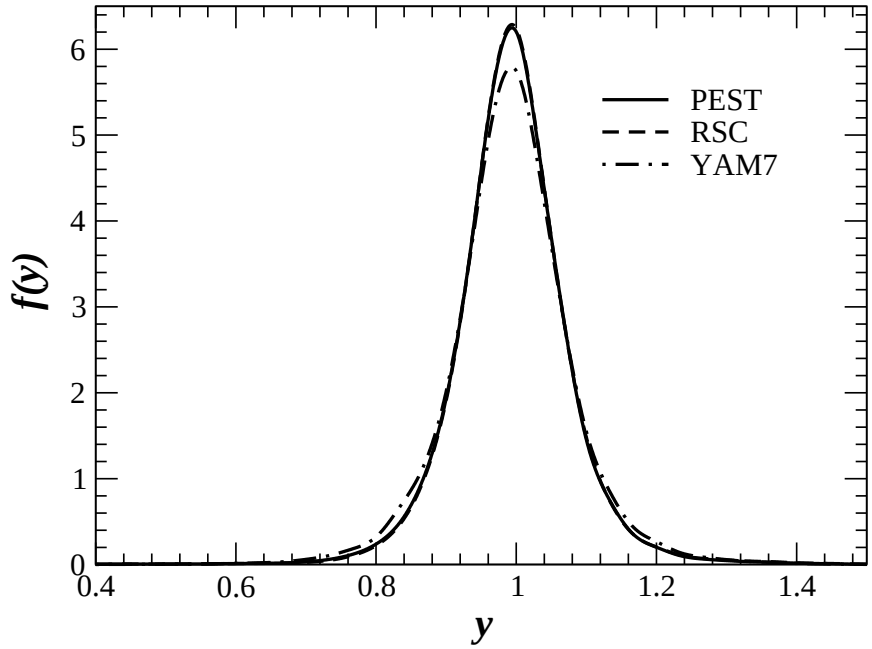

Figure 4.3: Proton light-cone momentum distribution in ^{3}He for various potentials.

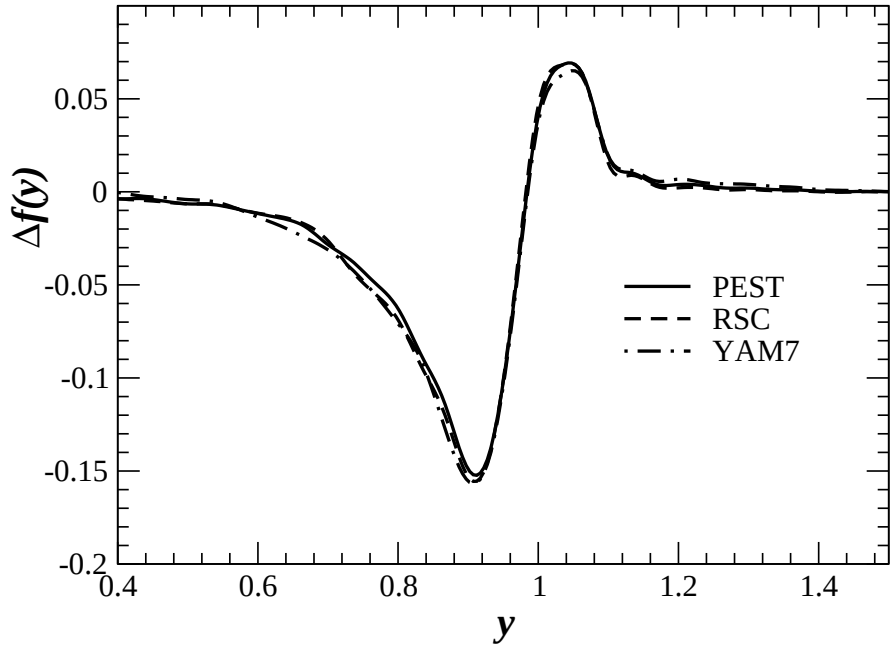

Figure 4.4: Proton polarised light-cone momentum distribution in ^{3}He for various potentials.

Table 4.1: Effective polarisation of the nucleons in ^{3}He for various potentials.

	$\sum P(X)$				$\int f(y)$			
	n^+	n^-	p^+	p^-	n^+	n^-	p^+	p^-
PEST	93.97%	6.03%	48.96%	51.04%	93.62%	6.32%	48.98%	50.96%
RSC	93.45%	6.55%	48.83%	51.17%	92.92%	6.79%	48.76%	50.95%
YAM7	93.66%	6.34%	48.81%	51.19%	93.25%	6.35%	48.69%	50.92%

Table 4.2: Effective polarisation of the nucleons in ^{3}He and ^{3}H, with two-body interaction adjusted to produce the experimental binding energies.

	$\sum P(X)$				$\int f(y)$			
	n^+	n^-	p^+	p^-	n^+	n^-	p^+	p^-
^{3}He	93.97%	6.03%	48.91%	51.09%	93.73%	6.24%	48.94%	51.02%
^{3}H	48.85%	51.15%	93.45%	6.55%	48.89%	51.10%	93.86%	6.13%

does not include short range repulsion. It is also important to note that to have consistent results one needs to use a deuteron wave function computed with the same potential as the three nucleon system. In Figs. 4.3 and 4.4 we show the proton and neutron polarised light-cone momentum distributions for the same potentials used in Figs. 4.1 and 4.2. The polarised neutron light-cone momentum distribution shows the same behaviour and is similar in size to its unpolarised counterpart. However, for the proton the polarised momentum distribution is far smaller than its unpolarised counterpart. In this case all the potentials give very similar results. We note that one can extract more information from the polarised momentum distributions. While in the unpolarised case the distributions are normalised to one, in the polarised case they are normalised to the polarisation of the given nucleon. From Ref. [33] one can compute these polarisations analytically in terms of the S, S' and D waves probabilities (neglecting the small contribution of the P waves). One can compute those probabilities from the wave function and then compare them with the values extracted from the momentum distributions. From Ref. [33] we have the following relations

$$n^+ = \int dy f_n^+(y) = 1-\frac{1}{3}\left(P(S')+2P(D)\right), \tag{4.22}$$

$$n^- = \int dy f_n^-(y) = \frac{1}{3}\left(P(S')+2P(D)\right), \tag{4.23}$$

$$p^+ = \int dy f_p^+(y) = \frac{1}{2}-\frac{1}{6}\left(P(D)-P(S')\right), \tag{4.24}$$

$$p^- = \int dy f_p^-(y) = \frac{1}{2}+\frac{1}{6}\left(P(D)-P(S')\right). \tag{4.25}$$

In Table 4.1 we compare the numerical values of these two expressions in ^{3}He, for our various potentials. The results are in quite good agreement, with the small discrepancies arising from numerical errors in the computation of many nested integrals. (Note, for example, that the overall normalisation is correct to about 0.06%.) In Table 4.2 we make the same comparison but with wave functions in which we have adjusted the binding energies to the experimental values.

Chapter 5

Unpolarised structure functions of the three nucleon system

5.1 Parton model

As we explained in chapter 3, in the unpolarised deep inelastic scattering of a charged lepton on a nuclear target, all the target information is included in the two structure functions F_1 and F_2. In our computations we will use a simple quark parton model (QPM) for the structure functions of the free nucleon. One can find a derivation of the QPM in various text books and lectures such as Refs. [19, 59, 60, 61]. We will not derive the QPM here, but we will recall its main assumptions and results regarding structure functions.

The relevant time scale involved in DIS is $\mathcal{O}(1/\sqrt{Q^2})$ and is far shorter than the time scale which characterises strong interactions. Therefore the virtual photon probes a frozen nucleon, where the partons (*i.e.* quarks and gluons) are quasi-free and do not interact. The last two assumptions constitute the impulse approximation on which the QPM is based.

Those assumptions are similar to the ones we have seen in Section 3.3.1, describing the PWIA, when we were studying the convolution formalism. The derivation of the formulae for the structure functions of the free nucleon have some similarity with the derivation of the convolution formalism. The hadronic tensor for the nucleon is a convolution of the probability of finding a given parton with the tensor for the parton. The main difference between the QPM and the convolution formalism, is that the quarks and gluons, like the leptons, are elementary particles and their tensor is easy to write down. In the end, if one neglects the transverse momentum of the quarks, we have:

$$F_1(x,Q^2) = \frac{1}{2}\sum_i e_i^2 q_i(x,Q^2), \tag{5.1}$$

$$F_2(x,Q^2) = 2xF_1(x,Q^2) = x\sum_i e_i^2 q_i(x,Q^2). \tag{5.2}$$

In the previous equations $q_i(x,Q^2)$ is usually interpreted as the number density of quarks of flavour i and fraction of the nucleon momentum x[1] at the momentum scale Q^2. e_i is the electric charge of the parton of flavour i. The first part of Eq. (5.2) is called the Callan-Gross relation [62]. This relation is valid for a simple parton model if one neglects the transverse momentum of the partons and if they have spin 1/2. A more general relation between F_1 and F_2 [17] is:

$$F_2(x,Q^2) = 2xF_1(x,Q^2)\frac{1+R}{1+2xm_N/\nu}, \tag{5.3}$$

[1]Here x is defined by $x = k^+/p^+$, where k is the four-momentum of the struck quark inside the nucleon of four-momentum p. In the QPM this quantity is equal to the Bjorken variable x, defined by Eq. (3.10).

where R is the ratio of the cross section for absorbing a longitudinal photon to that for a transverse photon. Given the relation between F_1 and F_2, most studies concentrate on the latter and we will do so as well using, Eq. (5.2) to compute F_2 in this study.

5.2 EMC effect

The convolution formula between the free and in medium structure functions [17, 25] are

$$\tilde{F}_1^N(x,Q^2) = \int_x^{\frac{M_A}{m}} dy \frac{f_N(y)}{y} F_1^N\left(\frac{x}{y},Q^2\right), \tag{5.4}$$

$$\tilde{F}_2^N(x,Q^2) = \int_x^{\frac{M_A}{m}} dy f_N(y) F_2^N\left(\frac{x}{y},Q^2\right). \tag{5.5}$$

Hence the F_2 structure function of a nucleus of mass number A and proton number Z is given by

$$F_2^{\rm A}(x,Q^2) = \int_x^{\frac{M_A}{m}} dy \left(Z f_p(y) F_2^p\left(\frac{x}{y},Q^2\right) + (A-Z) f_n(y) F_2^n\left(\frac{x}{y},Q^2\right)\right). \tag{5.6}$$

In comparing the F_2 structure functions on various targets, the European Muon Collaboration (Aubert et al. [42]) discovered what is now called the "EMC" effect. We define a theoretical EMC ratio as the ratio of the F_2 structure function of the nucleus to the sum of the free structure functions of the nucleons in this nucleus:

$$R_t = \frac{F_2^{\rm A}}{Z F_2^p + (A-Z) F_2^n}. \tag{5.7}$$

On the other hand, it is more common to compare the ratio of the F_2 structure function of the nucleus to that of deuterium:

$$R_x = \frac{F_2^{\rm A}/A}{F_2^{\rm D}/2}. \tag{5.8}$$

This should be close to R_t if the deuteron is a quasi-free system of a proton and a neutron and if the nucleus studied is symmetric, or almost, in its

content of neutrons and protons. ^{3}He and ^{3}H are highly asymmetric nuclei, as their content in one type of nucleon is twice as much as the other. To take this into account, it is common to add an isosymmetric correction so that the ratio studied is [25]:

$$R_A(x,Q^2) = \frac{F_2^{\rm A}(x,Q^2)}{F_2^{\rm D}(x,Q^2)} I(x,Q^2), \tag{5.9}$$

with:

$$I(x,Q^2) = \frac{F_2^p(x,Q^2)+F_2^n(x,Q^2)}{ZF_2^p(x,Q^2)+(A-Z)F_2^n(x,Q^2)}. \tag{5.10}$$

This ratio is, strictly speaking, the ratio of the EMC ratios of the nucleus A and the deuteron. Following the same kind of procedure used in the previous section, one can compute the light-cone momentum distribution of a nucleon in the deuteron. To be consistent, this ratio has to be computed with the same interaction for both the three nucleon system and the deuteron. To compute R_A we used several parametrisations for the quark distributions:

- The parametrisation "CTEQ5" from the CTEQ collaboration [37]. This collaboration gives several parametrisations, but we mainly used the one called "leading order", and it will be the one used when we talk about the CTEQ5 parametrisation, unless explicitly stated otherwise.

- The "GRV" parametrisation from Glück, Reya and Vogt [43].

- The "DOLA" parametrisation from Donnachie and Landshoff [44].

These distributions are usually given for quarks in a proton and in order to compute neutron structure functions we used charge symmetry[2] [45]. In Figs. 5.1 and 5.2 one can see the ratio R_3 for ^{3}He and ^{3}H, with the CTEQ5 parametrisation at $Q^2 = 10$ GeV^2, for the three potentials studied. In Fig. 5.3 we show R_3 in ^{3}He for the PEST potential alone but for all three quark distributions (again at $Q^2 = 10$ GeV^2). We also studied the effect of adjusting the binding energy as described at the end of the first section but did not include it in Figs. 5.1 and 5.2 because it would have confused the plot. This adjustment of the binding energy caused a slightly deeper EMC effect in both ^{3}He and ^{3}H and also a slightly steeper increase at high x.

[2]With the exception of the DOLA distribution which gives proton and deuteron distributions. In this case we took the neutron as the difference between the deuteron and the proton.

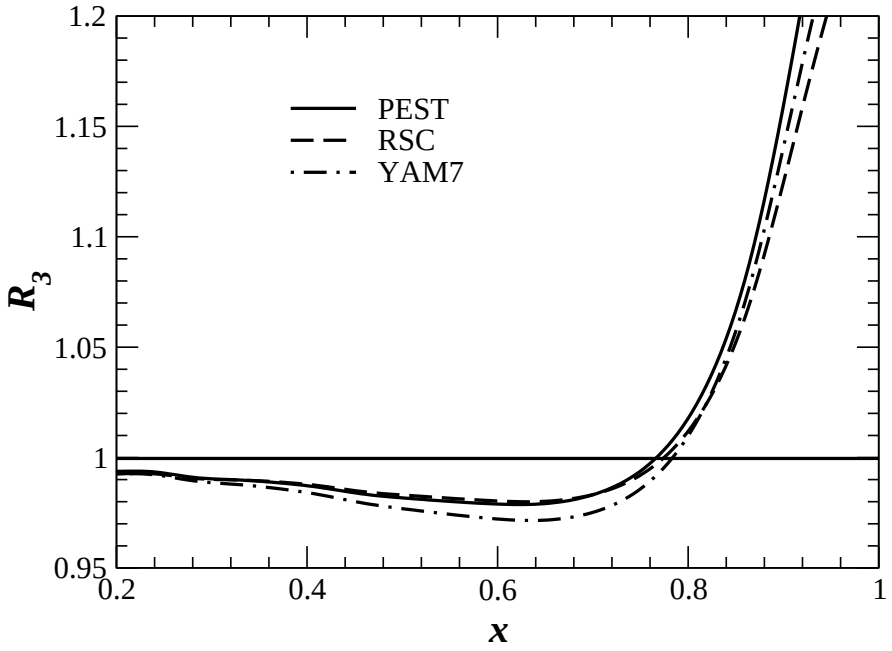

Figure 5.1: The ratio R_3, given in Eq.(5.9), for ^{3}He, at $Q^2 = 10$ GeV^2, calculated for various potentials using the CTEQ5 quark distributions.

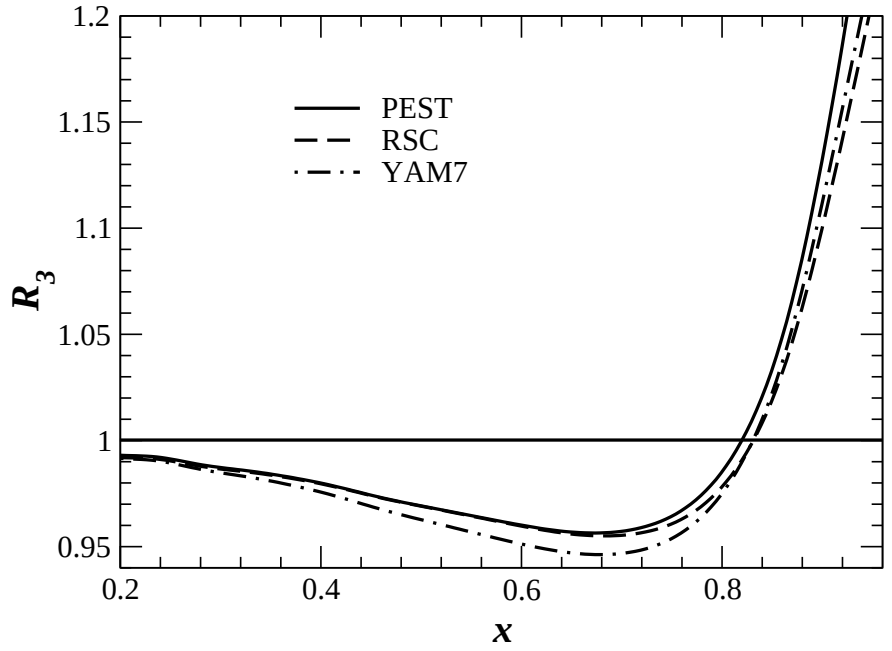

Figure 5.2: The ratio R_3, given in Eq.(5.9), for ^{3}H, at $Q^2 = 10$ GeV^2, calculated for various potentials using the CTEQ5 quark distributions.

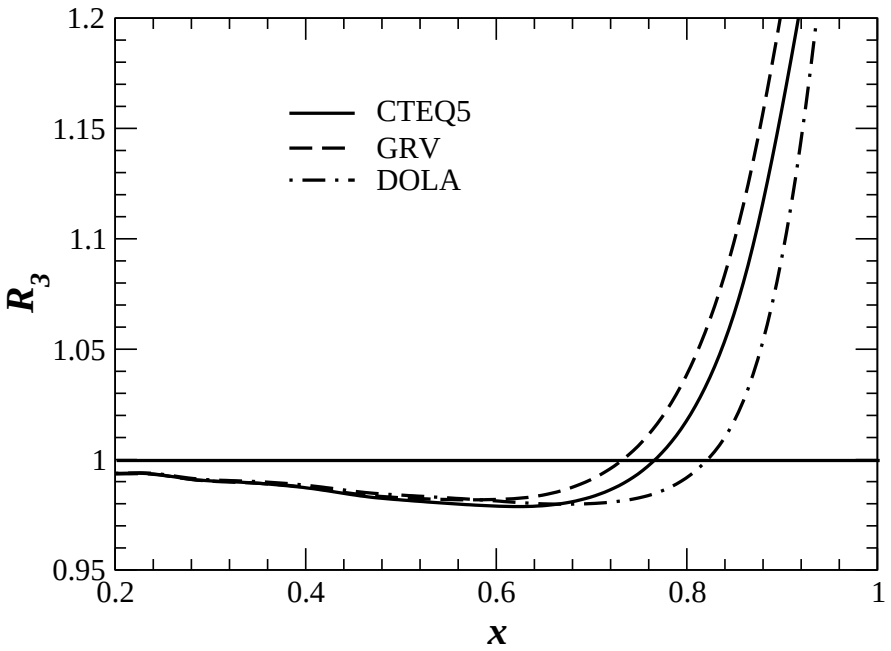

Figure 5.3: The ratio R_3, given in Eq.(5.9), for ^{3}He, at $Q^2 = 10$ GeV^2, calculated for the PEST potential, using various quark distributions for the nucleons.

5.3 Gottfried sum rule

Since we have computed the structure functions for both ^{3}He and ^{3}H we can investigate the Gottfried sum rule (GSR) in the tri-nucleon system. The GSR provides a way to probe the flavour asymmetry of the quark. For example, in a simple parton model where we assume charge symmetry, we have

$$\begin{aligned} F_2^p(x) - F_2^n(x) &= \frac{1}{3}x\left[u(x) - d(x)\right] + \frac{1}{3}x\left[\bar{u}(x) - \bar{d}(x)\right], \\ &= \frac{1}{3}x\left[u_v(x) - d_v(x)\right] + \frac{2}{3}x\left[\bar{u}(x) - \bar{d}(x)\right]. \end{aligned} \tag{5.11}$$

In Eq. (5.11), q_v is the valence distribution of the quark q and we have $q_v = q - \bar{q}$. This is why we have a factor 2 in front of the anti-quark distribution in the second line. The difference expressed in Eq. (5.11), divided by x and integrated, gives the Gottfried sum, I_G^N. For the nucleon it gives

$$I_G^N(z) = \int_z^1 dx \frac{F_2^p(x) - F_2^n(x)}{x}. \tag{5.12}$$

Using the normalisation of the valence quark distributions in the proton immediately leads to

$$I_G^N(0) = \frac{1}{3} + \frac{2}{3}\int_0^1 dx \left[\bar{u}(x) - \bar{d}(x)\right]. \tag{5.13}$$

This quantity provides a measure of flavour asymmetry. If the sea was flavour symmetric, *i.e.* $\bar{u}(x) = \bar{d}(x)$, the GSR would simply give $I_G^N(0) = 1/3$. However, the experimental value obtained by the NMC collaboration [38] was $I_G^N(0) = 0.235 \pm 0.026$ (at $Q^2 = 4$ GeV^2). This value is clearly less than $1/3$, and it implies that $\bar{d}(x)$ exceeds $\bar{u}(x)$ in the proton [38, 39]:

$$\int_0^1 dx \left[\bar{d}(x) - \bar{u}(x)\right] = 0.148 \pm 0.039. \tag{5.14}$$

The origin of the flavour asymmetry in the proton may be attributed to either the pion cloud required by chiral symmetry [34, 100] or to the Pauli exclusion principle at the quark level [35, 36, 100], or both. The existence of a pion cloud around the proton can generate pairs of $d\bar{d}$ quarks. For example, in the pion cloud picture the proton can undergo the following process: $p \to n + \pi^+$. The proton, on the left hand side, has the following quark content: (uud), while the neutron and pion on the right hand side have the following quark content: $(udd) + (u\bar{d})$. One can immediately see that a $d\bar{d}$ pair is generated in the process. The Pauli exclusion principle would also favour the creation of $d\bar{d}$ pair over $u\bar{u}$ in the proton, as the two u quarks are already filling more degrees of freedom than the single d quark.

Our point of interest here is to see how the GSR changes in a nucleus, and especially in the three nucleon system. The study of the flavour asymmetry of a bound nucleon may gives us insight into the non-perturbative structure of the nucleon in nuclear matter. We will now consider the "nuclear Gottfried sum" defined on a pair of mirror nuclei as

$$I_G^{\mathrm{A,A'}}(z) = \int_z^A dx \frac{F_2^{\mathrm{A}}(x) - F_2^{\mathrm{A'}}(x)}{x}, \tag{5.15}$$

where A and A' are mirror nuclei, A being proton rich (here ^{3}He) while A' is neutron rich (here ^{3}H). To compute the nuclear Gottfried sum we have used the wave function given by the PEST potential, adjusted to reproduce the binding energy of the corresponding nuclei. However, it turns out that

the difference of structure functions is not very sensitive to this change in the wave function, so we can expect the charge symmetry breaking to be very small in our study. We have used the CTEQ5 parametrisation for the free nucleon structure functions. This incorporates the measured flavour asymmetry in the free nucleon [37]. We restrict ourselves to $x \geqslant 0.1$ because the study of the small x region should include correction to take into account nuclear shadowing and physics neglected in the convolution formalism.

The effect of charge symmetry breaking is to break the nuclear Gottfried sum rule:

$$I_G^{\mathrm{A,A'}}(0) = Y \times I_G^N(0), \tag{5.16}$$

where Y is the excess proton (neutron) number in A (A') – in our case $Y = 1$. Eq. (5.16) should hold if the nuclear environment does not affect the flavour asymmetry. In Fig. 5.4 we show $F_2^{\mathrm{A}}(x) - F_2^{\mathrm{A'}}(x)$ for both the tri-nucleon system and the free nucleon. The curve that one gets using an isosymmetric wave function for the three nucleon system is identical. We can see in Fig. 5.4 that the difference between the free nucleon and three nucleon system case is very small. In the present calculation we find that for $Q^2 = 10$ GeV^2, we have $I_G^N(0.1) = 0.152$ whereas $I_G^{^3\mathrm{He},^3\mathrm{H}}(0.1) = 0.150$[3], so charge symmetry breaking in the $A = 3$ system gives very little change in the distribution $\bar{d}$–$\bar{u}$, at least for $x \geqslant 0.1$. As one can see in Fig. 5.5 there may be an increase in the difference between the free case and the three nucleon case at small x.

5.4 The neutron structure function F_2^n

One of the most interesting things about the tri-nucleon system is the fact that we can extract data on the free neutron. Either by experiments on ^{3}He alone, as we will see in the next chapter, or by combining results from experiments on both ^{3}He and ^{3}H, as we will see here. So far most parametrisations of the structure functions of the nucleon use data from proton and deuteron experiments and several assumptions, like, but not limited to, charge symmetry. The charge symmetry assumption seems to be valid in most cases, however the extraction of neutron data from deuteron experiments is at best problematic for values of x that are not small ($x \gtrsim 0.4$), see for example [63, 64, 65, 66]. We present here another way to access the structure func-

[3] If we use isosymmetric wave functions for ^{3}H and ^{3}He we have $I_G^{^3\mathrm{He},^3\mathrm{H}}(0.1) = 0.153$.

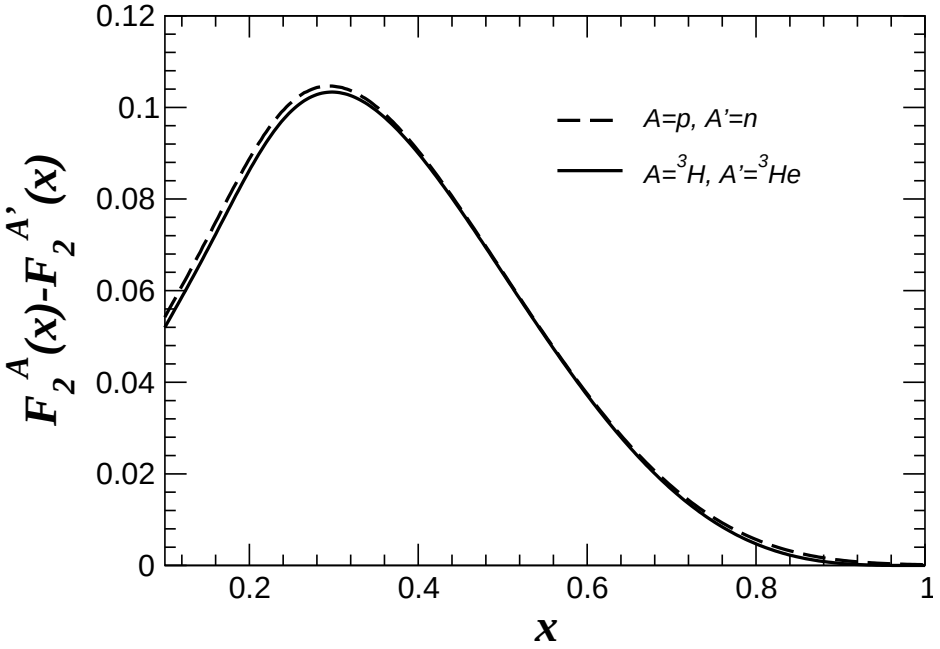

Figure 5.4: The difference $F_2^{\rm A}(x)$–$F_2^{\rm A'}(x)$ for both the tri-nucleon system and the free nucleon, at $Q^2 = 10$ GeV^2, using the CTEQ5 quark distributions.

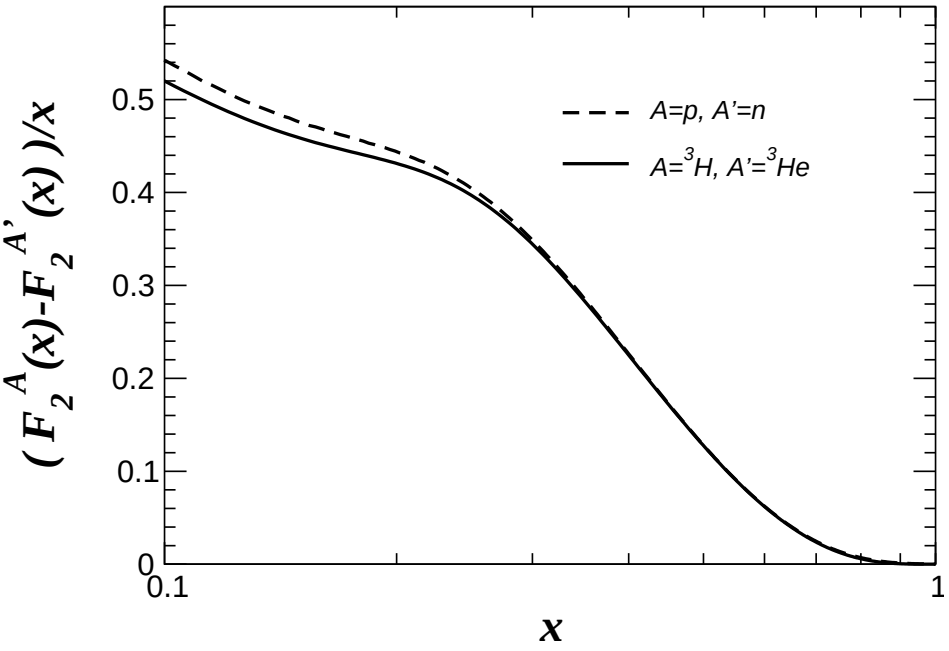

Figure 5.5: The difference $(F_2^{\rm A}(x)$–$F_2^{\rm A'}(x))/x$ for both the tri-nucleon system and the free nucleon, at $Q^2 = 10$ GeV^2, using the CTEQ5 quark distributions.

tion F_2^n of the neutron. From Eq. (5.7) we have:

$$R_t(^3\mathrm{He}) = \frac{F_2^{^3\mathrm{He}}}{2F_2^p+F_2^n}, \tag{5.17}$$

$$R_t(^3\mathrm{H}) = \frac{F_2^{^3\mathrm{H}}}{F_2^p+2F_2^n}. \tag{5.18}$$

Now we can form the ratio of EMC ratios:

$$\mathcal{R} = \frac{R_t(^3\mathrm{He})}{R_t(^3\mathrm{H})} = \frac{F_2^{^3\mathrm{He}}}{F_2^{^3\mathrm{H}}}\frac{F_2^p+2F_2^n}{2F_2^p+F_2^n}. \tag{5.19}$$

This expression can now be inverted to give us the ratio of the free neutron to proton structure functions as a function of $\mathcal{R}$:

$$\frac{F_2^n}{F_2^p} = \frac{2\mathcal{R}-F_2^{^3\mathrm{He}}/F_2^{^3\mathrm{H}}}{2F_2^{^3\mathrm{He}}/F_2^{^3\mathrm{H}}-\mathcal{R}}. \tag{5.20}$$

The ratio $F_2^{^3\mathrm{He}}/F_2^{^3\mathrm{H}}$ can be measured experimentally in the same way one measures the ratio R_x of Eq. (5.8). So the extracted ratio F_2^n/F_2^p depends, not on the size of the EMC effect in either ^{3}He or ^{3}H, but on the ratio of the EMC effects in ^{3}He and ^{3}H. If the neutron and proton distributions in tri-nucleon system are not dramatically different, one can expect $\mathcal{R} \approx 1$. Incidentally one can see that we have $\mathcal{R} = R_3(^3\mathrm{He})/R_3(^3\mathrm{H})$, so by studying Figs. 5.1 and 5.2 we can already see that indeed $\mathcal{R}$ is close to 1, within a few percent up to $x \approx 0.8$, the variation with x is quite rapid.

We computed $\mathcal{R}$ in our approach for various potentials for the light cone momentum distributions and various quark parametrisations for the structure functions. What we want to establish is that we can set $\mathcal{R}$ to "a central value" from which it deviates only a few percent, independent of the chosen model. The smaller the deviation the better the extraction of the ratio F_2^n/F_2^p.

Figs. 5.6 to 5.7 show the super-ratio, $\mathcal{R}$, for various potentials and quark distributions. In Fig. 5.6 we plot $\mathcal{R}$ computed using our three different kinds of potential and the CTEQ5 quark distribution at $Q^2 = 10$ GeV^2. As one can see on this figure, $\mathcal{R}$ seems to depend very little on the potential and is very close to unity. In Fig. 5.7 we investigate the effect on the isospin breaking in the three-nucleon wave function. The curve labelled PEST is identical to the one labelled PEST in Fig. 5.6 and corresponds to the use of an isospin symmetric wave function for ^{3}He and ^{3}H. The curve labelled PEST(E) corresponds to the use of binding energy adjusted wave functions for ^{3}He and ^{3}H, which are not isospin symmetric anymore. The effect observed here is

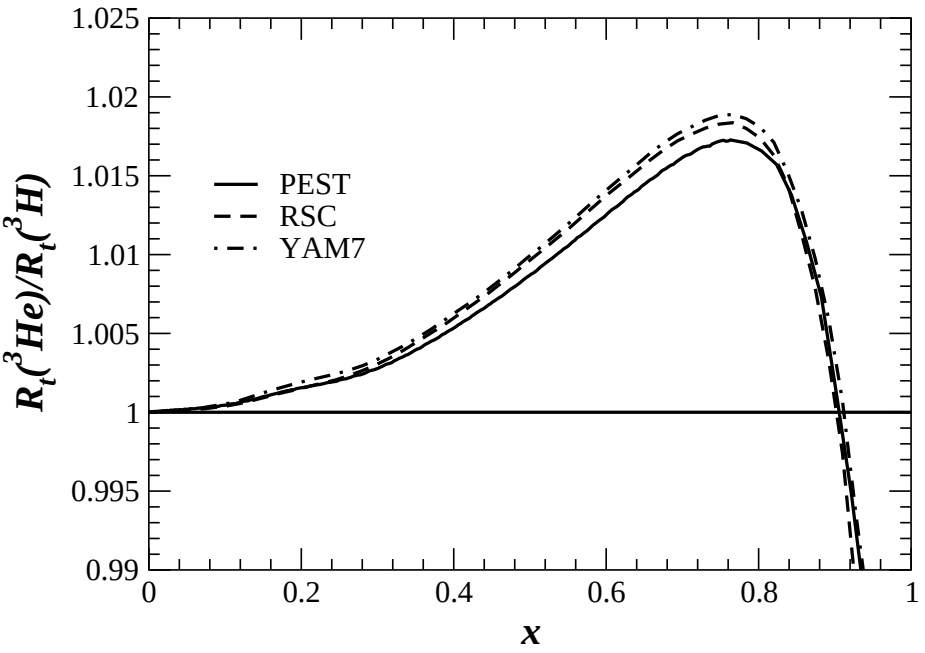

Figure 5.6: The ratio of ratios, Eq. (5.19), for various potentials, using the CTEQ5 parametrisation at $Q^2 = 10$ GeV^2.

much greater than those observed in Fig. 5.6. So the extraction of the ratio F_2^n/F_2^p may have some dependence on the model used for the wave functions of ^{3}He and ^{3}H.

In Fig. 5.8 we show $\mathcal{R}$ for various quark distributions using the PEST potential for the convolution formula. This figure is again at $Q^2 = 10$ GeV^2 except for the curve labelled BBS which is at $Q^2 = 4$ GeV^2. The solid curve is for CTEQ5 at leading order, the dash-dotted curve is the GRV parametrisation. There are two dashed curves for the DOLA parametrisation (labelled DL). The first one labelled DL(HT) includes a higher twist contribution to the structure function F_2, while none of the other parametrisations, including the one simply labelled DL, has it. This is why this curve behaves differently from the others. The curve labelled BBS uses the parametrisation of Ref. [76]. Most fits of parton distributions assume that the ratio $d/u \to 0$ as $x \to 1$, however that assumption can be questioned on theoretical and phenomenological grounds [77]. The BBS parametrisation incorporates constraints from perturbative QCD and forces the ratio $d/u \to 0.2$ as $x \to 1$.

As one can see, the dependence on the parton distributions is rather weak at low x but becomes large at high x. However this dependence is actually artificial and reflects the lack of knowledge of the neutron structure function

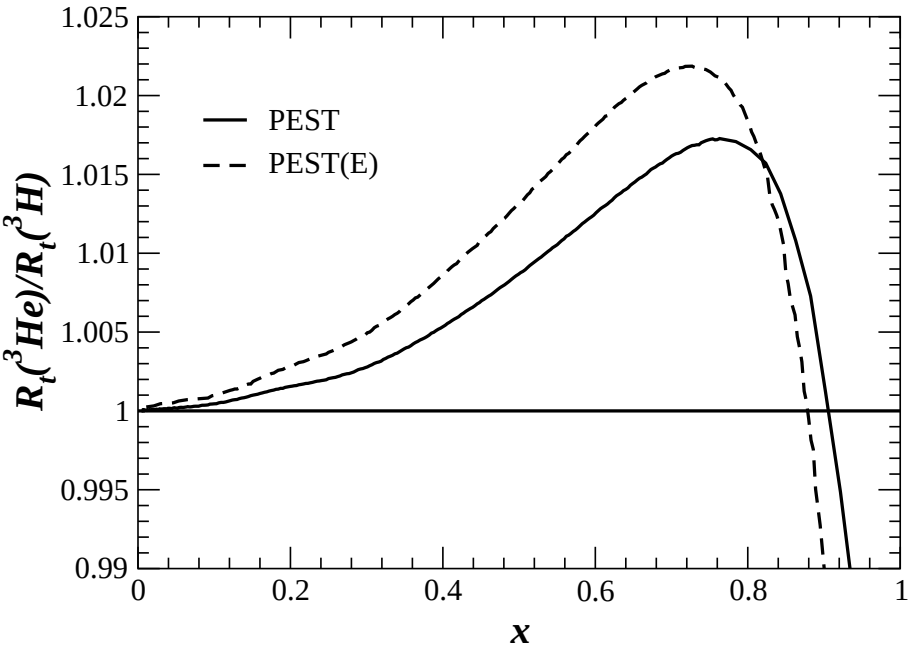

Figure 5.7: The ratio of ratios, Eq. (5.19), using the CTEQ5 quark parametrisation at $Q^2 = 10$ GeV^2, for isospin symmetric and non isospin symmetric three-nucleon wave functions.

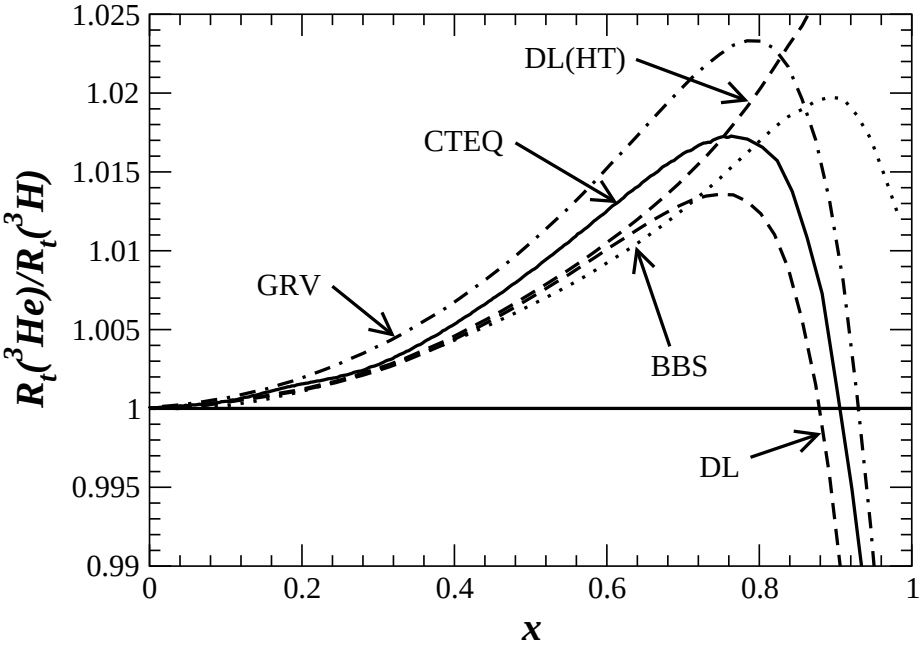

Figure 5.8: The ratio of ratios, Eq. (5.19), for various quark distributions, using the PEST potential.

F_2^n. In practice, once the ratio $F_2^{^3\mathrm{He}}/F_2^{^3\mathrm{H}}$ is measured one can use an iterative procedure to eliminate this dependence altogether. After extracting F_2^n/F_2^p for some $\mathcal{R}$ one can use the resulting F_2^n to compute a new $\mathcal{R}$ and extract a new F_2^n. This procedure is iterated until convergence is achieved and a self-consistent solution for F_2^n/F_2^p and $\mathcal{R}$ is obtained.

So from this study it appears that main dependence in the extracted ratio F_2^n/F_2^p may come from the model used for the tri-nucleon wave function. But even this dependence as shown in Fig. 5.7 is not very strong and the ratio $\mathcal{R}$ still deviates only by approximately 2% from unity. This shows that the measurement of the ratio $F_2^{^3\mathrm{He}}/F_2^{^3\mathrm{H}}$ would enable us to have an accurate estimate of the neutron structure function F_2.

Chapter 6

Polarised structure functions of the three nucleon system

6.1 Parton model

If one does experiments with both a polarised lepton beam and a polarised spin $\frac{1}{2}$ nuclear target, one needs two more structure functions, g_1 and g_2, to completely describe the target. As we have mentioned in Section 3.2.2 it is possible to isolate the contribution of the polarised structure functions by using combinations of cross sections measured with different polarisations of the target and the beam. If we use the same QPM as in the previous chapter and neglect again the transverse momentum of the quarks one finds that [18, 19, 46, 47]:

$$g_1(x, Q^2) = \frac{1}{2} \sum_i e_i^2 \Delta q_i(x, Q^2), \tag{6.1}$$

$$g_2(x, Q^2) = 0. \tag{6.2}$$

In Eq. (6.1), x, Q^2 and e_i are the same as in Eqs. (5.1) and (5.2). The meaning of Δq_i is less trivial, we have [18, 19]:

$$q_i(x, Q^2) = q_i^+(x, Q^2) + q_i^-(x, Q^2), \tag{6.3}$$

$$\Delta q_i(x, Q^2) = q_i^+(x, Q^2) - q_i^-(x, Q^2), \tag{6.4}$$

where q_i^+ is the probability of finding a quark of flavour i with the same helicity as the nucleon and q_i^- is the probability of finding a quark of flavour i with opposite helicity compared to the nucleon. So the probability of finding a quark of flavour i, which we used in Eqs. (5.1) and (5.2), is just the sum of q_i^+ and q_i^-. On the other hand, in g_1 we need the difference of those probabilities. Eq. (6.2) shows that, at leading order in the QPM, $g_2 = 0$. In fact, g_2 does not have a simple, consistent parton model interpretation [18, 69], but from the previous facts, we can say it is small.

The polarised structure functions are smaller than their unpolarised counterparts, g_2 in particular, as we have just seen, is very small and very difficult to measure (see for example Refs. [67, 68] for such measurements). In practice, in most experiments measuring g_1, the contribution of g_2 is suppressed by a factor x^2/Q^2 [18] and so it is neglected. We will not study g_2 at all. As we have already seen in Section 4.3 and Tables 4.1 and 4.2, the figures for the polarisation of the various nucleons in the tri-nucleon system indicate that the contribution from the doubly represented nucleon will be considerably suppressed. Therefore the system should be a good approximation to a pure target of the singlet nucleon.

The following computation will be made with a next to leading order (NLO) parametrisation of the parton distribution and a NLO formula for g_1,

as found in Refs. [48, 70]. We will use hereafter the standard NLO scenario of the parton distribution given in [70] (GSRV00 hereafter). In Ref. [71] we made those computations with the previous version of this parametrisation (GSRV96 [48] hereafter) and the conclusions were similar.

6.2 Off-shell corrections

As we have mentioned at the end of Section 3.3.1, in the convolution formula (6.5) we should not use the free nucleon structure functions as the parametrisations we have of them are for on-shell nucleons, while in our present formalism the struck nucleons are off-shell. Because of our lack of knowledge on the off-shell structure functions, we have so far used on-shell structure functions for off-shell ones. Here we will also study the impact of the off-shell corrections for g_1, calculated within the QMC model [50] in Ref. [49]. This off-shell correction was calculated using a local density approximation to estimate the change of the parton distributions in a bound nucleon. This off-shell correction has only been given for polarised parton distributions, which is why we did not study the impact of this model on unpolarised structure functions earlier.

In this model we have the following relation between the polarised quark distribution in a free nucleon and in a nucleon in ^{3}He:

$$\frac{\delta\tilde{q}_v(x)}{\delta q_v(x)} = \frac{1}{a_q x^{b_q} + c_q x^{d_q}(1-x)^{e_q}}\,, \tag{6.5}$$

where $\delta\tilde{q}_v$ is the quark distribution in a nucleon in ^{3}He and the parameters are the following:

$$\begin{array}{rcrcr} a_u = & 118.41 & , & a_d = & 8.964, \\ b_u = & 18.97 & , & b_d = & 7.5848, \\ c_u = & 1.0758 & , & c_d = & 1.0515, \\ d_u = & 0 & , & d_d = & -0.0048, \\ e_u = & 0.0335 & , & e_d = & 0.01086. \end{array} \tag{6.6}$$

Notice that in Eq. (6.5) the relation is between valence quark distributions and that we do not have any corrections for quarks from the sea. So, this correction is most useful for the the region of x dominated by valence quarks, namely for $0.2 \leq x \leq 0.8$. (The upper limit is determined by uncertainties in the structure functions calculated for the MIT bag, which underlies the QMC model.) However, since we will be using NLO formula in the $\overline{\rm MS}$ scheme for the parton distribution [48, 70] for g_1, a correction applied on a limited range

of x for the quark distribution will have an impact on all x for g_1. This is not true for a leading order calculation in any scheme, but we should note that the use of this correction is scheme dependent in NLO. While those corrections have been initially computed for ^{3}He we will apply them to the case of ^{3}H as well.

6.3 Non-nucleonic degrees of freedom

The convolution formula we will use to produce ^{3}He and ^{3}H polarised structure functions are the following:

$$g_1^{^3\mathrm{He}}(x,Q^2) = \int_x^{\frac{M_A}{m}} \frac{dy}{y}\left(\Delta f_n(y)\tilde{g}_1^n\left(\frac{x}{y},Q^2\right)+2\Delta f_p(y)\tilde{g}_1^p\left(\frac{x}{y},Q^2\right)\right), \quad (6.7)$$

$$g_1^{^3\mathrm{H}}(x,Q^2) = \int_x^{\frac{M_A}{m}} \frac{dy}{y}\left(\Delta f_n(y)\tilde{g}_1^p\left(\frac{x}{y},Q^2\right)+2\Delta f_p(y)\tilde{g}_1^n\left(\frac{x}{y},Q^2\right)\right), \quad (6.8)$$

where it is assumed that the polarised light-cone momentum distribution of the proton (neutron) in ^{3}H is equal to the light-cone momentum distribution of the neutron (proton) in ^{3}He, thanks to isospin symmetry. In these equations $\tilde{g}_1$ stands for the off-shell structure function of the corresponding nucleon in medium.

As has been already mentioned in section 3.3.1, a nucleus is more than just a collection of protons and neutrons and can contain other particles which should also be taken into account in the convolution formalism. We have here a perfect example of such a thing with the tri-nucleon system [72]. The Bjorken sum rule [73] relates the difference of the first moments of the proton and neutron polarised structure function g_1, to the axial vector coupling constant of the neutron β-decay g_A, with $g_A = 1.2670 \pm 0.0035$ [74]:

$$\int_0^1 \left(g_1^p(x,Q^2)-g_1^n(x,Q^2)\right)dx = \frac{1}{6}g_A\left(1+\mathcal{O}\left(\frac{\alpha_s}{\pi}\right)\right). \quad (6.9)$$

In the previous equation $\mathcal{O}(\alpha_s/\pi)$ represents a standard QCD radiative correction. This sum rule can be generalised to the ^{3}He-^{3}H system:

$$\int_0^{\frac{M_A}{m}} \left(g_1^{^3\mathrm{H}}(x,Q^2)-g_1^{^3\mathrm{He}}(x,Q^2)\right)dx = \frac{1}{6}g_A(^3\mathrm{H})\left(1+\mathcal{O}\left(\frac{\alpha_s}{\pi}\right)\right), \quad (6.10)$$

where $g_A(^3\mathrm{H}) = 1.211 \pm 0.002$ [75] is the axial vector coupling constant measured in ^{3}H β-decay. Taking the ratio of the two previous equations one gets:

$$\frac{\int_0^{\frac{M_A}{m}} \left(g_1^{^3\mathrm{H}}(x,Q^2) - g_1^{^3\mathrm{He}}(x,Q^2) \right) dx}{\int_0^1 (g_1^p(x,Q^2) - g_1^n(x,Q^2))\, dx} = \frac{g_A(^3\mathrm{H})}{g_A} = 0.956 \pm 0.004 \ . \tag{6.11}$$

Note that the QCD corrections to both Eqs. (6.9) and (6.10) cancels exactly. We can now compare the experimental value of Eq. (6.11) with the prediction we get using the convolution formalism and Eqs. (6.7) and (6.8). Using the following property of the convolution formalism:

$$\int_0^A dx \int_x^A \frac{dy}{y} C(y) f\left(\frac{x}{y}\right) = \int_0^A dy C(y) \int_0^1 dx f(x) \ , \tag{6.12}$$

and remembering Eqs. (4.15) to (4.18), we define $P_n = n^+ - n^- = \int dy \Delta f_n(y)$ and $P_p = p^+ - p^- = \int dy \Delta f_p(y)$, which are the effective polarisations of the neutron and proton (proton and neutron) in ^{3}He (^{3}H). We also define the first moment of the polarised structure function g_1 by $\Gamma_\mathrm{N} = \int dx g_1^\mathrm{N}(x,Q^2)$. Then, using the value for the PEST potential in table 4.1, we can rewrite the left hand side of Eq. (6.11) as:

$$\frac{\int_0^{\frac{M_A}{m}} \left(g_1^{^3\mathrm{H}}(x,Q^2) - g_1^{^3\mathrm{He}}(x,Q^2) \right) dx}{\int_0^1 (g_1^p(x,Q^2) - g_1^n(x,Q^2))\, dx} = (P_n - 2P_p)\frac{\tilde{\Gamma}_p - \tilde{\Gamma}_n}{\Gamma_p - \Gamma_n} = 0.921 \frac{\tilde{\Gamma}_p - \tilde{\Gamma}_n}{\Gamma_p - \Gamma_n} \ . \tag{6.13}$$

Since off-shell corrections [49] slightly decrease the value of the structure function g_1 we have $(\tilde{\Gamma}_p - \tilde{\Gamma}_n)/(\Gamma_p - \Gamma_n) < 1$, and thus this theoretical prediction underestimates the result of Eq. (6.11). Note that if we do not include off-shell corrections, the right hand side of Eq. (6.13) becomes $P_n - 2P_p = 0.921$ which also underestimates the ratio of Bjorken sum rules. This simple computation demonstrates the needs for new nuclear effects that are not included in the convolution formula (6.7) and (6.8).

Our theoretical result from Eq. (6.13) underestimates the experimental result from Eq. (6.11) by about 3.5%. An effect has been proposed that can make up for this discrepancy [72]. The direct correspondence between the calculations of the Gamow-Teller matrix element in the triton β-decay

and the Feynman diagrams of DIS on ^{3}He and ^{3}H suggests that two-body exchange currents should play an equal role in both processes. Of particular interest is the fact that analyses [78] have shown that the two-body exchange currents involving a $\Delta(1232)$ isobar increase the theoretical prediction for the axial vector coupling of the triton ($g_A(^3\mathrm{H})$) by about 4%, making it consistent with the experimental value. In the same way, this process should increase the value of the Bjorken sum rule in the tri-nucleon system, making the theoretical value of Eq. (6.13) consistent with the experimental value given in Eq. (6.11).

The $\Delta(1232)$ isobar contributes to $g_1^{^3\mathrm{He}}$ and $g_1^{^3\mathrm{H}}$ through Feynman diagrams involving the non diagonal transitions: $n \to \Delta^0$ and $p \to \Delta^+$. This requires the introduction of new polarised structure functions, $g_1^{n\to\Delta^0}$ and $g_1^{p\to\Delta^+}$, as well as the corresponding light-cone momentum distributions, $\Delta f_{n\to\Delta^0}$ and $\Delta f_{p\to\Delta^+}$. If we suppose that these light-cone momentum distributions are peaked enough around y equal one, then we can replace them by the effective polarisations[1] $P_{n\to\Delta^0}$ and $P_{p\to\Delta^+}$ times the delta function $\delta(1-y)$. With this addition Eqs. (6.7) and (6.8) become:

$$\begin{aligned} g_1^{^3\mathrm{He}}(x,Q^2) &= \int_x^{\frac{M_A}{m}} \frac{dy}{y}\left(\Delta f_n(y)\tilde{g}_1^n\left(\frac{x}{y},Q^2\right)+2\Delta f_p(y)\tilde{g}_1^p\left(\frac{x}{y},Q^2\right)\right) \\ &\quad +2P_{n\to\Delta^0}g_1^{n\to\Delta^0}+4P_{p\to\Delta^+}g_1^{p\to\Delta^+}\ , \qquad (6.14) \\ g_1^{^3\mathrm{H}}(x,Q^2) &= \int_x^{\frac{M_A}{m}} \frac{dy}{y}\left(\Delta f_n(y)\tilde{g}_1^p\left(\frac{x}{y},Q^2\right)+2\Delta f_p(y)\tilde{g}_1^n\left(\frac{x}{y},Q^2\right)\right) \\ &\quad -2P_{n\to\Delta^0}g_1^{p\to\Delta^+}-4P_{p\to\Delta^+}g_1^{n\to\Delta^0}\ . \qquad (6.15) \end{aligned}$$

The minus sign in front of the contribution from the Δ in the formula for $g_1^{^3\mathrm{H}}$ comes from the convention that $P_{n\to\Delta^0} \equiv P_{n\to\Delta^0/^3\mathrm{He}} = -P_{p\to\Delta^+/^3\mathrm{H}}$ and $P_{p\to\Delta^+} \equiv P_{p\to\Delta^+/^3\mathrm{He}} = -P_{n\to\Delta^0/^3\mathrm{H}}$.

In the quark parton model, the interference structure functions $g_1^{n\to\Delta^0}$ and $g_1^{p\to\Delta^+}$ can be related to the usual structure functions g_1^p and g_1^n thanks to the general form of the $SU(6)$ nucleon wave function [79]:

$$g_1^{n\to\Delta^0} = g_1^{p\to\Delta^+} = \frac{2\sqrt{2}}{5}\left(g_1^p - 4g_1^n\right)\ . \qquad (6.16)$$

This relation is valid in the domain of x and Q^2 where the contributions from sea quarks and gluons to g_1 can be omitted, that is for $0.2 \le x \le 0.8$ and

[1] Those effective polarisations are defined as the integral over x of the corresponding light-cone momentum distributions.

$0.5 \leq Q^2 \leq 5$ GeV^2 in the case of the parametrisation GSRV00. However, as shown in Ref. [81], this expression can be extended to all x, as it provides a satisfactory value for the following sum rule $\int (g_1^{n\to\Delta^0}(x)+g_1^{p\to\Delta^+}(x))dx$, when the integral is performed over all x.

Effective polarisations $P_{n\to\Delta^0}$ and $P_{p\to\Delta^+}$, as well as the corresponding light-cone momentum distributions, could be computed with the help of a tri-nucleon wave function including the Δ resonance. This would require the computation of new wave functions and would involve computational methods beyond the scope of the present study. Instead, we will fix the effective polarisation by requiring that the ratio of Bjorken sum rules is consistent with the experimental result. This leads to the following condition:

$$-2(P_{n\to\Delta^0}+2P_{p\to\Delta^+})\frac{\int dx\left(g_1^{n\to\Delta^0}(x)+g_1^{p\to\Delta^+}(x)\right)}{\Gamma_p-\Gamma_n} = 0.956-0.921\frac{\tilde{\Gamma}_p-\tilde{\Gamma}_n}{\Gamma_p-\Gamma_n}\ . \tag{6.17}$$

Then using Eq. (6.16) to link the interference structure functions to the off-shell neutron and proton polarised structure functions g_1 we have:

$$2(P_{n\to\Delta^0}+2P_{p\to\Delta^+}) = \frac{0.814(\tilde{\Gamma}_p-\tilde{\Gamma}_n)-0.845(\Gamma_p-\Gamma_n)}{\tilde{\Gamma}_p-4\tilde{\Gamma}_n} = -0.024\ . \tag{6.18}$$

The numerical value in Eq. (6.18) has been computed at 4 GeV^2 with the standard NLO parametrisation of GSRV00 for the quark distributions. This correction has also been computed with the PEST potential and other potentials could yield slightly different results.

6.4 The neutron in ^{3}He

Computing $g_1^{^3\mathrm{He}}$ using Eq. (6.7) and our three usual potentials, we found that the results are sufficiently close that we can limit ourselves to the PEST potential in the following. We will compute the polarised structure function g_1 of ^{3}He for three cases:

- Simple convolution using Eq. (6.7) but without off-shell corrections.
- Convolution including off-shell corrections as per Eq. (6.7).
- Same as above plus corrections from the inclusion of the Δ resonance as per Eq. (6.14) and using the results of Eqs. (6.16) and (6.18).

In Fig. 6.1 we show four curves at $Q^2 = 4$ GeV^2: $xg_1(x)$ for the free neutron and $xg_1(x)$ for ^{3}He for each one of our three cases. As one can see, the four

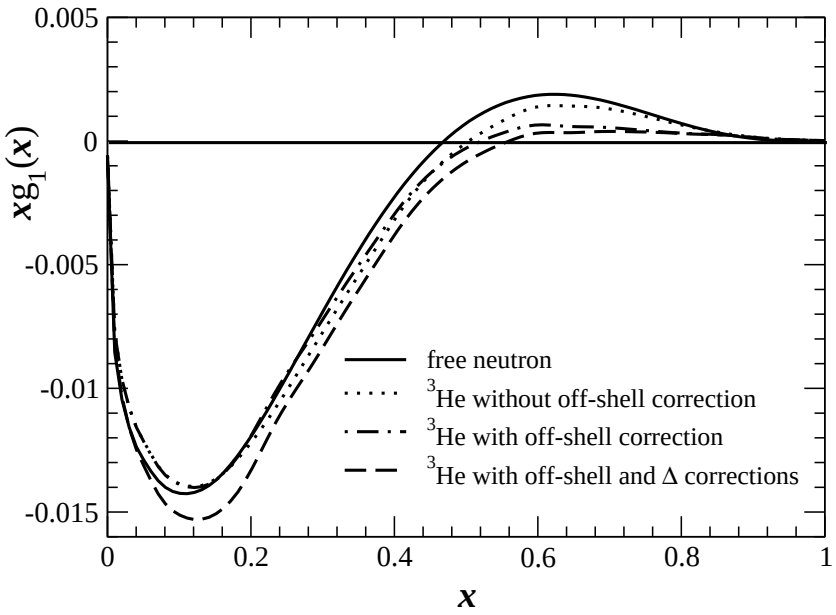

Figure 6.1: Comparison of several calculations of $xg_1(x)$ for ^{3}He and the free neutron at $Q^2 = 4$ GeV^2.

curves are quite close. There are two main sources of complications when one tries to extract g_1^n from ^{3}He. As one can see from Fig. 6.1, the contribution of the Δ resonance can be important for values of x less or equal to 0.2. Another complication is the contribution of the proton. The free proton spin structure function is very big compared with that of the neutron, so while the proton contribution in ^{3}He is severely reduced by the low effective polarisation, it may not be negligible. One way to estimate the size of the contribution of the proton is to compare $g_1^{^3\mathrm{He}}$ with a formula often used in experimental analysis[2]:

$$g_1^{^3\mathrm{He}} \approx \Delta_n g_1^n + 2\Delta_p g_1^p. \tag{6.19}$$

If the contribution of the proton to $g_1^{^3\mathrm{He}}$ is negligible, Eq. (6.19) is equivalent to: $g_1^{^3\mathrm{He}} \approx \Delta_n g_1^n$. To estimate the effect of the proton contribution in the extraction of g_1^n, we plotted the following differences:

$$\Delta_g = \frac{g_1^{^3\mathrm{He}} - 2\Delta_p g_1^p}{\Delta_n} - g_1^n, \tag{6.20}$$

[2]There are several ways to find this result. One would be to use the same argument we already used for the Δ isobar in the previous section. See Ref. [19] for another derivation.

and

$$\Delta_g^{'} = \frac{g_1^{^3\mathrm{He}}}{\Delta_n} - g_1^n. \tag{6.21}$$

In Figs. 6.2 and 6.3 we plot Δ_g, $\Delta_g^{'}$ and g_1^n. We have plotted g_1^n as one ultimately wants to extract it and one needs to have an idea of the relative size of the error. In Fig. 6.2 the dotted curve is g_1^n, the dash-dotted curve is $\Delta_g^{'}$, where $g_1^{^3\mathrm{He}}$ has been computed with Eq. (6:7), including the off-shell effects of Ref. [49], the dashed curve is Δ_g, where $g_1^{^3\mathrm{He}}$ is the same as for the dash-dotted curve, finally the solid curve is Δ_g where $g_1^{^3\mathrm{He}}$ as been computed as per Eq. (6.14), that is, with both off-shell effects and the Δ isobar. In Fig. 6.3 we plotted the same curves as in Fig. 6.2 (except the solid curve), without including the off-shell effects of Ref. [49] in the computation of $g_1^{^3\mathrm{He}}$. These computations have been done at $Q^2 = 4$ GeV^2. We do not plot the ratio of structure functions because in both the neutron and ^{3}He cases g_1 can be zero, leading to singularities in the plots.

If we do not include off-shell effects, it is clear from Fig. 6.4, that one gets more accurate results for most values of x, by taking into account the contribution of the protons. In Fig. 6.2, one can see that once we turn on the off-shell effects of Ref. [49], one gets more accurate results on $0.5 \leq x \leq 0.8$ by including the contribution of the protons. However on $0.2 \leq x \leq 0.5$ both computations give similar errors. Surprisingly, when we include the contribution of the Δ isobar, Eq. (6.19) is very accurate for $x \geq 0.2$. In this case the inclusion of the protons contribution is essential as without it, we get a far greater error than with any other computations. In all cases, the relative error is at its biggest, for $0.2 \leq x \leq 0.8$, around the point where g_1^n cross the x-axis.

For values of x below 0.2, all computations give big absolute differences and one clearly needs some other tools to accurately extract the free neutron structure function, even if the relative difference seems to be small. For values of x over 0.8, the differences are all very small, but so is the structure function g_1^n. For those values of x, Fermi motion effects are significant, but this cannot be shown on a difference plot. Fermi motion effects will be more apparent for ^{3}H, in the next section. We find similar curves for other parton distributions, such as those from Refs. [54, 48].

In Figs. 6.4 and 6.5, we apply our previous results to experimental data. Fig. 6.4 shows results from E154 [82] while Fig. 6.5 shows results from HERMES [52]. In the following we compute the value of Δ_g, defined in Eq. (6.20), using the standard NLO parton distribution of Ref. [70], for each experimental point, including the various corrections we studied previously. Then we apply this correction, Δ_g, to the experimental data. In both figures the white

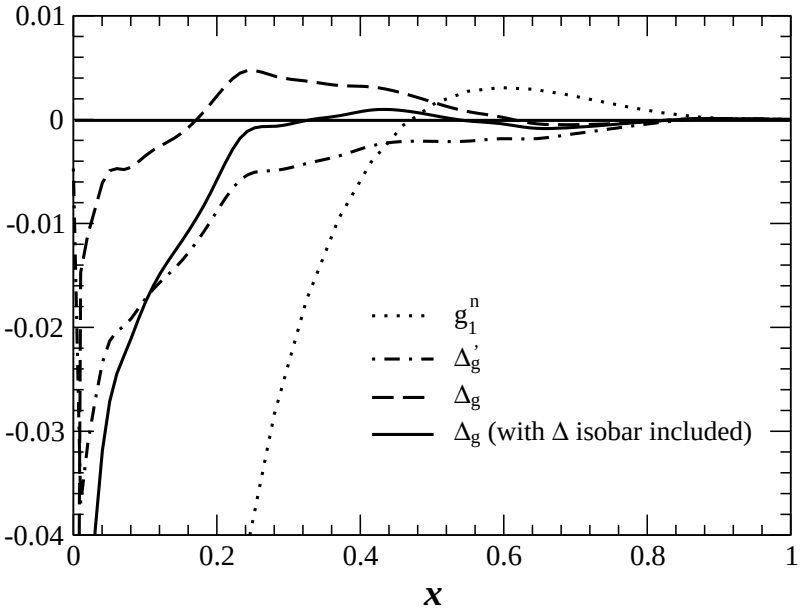

Figure 6.2: Δ_g, $\Delta_g^{'}$ and g_1^n at $Q^2 = 4$ GeV^2.

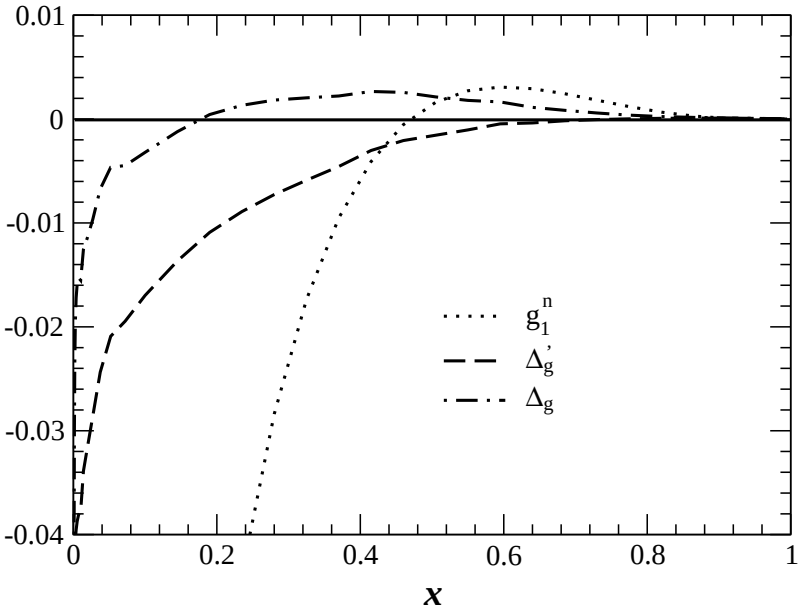

Figure 6.3: Δ_g, $\Delta_g^{'}$ and g_1^n, without off-shell corrections, at $Q^2 = 4$ GeV^2.

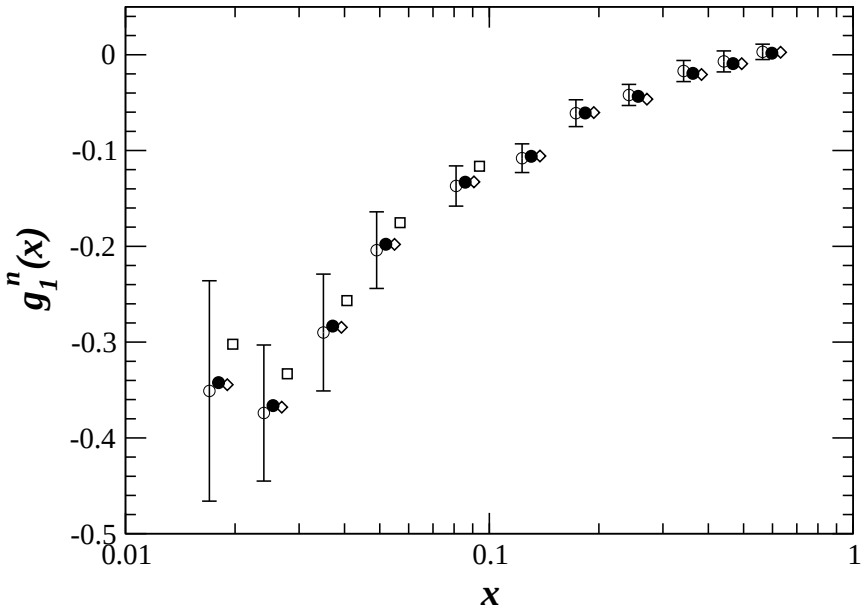

Figure 6.4: Corrections to g_1^n data from E154. White circles represent the original data. Black circles are corrected for binding energy and nuclear effects. Diamonds have all corrections from the black circles as well as off-shell corrections. Squares have all the corrections from the diamonds as well as Δ isobar corrections. The error bars are statistical errors.

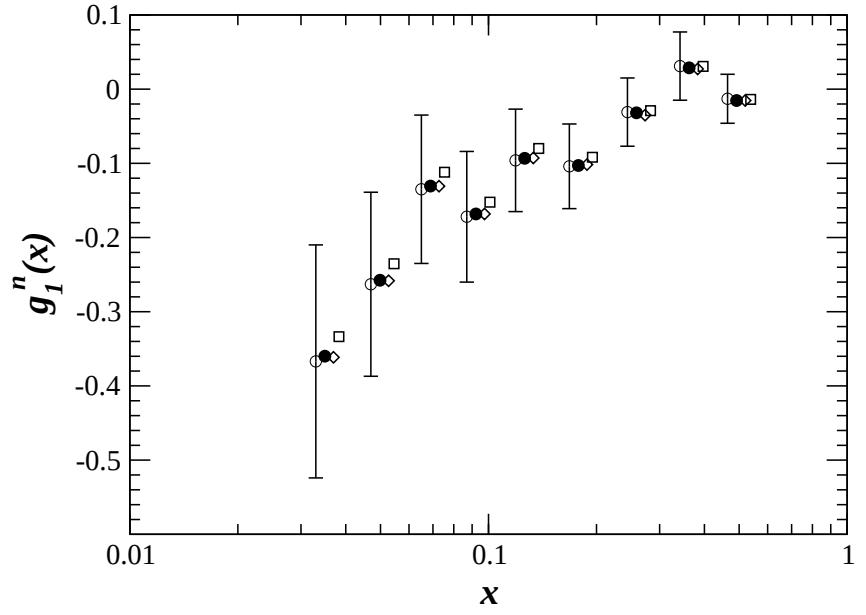

Figure 6.5: Corrections to g_1^n data from HERMES. White circles represent the original data. Black circles are corrected for binding energy and nuclear effects. Diamonds have all corrections from the black circles as well as off-shell corrections. Square have all the corrections from the diamond as well as Δ isobar corrections. The error bars are statistical errors.

circles represent the original data given in Refs. [52, 82] and are assumed to have been extracted as per Eq. (6.19). One gets the black circles by correcting for the nuclear effects included in the convolution formalism. One gets the diamonds by including the off-shell effects of Ref. [49], and finally, one gets the squares by including the correction from the Δ isobar discussed in section 6.3.

In Fig. 6.4, we did not apply the correction associated with the Δ isobar on all points, as for points with $x \geq 0.1$ the corresponding Q^2 is more than 6 GeV^2 which is outside the range of application of the model used. The E154 collaboration has evolved its data to $Q^2 = 5$ GeV^2 which would be in the limit of applicability of the model, however, we believe that data should be corrected before being evolved. So, we will not use the evolved data of E154. In Fig. 6.5 we did apply the Δ isobar correction to the last point, $x = 0.464$ and $Q^2 = 5.25$ GeV^2, as it is not far off the limit of applicability of our model. Both figures show that the most important correction comes from the inclusion of the Δ isobar for values of x smaller than 0.2. All other corrections are small and well within error bars. However at small x, one probably needs to take into account some other physics to get a good description of the system. This suggests that we can make an accurate extraction of g_1^n from ^{3}He data for medium and large values of x. In the small x region, however, one may need other tools to perform an accurate extraction of g_1^n from $g_1^{^3\mathrm{He}}$.

6.5 The proton in tritium

For tritium we will compute the polarised structure function g_1 using Eqs. (6.8) and (6.15). In this case one can plot a ratio, as g_1^p and $g_1^{^3\mathrm{H}}$ do not change sign. Therefore, to illustrate the effect of the neutron contribution in this case one can plot:

$$R_g = \frac{g_1^{^3\mathrm{H}} - 2\Delta_n g_1^n}{\Delta_p g_1^p}, \tag{6.22}$$

and

$$R_g^{'} = \frac{g_1^{^3\mathrm{H}}}{\Delta_p g_1^p}. \tag{6.23}$$

In Fig. 6.6 we show both ratios (R_g is the solid line and $R_g^{'}$ is the dashed line) without including the off-shell corrections [49] as well as R_g with the off-shell corrections (dot-dashed line). In this figure we can clearly see that on most of the interval the contribution of the neutron is negligible, some difference appearing for small x. This is expected simply because g_1^n is significantly smaller than g_1^p for most values of x, but starts to grow at small

x in most parametrisations. For the next figure we will concentrate on $R_g^{'}$. Since this ratio does not depend on the structure function of the neutron it may be more accurately compared with experiment.

In Fig. 6.7 we study the impact of off-shell corrections and Δ isobar corrections on $R_g^{'}$. On this figure there are three curves. The dotted curve is identical to the dashed one in Fig. 6.6 and does not include any corrections. The dashed line includes the off-shell corrections of Ref. [49] for $0.2 \leq x \leq 0.8$. As one can see, on this curve there is a correction of at least 5% for all x. One can also see that there is also a big drop of $R_g^{'}$ for $x \approx 0.8$. At its lowest point, in this dip we have $R_g^{'} \approx 0.68$. If apply these off-shell corrections for all x this dip is present and we have $R_g^{'} \approx 0.44$ at its lowest point. This dip is almost certainly spurious and may come from the inclusion of the off-shell correction outside its domain of validity. If we limit the off-shell corrections to $0.2 \leq x \leq 0.7$ the dip remains but its lowest point is now $R_g^{'} \approx 0.85$, which is more credible. We also note that we now have a "jump" in $R_g^{'}$ at $x = 0.2$, so the behaviour at small x is not clearly determined as the transition should be smoother. The solid line includes corrections from both off-shell effects and Δ isobar. The Δ isobar has no effects on the dip around $x \approx 0.8$, but it reduces the contribution of off-shell effects for $0.2 \leq x \leq 0.6$. For $x \leq 0.2$ the Δ increases $g_1^{^3\mathrm{H}}$ compare to g_1^p, however, as in the case of ^{3}He one probably needs to take into account some additional physics, such as shadowing and meson exchange currents, in order to get an accurate description of $g_1^{^3\mathrm{H}}$.

From Fig. 6.7 we can conclude that any corrections from the nuclear medium can probably be put in evidence in the ratio $R_g^{'}$ at moderate x. In the high x region the behaviour of this ratio is still unclear. The dip observed in Fig. 6.7 can have two origins. One is that off-shell corrections are not properly handled at high x, which is why we tried to reduce the range on which we apply the correction. The second may be a breakdown of the convolution formalism we used for those values. However, if both the convolution formalism and the off-shell corrections hold for values of x as high as 0.8 we would have a very big effect on the ratio that could definitely be measured. In fact even if the off-shell corrections applies to a smaller range of x, a dip may still be spotted – basically because the effects from off-shell corrections act against the effect of Fermi motion[3]

[3]In Ref. [71] where the OSC were put by taking the inverse of Eq. (6.5), the effects of OSC goes in the same way as the Fermi motion and thus there is no dip, but the effect is added to the Fermi motion making it seem to start earlier and be bigger.

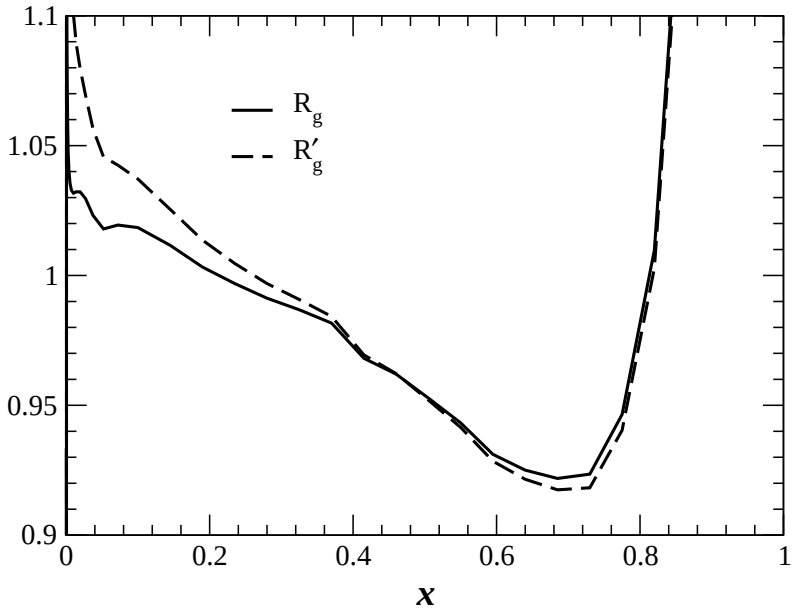

Figure 6.6: The ratio R_g and R'_g of Eqs. (6.22) and (6.23) at 4 GeV^2, without any off-shell corrections.

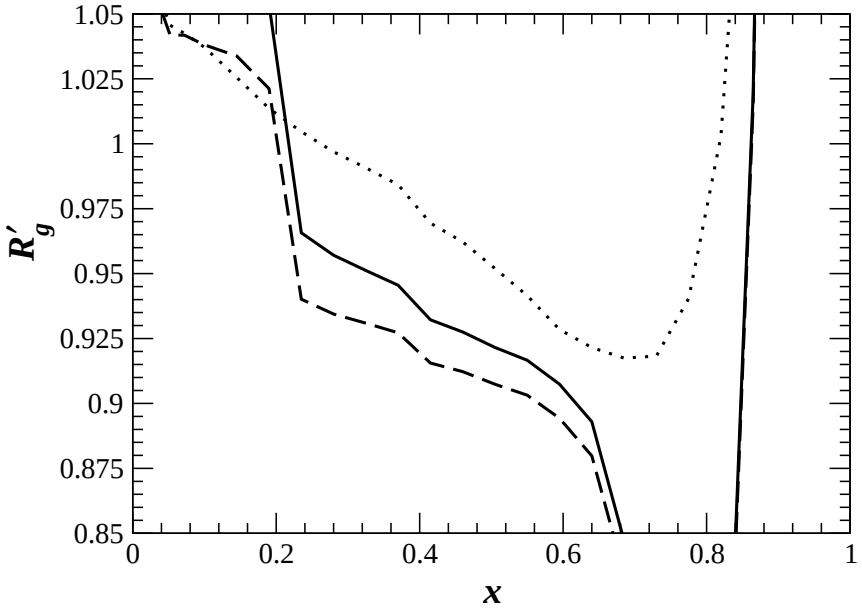

Figure 6.7: The ratio R'_g of Eq. (6.23) at 4 GeV^2. The dotted line is without off-shell corrections. The dashed line is with off-shell corrections and the solid line include both off-shell corrections and Δ isobar corrections.

Chapter 7

Conclusions

In the first part of this work we have shown how to derive the Faddeev equation and how to write them down in order to be used with a separable potential. We have used these equations to get the wave function of the three nucleon system with several potentials. We compared the figures for the binding energy and the contribution of the different partial waves to the wave function. We have concluded that most realistic potentials under-bind the three nucleon system. This problem may have several origins, such as the lack of a contribution from genuine three-body forces in our computation or from a misrepresentation of the short range behaviour of the two-body potential. However, these kinds of potentials have proved to be able to give a good description of a wide range of phenomena both in the two-nucleon and the three-nucleon sector. While in that chapter we have focused on systems made up of identical particles, this work can be easily extended to systems made of different kinds of particles.

Then, we presented, how from first principles one can write the cross-section of an electromagnetic probe with a nuclear target of spin 1/2. We pointed out that such a cross-section depends on four nuclear unknowns, the structure functions. We then presented a short derivation of the convolution formalism. This formalism gave us basic tools to link the structure functions of simple objects like the nucleons to the structure functions of more complex objects, made of nucleons, like ^{3}He and ^{3}H. During the presentation of this formalism we have carefully enumerated the hypotheses and approximations made in its derivation. This formalism supposes that only one photon exchange occurs and that there is no rescattering. It is know that in the small x region multiple scattering is likely to occur, so the convolution formalism cannot be used to make predictions for small x. It also supposes that there is no interaction between the components of the final state of the reaction. If it is known that such interactions are important then, it is likely to have consequences for the applicability of the formalism.

We moved on to the computation of the fundamental ingredients of the convolution formalism: the light-cone momentum distributions. We have shown how one can compute those quantities from the tri-nucleon wave function we first computed. The light-cone momentum distributions we get from different potentials are very similar, curves computed from the PEST and RSC potentials are very close, while there is some discrepancy between those and the Yamaguchi type of potential. These discrepancies were already present in the computed value of the binding energy of the wave function and it was likely to have an influence on the light-cone momentum distribution. We also studied the figures for the polarisation of the nucleon in ^{3}He and saw that they were in agreement with the figures given in the literature, with the exception of the polarisation of the proton, which is very slightly

underestimated.

Next, we studied the structure functions of the three nucleon system. We started with the unpolarised structure functions. Using the QPM, we wrote down the expression of the structure functions of the free nucleons in terms of quark distribution. Using the convolution we then computed the unpolarised structure functions of both ^{3}He and ^{3}H. We, then, used these results to compute the EMC effect in the three nucleon system (*i.e.* for both ^{3}He and ^{3}H). We studied the dependence of the EMC effect to both the potential used and the quark distribution. We found that all the potentials we used give similar results. In fact, we found that our predictions for the EMC effect are more dependent on the quark distributions used than the potential. After computing the EMC effect we evaluated the Gottfried sum rule in the (^{3}He, ^{3}H) system. We found, that according to our model, the nuclear medium in the three nucleon system had little effect on the Gottfried sum rule. This implied that the flavour asymmetry of the quark sea in the tri-nucleon system is the same as in the nucleons.

At last, in this chapter we have shown how one can extract the structure function F_2 of the neutron by measuring the EMC effect in both ^{3}He and ^{3}H. This work led to a proposal for a experiment a TJNAF [56, 94] to cross check previous results from deuteron experiments and to determine the behaviour of F_2^n at high x. This, in turn, could lead to re-analysis of most current quark distributions which enforce the following behaviour: $d/u \to 0$ as $x \to 1$. However, computations from perturbative QCD predict the following behaviour: $d/u \to 1/5$ as $x \to 1$. This experiment will help clarify the behaviour of the ratio d/u as x goes towards 1. Our perspective on the behaviour of quark distribution in the limit $x \to 1$ could be changed completely by this experiment.

After studying the unpolarised structure functions of the three nucleon system we moved to the study of the polarised one. One the main interests in the study of the polarised structure functions of ^{3}He, is the extraction of the neutron ones. So, we have analysed the usual formula used to extract g_1^n from $g_1^{^3\mathrm{He}}$ and the effects of the most important corrections that one can make in this extraction. First, the convolution formalism required the use of off-shell structure functions. In this work we have studied the effect of novel off-shell corrections computed with the help of the QMC [49, 50]. We also included the contribution of the resonance $\Delta(1232)$ in the computation of the $g_1^{^3\mathrm{He}}$. This contribution is needed if one wants to recover the Bjorken sum rule in the tri-nucleon system. In the absence of the contribution of the Δ resonance the convolution formalism, with or without the inclusion of off-shell corrections, cannot satisfy this sum rule. We found that the results from the experiments HERMES [52] and E154 [82] were almost not changed

by our corrections except at small x were the applicability of our method is uncertain. This shows that the data extracted from these experiments are quite reliable.

In the last part of this chapter we have shown that one could detect effects of the nuclear medium on the proton in ^{3}H. As polarised ^{3}He behaves almost as a polarised neutron, polarised ^{3}H behaves almost like a polarised proton. However, while in ^{3}He we must be careful to include the contribution from the proton to $g_1^{^3\mathrm{He}}$, in ^{3}H we can discard totally the small contribution of the neutron to $g_1^{^3\mathrm{H}}$. So, ^{3}H is a perfect target to measure effects of the light nuclear medium on the polarised proton structure function. Using the same corrections discussed for ^{3}He we have shown that for $0.7 \leq x \leq 0.8$ there is a very big discrepancy between results computed with and without off-shell corrections. This shows that measurements of the polarised structure function of ^{3}H could help us understand the effect of the light nuclear medium on nucleons. Such an experiment, while technically possible at TJNAF, cannot be done safely at the moment. Thus, it constitutes a future test of the QMC.

This work can have several natural extensions. First, as the Faddeev equations can be cast for a system made several kinds of particle, we could explicitly break the isospin symmetry we have used in most of this thesis and use different potential for proton-proton, neutron-proton and neutron-neutron interactions. Some potentials, for example, include the Coulomb corrections in their proton-proton potential. In this work, we neglected the second polarised structure function g_2. While the study of g_2 is more difficult than the study of g_1, one can derive a convolution formula for it and study the relationship between g_2 in the tri-nucleon system and g_2 of the free nucleon, and g_2^n in particular.

To extract the structure functions of the neutron, ^{3}He is not the only choice of target. Of course, deuterium has already been used, and will probably be used again for that purpose. But, some other target like ^{6}Li, may be used for that purpose as well. In first approximation, ^{6}Li can be described as an α-particle plus two nucleons (one proton and one neutron) more weakly bound. This system can be described as a three-body system provided that one does not probe the α-particle very deeply. In that case, one can hope that the weakly bound peripheral neutron can give useful information on the free neutron structure functions.

Such a study would re-use the Faddeev equations, for two different kinds of particles this time (α-particle and nucleon), to compute the wave function of ^{6}Li and the same convolution formalism. If one does not break the α-particle, the final state of the reaction can only be a scattering state (if one nucleon or the α-particle is struck) or a deuteron state (if the α-particle is

struck). This similarly to the case of ^{3}He. Good care should be taken of the fact that ^{6}Li is not a spin 1/2 target but a spin 1 target. However, similar studies have been done on the deuteron which has the same spin, and should be readily usable. A similar study to that performed on $g_1^{^3\mathrm{H}}$ could be done in the hope of finding a clear signature of the effects of nuclear medium on free nucleon, such a study could be done with the help of off-shell corrections computed with the QMC and readily available [49].

Appendix A

The kernel of the homogeneous Faddeev equation

We now review the derivation of the kernel of the homogeneous Faddeev equation, $Z^{JI}_{\ell_\alpha N_\alpha;\ell_\beta N_\beta}$. We note that the derivation of the permutation term will be very similar. First of all we will use the following notation for the z-projections of the various angular momenta: m_α, m_β and m_γ for the z-projections of j_α, j_β and j_γ; σ_α for s_α; $\overline{m}_\alpha$ for $\bar{\jmath}_\alpha$; λ_α for ℓ_α; Λ_α for L_α; Σ_α for S_α and M for J. If for simplicity we forget isospin and use the notation $\hat{J} = \sqrt{2J+1}$, we have

$$\begin{aligned} Z^J_{\ell_\alpha N_\alpha;\ell_\beta N_\beta}(p_\alpha, p_\beta, E) &\equiv \left\langle g^{n_\alpha}_{\ell_\alpha}; \ell_\alpha N_\alpha; p_\alpha \middle| G_0(E) \middle| p_\beta; \ell_\beta N_\beta; g^{n_\beta}_{\ell_\beta} \right\rangle \\ &= \frac{1}{\hat{J}^2} \sum_{\substack{\text{all} \\ \text{z-projections}}} \langle j_\beta\, m_\beta\, j_\gamma\, m_\gamma | s_\alpha\, \sigma_\alpha \rangle \, \langle j_\gamma\, m_\gamma\, j_\alpha\, m_\alpha | s_\beta\, \sigma_\beta \rangle \\ &\times \langle \ell_\alpha\, \lambda_\alpha\, s_\alpha\, \sigma_\alpha | \bar{\jmath}_\alpha\, \overline{m}_\alpha \rangle \, \langle \ell_\beta\, \lambda_\beta\, s_\beta\, \sigma_\beta | \bar{\jmath}_\beta\, \overline{m}_\beta \rangle \\ &\times \langle \bar{\jmath}_\alpha\, \overline{m}_\alpha\, j_\alpha\, m_\alpha | S_\alpha\, \Sigma_\alpha \rangle \, \langle \bar{\jmath}_\beta\, \overline{m}_\beta\, j_\beta\, m_\beta | S_\beta\, \Sigma_\beta \rangle \\ &\times \langle L_\alpha\, \Lambda_\alpha\, S_\alpha\, \Sigma_\alpha | J\, M \rangle \, \langle L_\beta\, \Lambda_\beta\, S_\beta\, \Sigma_\beta | J\, M \rangle \\ &\times \left\langle g^{n_\alpha}_{\ell_\alpha}; \mathcal{Y}_{\ell_\alpha\lambda_\alpha}; \mathcal{Y}_{L_\alpha\Lambda_\alpha}; p_\alpha \middle| G_0(E) \middle| p_\beta; \mathcal{Y}_{\ell_\beta\lambda_\beta}; \mathcal{Y}_{L_\beta\Lambda_\beta}; g^{n_\beta}_{\ell_\beta} \right\rangle. \end{aligned} \tag{A.1}$$

The last term in Eq. (A.1) is given by

$$\begin{aligned} \mathcal{G} &= \left\langle g^{n_\alpha}_{\ell_\alpha}; \mathcal{Y}_{\ell_\alpha\lambda_\alpha}; \mathcal{Y}_{L_\alpha\Lambda_\alpha}; p_\alpha \middle| G_0(E) \middle| p_\beta; \mathcal{Y}_{\ell_\beta\lambda_\beta}; \mathcal{Y}_{L_\beta\Lambda_\beta}; g^{n_\beta}_{\ell_\beta} \right\rangle \\ &= \int d^3\vec{p}'_\alpha d^3\vec{q}_\alpha d^3\vec{p}'_\beta d^3\vec{q}_\beta\, \mathcal{Y}_{\ell_\alpha\lambda_\alpha}(\hat{q}_\alpha) \mathcal{Y}_{L_\alpha\Lambda_\alpha}(\hat{p}'_\alpha) \mathcal{Y}^*_{\ell_\beta\lambda_\beta}(\hat{q}_\beta) \mathcal{Y}^*_{L_\beta\Lambda_\beta}(\hat{p}'_\beta) \\ &\times \frac{g^{n_\beta\dagger}_{\ell_\beta}(q_\beta) g^{n_\alpha}_{\ell_\alpha}(q_\alpha)}{E - \frac{p'^2_\alpha}{2m} - \frac{p'^2_\beta}{2m} - \frac{(\vec{p}'_\alpha + \vec{p}'_\beta)^2}{2m}} \frac{\delta(p'_\alpha - p_\alpha)}{p^2_\alpha} \frac{\delta(p'_\beta - p_\beta)}{p^2_\beta} \\ &\times \delta^3\left(\vec{q}_\alpha - (\vec{p}'_\beta + \rho_\alpha \vec{p}'_\alpha)\right) \delta^3\left(\vec{q}_\beta - (-\vec{p}'_\alpha - \rho_\beta \vec{p}'_\beta)\right). \end{aligned} \tag{A.2}$$

In the last equation the integrals are only on $\hat{p}'_\alpha$ and $\hat{p}'_\beta$. $\vec{q}_\alpha$ and $\vec{q}_\beta$ are completely determined once we know $\vec{p}'_\alpha$ and $\vec{p}'_\beta$, as shown by the delta functions present in the integral. For a system of particles with identical masses we have $\rho_\alpha = \rho_\beta = 1/2$ in Eq. (A.2). Since $\hat{p}'_\alpha$ and $\hat{p}'_\beta$ are the only indepent variables in Eq. (A.2), one needs to express every components of the integral in terms of them. The spherical harmonics in $\hat{q}_\alpha$ and $\hat{q}_\beta$ can be expressed in terms of $\hat{p}'_\alpha$ and $\hat{p}'_\beta$ using the following [1]

$$\begin{aligned} p^\ell \mathcal{Y}_{\ell m}(\hat{p}) = \sum_{\substack{ab \\ m_a m_b}} \delta_{\ell,a+b} \sqrt{\frac{4\pi(2\ell+1)!}{(2a+1)!(2b+1)!}} \, \langle a\, m_a\, b\, m_b | \ell\, m \rangle \\ \times (\alpha q)^a \mathcal{Y}_{a m_a}(\hat{q}) (\beta r)^b \mathcal{Y}_{b m_b}(\hat{r}), \end{aligned} \tag{A.3}$$

with $\vec{p} = \alpha\vec{q} + \beta\vec{r}$. To completely eliminate the dependence on $\hat{q}_\alpha$ and $\hat{q}_\beta$ of $\mathcal{G}$, one needs to expand the products of the Green's function with the form factors in terms of spherical harmonics in $\hat{p}'_\alpha$ and $\hat{p}'_\beta$. That is

$$\frac{q_\beta^{-\ell_\beta} g_{\ell_\beta}^{n_\beta\dagger}(q_\beta) g_{\ell_\alpha}^{n_\alpha}(q_\alpha) q_\alpha^{-\ell_\alpha}}{E - \frac{p_\alpha^2}{2m} - \frac{p_\beta^2}{2m} - \frac{(\vec{p}'_\alpha + \vec{p}'_\beta)^2}{2m}} = 4\pi \sum_{\mathcal{L}M_\mathcal{L}} F_{n_\alpha,n_\beta}^{\mathcal{L},\ell_\alpha,\ell_\beta}(p_\alpha, p_\beta, E) \mathcal{Y}^*_{\mathcal{L}M_\mathcal{L}}(\hat{p}'_\beta) \mathcal{Y}_{\mathcal{L}M_\mathcal{L}}(\hat{p}'_\alpha), \tag{A.4}$$

with

$$F_{n_\alpha,n_\beta}^{\mathcal{L},\ell_\alpha,\ell_\beta}(p_\alpha, p_\beta, E) = \frac{1}{2} \int_{-1}^{+1} dx \frac{q_\beta^{-\ell_\beta} g_{\ell_\beta}^{n_\beta\dagger}(q_\beta) g_{\ell_\alpha}^{n_\alpha}(q_\alpha) q_\alpha^{-\ell_\alpha}}{E - \frac{p_\alpha^2}{2m} - \frac{p_\beta^2}{2m} - \frac{(\vec{p}'_\alpha + \vec{p}'_\beta)^2}{2m}} P_\mathcal{L}(x), \tag{A.5}$$

where $P_\mathcal{L}$ is the Legendre polynomial of order $\mathcal{L}$ and $x = \hat{p}'_\alpha \cdot \hat{p}'_\beta$. Using all the previous equations leads to an expression for $\mathcal{G}$ that contains 4 spherical harmonics in both $\hat{p}'_\alpha$ and $\hat{p}'_\beta$. Those can be reduced, using the following formula [2, 3]

$$\mathcal{Y}_{\ell_1 m_1}(\hat{p}) \mathcal{Y}_{\ell_2 m_2}(\hat{p}) = \sum_{\ell,m} \sqrt{\frac{(2\ell_1+1)(2\ell_2+1)(2\ell+1)}{4\pi}} \times \begin{pmatrix} \ell_1 & \ell_2 & \ell \\ m_1 & m_2 & m \end{pmatrix} \begin{pmatrix} \ell_1 & \ell_2 & \ell \\ 0 & 0 & 0 \end{pmatrix} \mathcal{Y}^*_{\ell m}(\hat{p}), \tag{A.6}$$

to a product of two spherical harmonics in each variable, for which we can use standard orthogonality relation between spherical harmonics. The result involves several vector coupling coefficients and 3-j symbols. Summing over some z-projections with the help of Eqs. (2.20) and (3.21) of Ref [2] one finds:

$$\begin{aligned} \mathcal{G} = (-1)^{\ell_\alpha+\lambda_\alpha+\Lambda_\alpha} \hat{\ell}_\alpha \hat{\ell}_\beta \hat{L}_\alpha \hat{L}_\beta \sum_{\mathcal{L}} (-1)^\mathcal{L} \hat{\mathcal{L}}^2 F_{n_\alpha,n_\beta}^{\mathcal{L},\ell_\alpha,\ell_\beta}(p_\alpha, p_\beta, E) \\ \times \sum_{aa'bb'} \delta_{\ell_\alpha,a+b} \delta_{\ell_\beta,a'+b'} \rho_\alpha^a \rho_\beta^{b'} p_\alpha^{a+a'} p_\beta^{b+b'} \sqrt{\frac{(2\ell_\alpha+1)!(2\ell_\beta+1)!}{(2a)!(2b)!(2a')!(2b')!}} \\ \times \sum_{\Lambda\Lambda' f} \left(\hat{f}\hat{\Lambda}\hat{\Lambda}'\right)^2 \begin{pmatrix} a & a' & \Lambda \\ 0 & 0 & 0 \end{pmatrix} \begin{pmatrix} b & b' & \Lambda' \\ 0 & 0 & 0 \end{pmatrix} \begin{pmatrix} \Lambda & \mathcal{L} & L_\alpha \\ 0 & 0 & 0 \end{pmatrix} \begin{pmatrix} \Lambda' & \mathcal{L} & L_\beta \\ 0 & 0 & 0 \end{pmatrix} \\ \times \begin{Bmatrix} L_\alpha & L_\beta & f \\ \Lambda' & \Lambda & \mathcal{L} \end{Bmatrix} \begin{Bmatrix} \ell_\alpha & \ell_\beta & f \\ a & a' & \Lambda \\ b & b' & \Lambda' \end{Bmatrix} \sum_{m_f} \begin{pmatrix} \ell_\alpha & \ell_\beta & f \\ -\lambda_\alpha & \lambda_\beta & m_f \end{pmatrix} \begin{pmatrix} L_\alpha & L_\beta & f \\ \Lambda_\alpha & -\Lambda_\beta & m_f \end{pmatrix}. \end{aligned} \tag{A.7}$$

Going back to the expression for the kernel one can replace all Clebsch-Gordan coefficients by 3-j symbols[1] and then use the following relations to simplify the expression:

$$\sum_{\Lambda_\alpha \Lambda_\beta M} (-1)^{\Lambda_\beta - 2M} \begin{pmatrix} L_\alpha & L_\beta & f \\ \Lambda_\alpha & -\Lambda_\beta & m_f \end{pmatrix} \begin{pmatrix} L_\alpha & S_\alpha & J \\ \Lambda_\alpha & \Sigma_\alpha & -M \end{pmatrix} \begin{pmatrix} L_\beta & S_\beta & J \\ \Lambda_\beta & \Sigma_\beta & -M \end{pmatrix}$$
$$= (-1)^{J-f+\Sigma_\alpha} \begin{pmatrix} S_\alpha & S_\beta & f \\ -\Sigma_\alpha & \Sigma_\beta & m_f \end{pmatrix} \begin{Bmatrix} S_\alpha & S_\beta & f \\ L_\beta & L_\alpha & J \end{Bmatrix}, \quad \text{(A.8)}$$

and

$$\sum_{\substack{\text{all} \\ \text{z-projections}}} (-1)^{-\Sigma_\alpha - \overline{m}_\alpha - \overline{m}_\beta - \sigma_\alpha - \sigma_\beta + \lambda_\alpha} \begin{pmatrix} S_\alpha & S_\beta & f \\ -\Sigma_\alpha & \Sigma_\beta & m_f \end{pmatrix} \begin{pmatrix} \ell_\alpha & \ell_\beta & f \\ -\lambda_\alpha & \lambda_\beta & m_f \end{pmatrix}$$
$$\times \begin{pmatrix} \bar{\jmath}_\alpha & j_\alpha & S_\alpha \\ \overline{m}_\alpha & m_\alpha & -\Sigma_\alpha \end{pmatrix} \begin{pmatrix} \bar{\jmath}_\beta & j_\beta & S_\beta \\ \overline{m}_\beta & m_\beta & -\Sigma_\beta \end{pmatrix} \begin{pmatrix} \ell_\alpha & s_\alpha & \bar{\jmath}_\alpha \\ \lambda_\alpha & \sigma_\alpha & -\overline{m}_\alpha \end{pmatrix} \begin{pmatrix} \ell_\beta & s_\beta & \bar{\jmath}_\beta \\ \lambda_\beta & \sigma_\beta & -\overline{m}_\beta \end{pmatrix}$$
$$\times \begin{pmatrix} j_\beta & j_\gamma & s_\alpha \\ m_\beta & m_\gamma & -\sigma_\alpha \end{pmatrix} \begin{pmatrix} j_\gamma & j_\alpha & s_\beta \\ m_\gamma & m_\alpha & -\sigma_\beta \end{pmatrix}$$
$$= (-1)^{2f+2S_\beta+2\ell_\alpha+2\bar{\jmath}_\beta - s_\alpha + 2s_\beta - j_\alpha + 2j_\beta} \begin{Bmatrix} j_\alpha & S_\alpha & S_\beta & j_\beta \\ \bar{\jmath}_\alpha & f & \bar{\jmath}_\beta & j_\gamma \\ s_\alpha & \ell_\alpha & \ell_\beta & s_\beta \end{Bmatrix}, \quad \text{(A.9)}$$

where the 12-j symbol is defined by Ord-Smith[58]. One can find these relations using the diagrammatic procedures of Ref. [4]. In the end the kernel can be expressed in the following way:

$$Z^{JI}_{\ell_\alpha N_\alpha; \ell_\beta N_\beta} \equiv \left\langle g^{n_\alpha}_{\ell'_\alpha}; \Omega^{JI}_{\ell'_\alpha N_\alpha} \middle| \, G_0(E) \middle| \Omega^{JI}_{\ell_\beta N_\beta}; g^{n_\beta}_{\ell_\beta} \right\rangle$$
$$= p_\beta^{\ell_\alpha} p_\alpha^{\ell_\beta} B_{N_\alpha N_\beta} \sum_{\mathcal{L}} F^{\mathcal{L}\ell_\alpha\ell_\beta}_{n_\alpha, n_\beta}(p_\alpha, p_\beta, E) \sum_{a=0}^{l_\alpha} \sum_{b=0}^{l_\beta} A^{\mathcal{L},a,b}_{\ell_\alpha N_\alpha; \ell_\beta N_\beta} \left(\frac{p_\alpha}{p_\beta} \right)^{a-b}. \quad \text{(A.10)}$$

The coefficients $A^{\mathcal{L},a,b}_{\ell_\alpha N_\alpha; \ell_\beta N_\beta}$ which result from the recoupling of the spin and

[1] We have the following relation between Clebsch-Gordan and 3-j symbol: $\langle j_1\, m_1\, j_2\, m_2 | j\, m \rangle = (-1)^{-j_1+j_2-m} \sqrt{2j+1} \begin{pmatrix} j_1 & j_2 & j \\ m_1 & m_2 & -m \end{pmatrix}$.

orbital angular momentum are given by

$$\begin{aligned} A^{\mathcal{L},a,b}_{\ell_\alpha N_\alpha;\ell_\beta N_\beta} &= (-1)^R \hat{\ell}_\alpha \hat{\ell}_\beta \hat{L}_\alpha \hat{L}_\beta \hat{S}_\alpha \hat{S}_\beta \hat{\bar{\jmath}}_\alpha \hat{\bar{\jmath}}_\beta \hat{s}_\alpha \hat{s}_\beta \hat{\mathcal{L}}^2 \rho^a_\alpha \rho^b_\beta \\ &\times \sqrt{\frac{(2\ell_\alpha+1)!(2\ell_\beta+1)!}{(2a)!(2b)!(2\ell_\alpha-2a)!(2\ell_\beta-2b)!}} \\ &\times \sum_{f\Lambda\Lambda'} \left(\hat{f}\hat{\Lambda}\hat{\Lambda}'\right)^2 \begin{Bmatrix} S_\alpha & S_\beta & f \\ L_\beta & L_\alpha & J \end{Bmatrix} \begin{Bmatrix} L_\alpha & L_\beta & f \\ \Lambda' & \Lambda & \mathcal{L} \end{Bmatrix} \\ &\times \begin{Bmatrix} j_\alpha & S_\alpha & S_\beta & j_\beta \\ \bar{\jmath}_\alpha & f & \bar{\jmath}_\beta & j_\gamma \\ s_\alpha & \ell_\alpha & \ell_\beta & s_\beta \end{Bmatrix} \begin{Bmatrix} \ell_\alpha & \ell_\beta & f \\ a & \ell_\beta - b & \Lambda \\ \ell_\alpha - a & b & \Lambda' \end{Bmatrix} \\ &\times \begin{pmatrix} a & \ell_\beta - b & \Lambda \\ 0 & 0 & 0 \end{pmatrix} \begin{pmatrix} \Lambda' & \mathcal{L} & L_\beta \\ 0 & 0 & 0 \end{pmatrix} \begin{pmatrix} \Lambda & \mathcal{L} & L_\alpha \\ 0 & 0 & 0 \end{pmatrix} \begin{pmatrix} \ell_\alpha - a & b & \Lambda' \\ 0 & 0 & 0 \end{pmatrix}, \end{aligned} \tag{A.11}$$

with the phase R defined as

$$R = -J + L_\alpha + L_\beta + S_\alpha + S_\beta + \bar{\jmath}_\alpha + \bar{\jmath}_\beta - j_\alpha + s_\beta + \ell_\alpha + \mathcal{L}. \tag{A.12}$$

Finally, the isospin recoupling coefficient $B_{N_\alpha N_\beta}$ is given in terms of a 6-j symbol by the relation

$$B_{N_\alpha N_\beta} = (-1)^{i_\alpha + i_\gamma - \bar{\imath}_\beta + 2I} \hat{i}_\alpha \hat{\bar{\imath}}_\beta \begin{Bmatrix} i_\beta & i_\gamma & \bar{\imath}_\alpha \\ i_\alpha & I & \bar{\imath}_\beta \end{Bmatrix}. \tag{A.13}$$

Appendix B

The permutation term

This section is devoted to the extraction of the form of Eq. (2.23). We call it the permutation term because it originates from Eq. (2.1). Its derivation has a lot of similarities with the derivation of the kernel. The contribution of a given channel $(\ell_\beta N_\beta)$ to a given channel $(\ell_\alpha N_\alpha)$ can be written as the sum over all z-projections over the same series of clebsch-gordan. Only the term we called $\mathcal{G}$ in the previous section will be different. For this reason we will call it $\mathcal{G}'$. We have

$$\begin{aligned}\mathcal{G}' &= \left\langle \mathcal{Y}_{\ell_\alpha\lambda_\alpha};\mathcal{Y}_{L_\alpha\Lambda_\alpha};p_\alpha q_\alpha\middle|\mathcal{Y}_{\ell_\beta\lambda_\beta};\mathcal{Y}_{L_\beta\Lambda_\beta};\eta^{JI1}_{\ell_\beta N_\beta}\right\rangle \\ &= \int d^3\vec{p}'_\alpha d^3\vec{q}'_\alpha d^3\vec{p}_\beta d^3\vec{q}_\beta\, \mathcal{Y}_{\ell_\alpha\lambda_\alpha}(\hat{q}'_\alpha)\mathcal{Y}_{L_\alpha\Lambda_\alpha}(\hat{p}'_\alpha)\mathcal{Y}^*_{\ell_\beta\lambda_\beta}(\hat{q}_\beta)\mathcal{Y}^*_{L_\beta\Lambda_\beta}(\hat{p}_\beta) \\ &\quad\times \eta^{JI1}_{\ell_\beta N_\beta}(p_\beta,q_\beta)\frac{\delta(p'_\alpha-p_\alpha)}{p^2_\alpha}\frac{\delta(q'_\alpha-q_\alpha)}{q^2_\alpha} \\ &\quad\times \delta^3\big(\vec{p}_\beta-(\vec{q}'_\alpha-\varrho_\alpha\vec{p}'_\alpha)\big)\,\delta^3(\vec{q}_\beta-(-\varrho_\beta\vec{q}_\alpha-\varrho_\gamma\vec{p}_\alpha))\,,\end{aligned} \tag{B.1}$$

with $\varrho_\alpha = 1/2$, $\varrho_\beta = 1/2$ and $\varrho_\gamma = 3/4$, for a system of particles with identical masses. Here the integral is really only on $\hat{p}'_\alpha$ and $\hat{q}'_\alpha$, the same way that the integral in Eq. (A.2) depends only on $\hat{p}'_\alpha$ and $\hat{p}'_\beta$. However we can use the delta function in Eq. (B.1) to make it an integral over $\hat{p}'_\alpha$ and $\hat{p}_\beta$ instead. The advantage being that we can reuse our derivation of the kernel to express the permutation term. The only significative difference will be in the expression of the coefficient F given by Eq. (A.5). What we want to express as an expansion in spherical harmonics here, is

$$\int dp_\beta \left(\frac{p_\beta}{q_\alpha}\right)^2 \frac{p_\beta^{\ell_\alpha+b-a}}{q'^{\ell_\alpha}_\alpha q^{\ell_\beta}_\beta}\eta^{JI1}_{\ell_\beta N_\beta}(p_\beta,q_\beta)\delta(q'_\alpha-q_\alpha) = 4\pi\sum_{\mathcal{L}M_\mathcal{L}} Q^{\mathcal{L},a,b}_{\ell_\beta N_\beta;\ell_\alpha}(p_\alpha,q_\alpha)\mathcal{Y}_{\mathcal{L}M_\mathcal{L}}(\hat{p}'_\alpha)\mathcal{Y}^*_{\mathcal{L}M_\mathcal{L}}(\hat{p}_\beta), \tag{B.2}$$

where we have

$$Q^{\mathcal{L},a,b}_{\ell_\beta N_\beta;\ell_\alpha}(p_\alpha,q_\alpha) = \int_{-1}^{+1} dx \int dp_\beta \left(\frac{p_\beta}{q_\alpha}\right)^2 \frac{p_\beta^{\ell_\alpha+b-a}}{q'^{\ell_\alpha}_\alpha q^{\ell_\beta}_\beta}\eta^{JI1}_{\ell_\beta N_\beta}(p_\beta,q_\beta)\delta(q'_\alpha-q_\alpha)P_\mathcal{L}(x), \tag{B.3}$$

where $x = \hat{p}'_\alpha\cdot\hat{p}_\beta$. We have to put the integral on p_β in the coefficient because p_β is dependent on x through the delta function $\delta(q'_\alpha-q_\alpha)$. From the integral on $\vec{q}'_\alpha$ and $\vec{q}_\beta$ we have $\vec{q}'_\alpha = \vec{p}_\beta+\rho_\alpha\vec{p}'_\alpha$ (see Eq. (A.2)). Therefore we have

$q'_\alpha = \sqrt{p_\beta^2+\rho_\alpha^2 p'^2_\alpha+2\rho_\alpha x p'_\alpha p_\beta}$ and p_β is dependent on x and q_α. So one can finally write the equivalent of Eq. (A.7) for $\mathcal{G}'$

$$\begin{aligned}\mathcal{G}' = (-1)^{\ell_\alpha+\lambda_\alpha+\Lambda_\alpha}\hat{\ell}_\alpha\hat{\ell}_\beta\hat{L}_\alpha\hat{L}_\beta\sum_{\mathcal{L}}(-1)^{\mathcal{L}}\hat{\mathcal{L}}^2\sum_{a=0}^{\ell_\alpha}\sum_{b=0}^{\ell_\beta}\\ \times Q^{\mathcal{L},a,b}_{\ell_\beta N_\beta;\ell_\alpha}(p_\alpha,q_\alpha)\rho_\alpha^a\rho_\beta^b p_\alpha^{\ell_\alpha+a-b}\sqrt{\frac{(2\ell_\alpha+1)!(2\ell_\beta+1)!}{(2a)!(2b)!(2\ell_\alpha-2a)!(2\ell_\beta-2b)!}}\\ \times\sum_{\Lambda\Lambda' f}\left(\hat{f}\hat{\Lambda}\hat{\Lambda}'\right)^2\begin{pmatrix}a & \ell_\beta-b & \Lambda\\ 0 & 0 & 0\end{pmatrix}\begin{pmatrix}\ell_\alpha-a & b & \Lambda'\\ 0 & 0 & 0\end{pmatrix}\begin{pmatrix}\Lambda & \mathcal{L} & L_\alpha\\ 0 & 0 & 0\end{pmatrix}\begin{pmatrix}\Lambda' & \mathcal{L} & L_\beta\\ 0 & 0 & 0\end{pmatrix}\\ \times\begin{Bmatrix}L_\alpha & L_\beta & f\\ \Lambda' & \Lambda & \mathcal{L}\end{Bmatrix}\begin{Bmatrix}\ell_\alpha & \ell_\beta & f\\ a & \ell_\beta-b & \Lambda\\ \ell_\alpha-a & b & \Lambda'\end{Bmatrix}\sum_{m_f}\begin{pmatrix}\ell_\alpha & \ell_\beta & f\\ -\lambda_\alpha & \lambda_\beta & m_f\end{pmatrix}\begin{pmatrix}L_\alpha & L_\beta & f\\ \Lambda_\alpha & -\Lambda_\beta & m_f\end{pmatrix}. \quad \text{(B.4)}\end{aligned}$$

Finally using the same formula as in appendix A, one can write the permutation term

$$\left\langle p_\alpha q_\alpha;\Omega^{JI}_{\ell_\alpha N_\alpha}\middle|\Omega^{JI}_{\ell_\beta N_\beta}\right\rangle\middle|\eta^{JI1}_{\ell_\beta N_\beta}\right\rangle = p_\alpha^{\ell_\alpha}B_{N_\alpha N_\beta}\sum_{\mathcal{L}}\sum_{a=0}^{\ell_\alpha}\sum_{b=0}^{\ell_\beta}p_\alpha^{a-b}Q^{\mathcal{L},a,b}_{\ell_\beta N_\beta;\ell_\alpha}A^{\mathcal{L},a,b}_{\ell_\alpha N_\alpha;\ell_\beta N_\beta}, \quad \text{(B.5)}$$

where the coefficients $A^{\mathcal{L},a,b}_{\ell_\alpha N_\alpha;\ell_\beta N_\beta}$ and $B_{N_\alpha N_\beta}$ are given by Eqs. (A.11) and (A.13).

Bibliography

[1] M. Moshinsky, Nucl. Phys. **13**,104 (1959).

[2] M. Rotenberg, R. Bivins,N. Metropolis and J. K. Wooten, Jr : *The 3-j and 6-j symbols* (The Technology Press, MIT 1959).

[3] A. J. Edmonds : *Angular momentum in Quantum Mechanichs* (Princeton University Press 1957).

[4] A. P. Yutsis, I. B. Levinson, V. V. Vanagas : *Mathematical Apparatus of the Theory of Angular Momentum* (Israel Program for Scientific Translations, Jerusalem 1962).

[5] J. Haidenbauer and W. Plessas, Phys. Rev. **C 30**, 1822 (1984); *ibid.* **C 32**, 1424 (1985).

[6] M. Lacombe, B. Loiseau, J. M. Richard, R. Vinh Mau, J. Côtè, P. Pirès, and R. de Tourreil, Phys. Rev. **C 21**, 861 (1980).

[7] W. C. Parke, Y. Koike, D. R. Lehman and L. C. Maximon, Few Body Syst. **11**, 89 (1991).

[8] T. Y. Saito and I. R. Afnan, Phys. Rev. **C 50**, 2756 (1994); Few Body Syst. **18**, 101 (1995).

[9] I. R. Afnan and J. M. Read, Aust. J. Phys. **26** 725 (1973); Phys. Rev. **C 8**,1294 (1973).

[10] R. V. Reid, Ann. Phys. (N.Y.) **50**, 411 (1968).

[11] Y. Yamaguchi and Y. Yamaguchi, Phys. Rev. **95**, 1635 (1954).

[12] I. R. Afnan and A. W. Thomas: "Fundamentals of Three-Body Scattering Theory" in *Modern Three-Hadron Physics*, ed. A. W. Thomas (Springer-Verlag, Berlin Heidelberg New York, 1977).

[13] C. Lovelace, Phys. Rev. **135B**, 1225 (1964).

[14] I. R. Afnan and N. D. Birrell, Phys. Rev. **C 16**, 823 (1977).

[15] R. Machleidt, F. Sammarruca and Y. Song, Phys. Rev. **C 53**, 1483 (1996) [nucl-th/9510023].

[16] B. F. Gibson, Nucl. Phys. **A 543**, 1e (1992); M. T. Peña, P. U. Sauer, A. Stalder and G. Gortemeyer, Phys. Rev. **C 48**, 2208 (1993); S. A. Coon and M. T. Peña, Phys. Rev. **C 48**, 2559 (1993); T. Y. Saito and J. Haidenbauer, Eur. Phys. J **A 7**,559 (2000).

[17] D. F. Geesaman, K. Saito and A. W. Thomas, Ann. Rev. Nucl. Part. Sci. **45**, 337 (1995).

[18] B. Lampe and E. Reya, Phys. Rept. **332**, 1 (2000).

[19] M. Anselmino, A. Efremov and E. Leader, Phys. Rept. **261**, 1 (1995).

[20] R. -W. Schulze and P. U. Sauer, Phys. Rev. **C 48**, 38 (1993).

[21] R. -W. Schulze and P. U. Sauer, Phys. Rev. **C 56**, 2293 (1997).

[22] L. Heller and A. W. Thomas, Phys. Rev. **C 41**, 2756 (1990).

[23] H. Meier-Hadjuk, U. Oelfke and P. U. Sauer, Nucl. Phys. **A 499**, 637 (1989).

[24] U. Oelfke, P. U. Sauer and F. Coester, Nucl. Phys. **A 518**, 593 (1990).

[25] T. Uchiyama and K. Saito, Phys. Rev. **C 38**, 2245 (1988).

[26] L. L. Frankfurt and M. I. Strikman, Phys. Lett. **B 64**, 433 (1976); Phys. Lett. **B 65**, 51 (1976); Phys. Lett. **B 76**, 333 (1978) ; Nucl. Phys. **B 148**, 107; Phys. Rept. **76**, 215 (1981).

[27] H-M. Jung and G. A. Miller, Phys. Lett. **B 200**, 351 (1988).

[28] C. Ciofi degli Atti and S. Liuti, Phys. Rev. **C 41**, 1100 (1990).

[29] C. Ciofi degli Atti, E. Pace and G. Salmè, Phys. Lett **141B**, 14 (1984).

[30] S. Frullani and J. Mougey, Adv. in Nucl. Phys. 14, 1 (1984).

[31] A. E. L. Dieperink and T. de Forest Jr., Ann. Rev. Nucl. Sc. **25**, 1 (1975).

[32] J. L. Friar, B. F. Gibson and G. L. Payne, Phys. Rev. **C 37**, 2869 (1988).

[33] J. L. Friar, B. F. Gibson, G. L. Payne, A. M. Bernstein and T. E. Chupp, Phys. Rev. **C 42**, 2310 (1990).

[34] A. W. Thomas, Phys. Lett. **B 126**, 97 (1983).

[35] R. D. Field and R. P. Feynman, Phys. Rev. **D 15**, 2590 (1977).

[36] A. I. Signal and A. W. Thomas, Phys. Rev. **D 40**, 2832 (1989).

[37] H. L. Lai et al., Eur. Phys. J. **C 12**, 375 (2000).

[38] New Muon Collaboration, M. Arnadeo et al., Phys. Rev. **D 50**, R1 (1994).

[39] FNAL E866/NuSea Collaboration, J. C. Peng et al, Phys. Rev. **D 58**, 092004 (1998).

[40] A. Kievsky, E. Pace, G. Salme and M. Viviani, Phys. Rev. **C 56**, 64 (1997) [nucl-th/9704050].

[41] C. Ciofi degli Atti, E. Pace and G. Salme, Phys. Rev. **C 51**, 1108 (1995) [nucl-th/9411006].

[42] J. J. Aubert *et al.*, Phys. Lett. **123B**, 275 (1983).

[43] M. Glück, E. Reya and A. Vogt, Z. Phys. **C 67**, 433 (1995).

[44] A. Donnachie and P. V. Landshoff, Z. Phys. **C 61**, 139 (1994).

[45] J. T. Londergan and A. W. Thomas, Prog. Part. Nucl. Phys. **41**, 49 (1998).

[46] R. M. Woloshyn, Nucl. Phys. **A 496**, 749 (1989); B. Blankleider and R. M. Woloshyn, Phys. Rev. **C 29**, 538 (1984).

[47] Y. Goto *et al.* [Asymmetry Analysis collaboration], Phys. Rev. **D 62**, 034017 (2000) [hep-ph/0001046].

[48] M. Glück, E. Reya, M. Stratmann and W. Vogelsang, Phys. Rev. **D 53**, 4775 (1996).

[49] F. M. Steffens, K. Tsushima, A. W. Thomas and K. Saito, Phys. Lett. **B 447**, 233 (1999).

[50] P. A. M. Guichon, K. Saito, E. Rodionov and A. W. Thomas, Nucl. Phys. **A601**, 349 (1996) [nucl-th/9509034]; K. Saito and A. W. Thomas, Phys. Rev. **C 51**, 2757 (1995) [nucl-th/9410031]; P. A. Guichon, Phys. Lett. **B 200**, 235 (1988).

[51] P. L. Anthony *et al.* [E142 Collaboration], Phys. Rev. **D 54**, 6620 (1996) [hep-ex/9610007].

[52] K. Ackerstaff *et al.* [HERMES Collaboration], Phys. Lett. **B 404**, 383 (1997) [hep-ex/9703005].

[53] C. Ciofi degli Atti, S. Scopetta, E. Pace and G. Salme, Phys. Rev. **C 48**, 968 (1993) [nucl-th/9303016].

[54] T. Gherman and W. J. Stirling, Z. Phys. **C 65**, 461 (1995).

[55] I. R. Afnan *et al.*, Phys. Lett. **B 493**, 36 (2000) [nucl-th/0006003].

[56] G. G. Petratos *et al.*, Jefferson Lab proposal (July 2000)

[57] E. Pace, G. Salme and S. Scopetta, Nucl. Phys. **A 689**, 453 (2001).

[58] R. J. Ord-Smith, Phys. Rev. **94**, 1227 (1954).

[59] R. G. Roberts: *The structure of the proton* (Cambridge University Press, 1990).

[60] R. L. Jaffe: "Deep inelastic scattering with application to nuclear targets", in *Los Alamos School on Relativistic Dynamics and Quark-Nuclear Physics*, ed. M. B. Jackson and A. Picklesimer (Jhon Wiley and Sons, New York, 1985).

[61] P. V. Landshoff and J. C. Polkinghorne, Phys. Rep. **5c**, 1 (1972).

[62] C. G. Callan and D. J. Gross, Phys. Rev. Lett. **22**, 156 (1969).

[63] G. B. West, Phys. Lett. **37B**, 509 (1971); W. B. Atwood and G. B. West, Phys. Rev. **D 7**, 773 (1973).

[64] L. P. Kaptari, A. Yu. Umnikov, Phys. Lett. **B 259**, 155 (1991); M. A. Braun, M. V. Tokarev, Phys. Lett. **B 320**, 381 (1994).

[65] W. Melnitchouck, A. W. Schreiber and A. W. Thomas, Phys. Lett. **B 335**, 11 (1994).

[66] W. Melnitchouck and A. W. Thomas, Phys. Lett. **B 377**, 11 (1996).

[67] K. Abe *et al*, Phys. Rev **D 58**, 112003 (1998).

[68] P. L. Anthony *et al.*, Phys. Lett. **B 463**, 339 (1999).

[69] R. L. Jaffe, Nucl. Phys. **19**, 239 (1990).

[70] M. Glück, E. Reya, M. Stratmann and W. Vogelsang, Phys. Rev. **D 63**, 094005 (2001).

[71] I. R. Afnan, F. Bissey and A. W. Thomas, Phys. Rev. **C 64**, 024004 (2001).

[72] L. Frankfurt, V. Guzey and M. Strickman, Phys. Lett. **B 381**, 379 (1996).

[73] J. D. Bjorken, Phys. Rev. **148**, 1467 (1966).

[74] Particle Data Group, C. Caso *et al.*, Eur. Phys. J. **C 3**, 1 (1998).

[75] B. Budick, J. Chen and H. Lin, Phys. Rev. Lett. **67**, 2630 (1991).

[76] S. J. Brodsky, M. Burkardt and I. Schmidt, Nucl. Phys. **B 441**, 197 (1995).

[77] W. Melnitchouk and A. W. Thomas, Phys. Lett. **B 377**, 11 (1994); W. Melnitchouk and J. C. Peng, Phys. Lett. **B 400**, 220 (1997); U. K. Yang and A. Bodek, Phys. Rev. Lett. **82**, 2467 (1999); M. Boglione and E. Leader, [hep-ph/0005092] .

[78] T. Y. Saito, Y. Wu, S. Ishikawa and T. Sasakawa, Phys. Lett. **B 242**, 12 (1990); J. Carlson, D. Riska, R. Schiavilla and R. B. Wiringa, Phys. Rev. **C 44**, 619 (1991).

[79] F. E. Close and A. W. Thomas, Phys. Lett. **B 212**, 227 (1988); C. Boros and A. W. Thomas, Phys. Rev. **D 60**, 074017 (1999).

[80] J. L. Friar, E. l. Tomusiak, B. F. Gibson and G. L. Payne, Phys. Rev. **C 24**, 677 (1981); G. Derrick and J. M. Blatt, Nucl. Phys. **8**, 310 (1958).

[81] C. Boros, V. Guzey, M. Strikman and A. W. Thomas, Phys. Rev. **D 64**, 014025 (2001); F. Bissey, V. Guzey, M. Strikman and A. W. Thomas, [hep-ph/0109069].

[82] E154 Collab., K. Abe *et al.*, Phys. Lett. **B 404**, 339 (1997); K. Abe *et al.*, *ibid.* **405**, 180 (1997); Phys. Rev. Lett. **79**, 26 (1997).

[83] H. Geiger and E. Marsden, Proc. Roy. Soc. Lond. **82**, 495 (1909); E. Rutherford, Philos. Mag. **21**, 669 (1911).

[84] R. Hofstadter and R. W. McAllister, Phys. Rev. **98**, 217 (1955); R.Hofstadter, Rev. Mod. Phys. **28**, 214 (1956).

[85] M. Gell-Mann, Phys. Lett. **8**, 214 (1964); G. Zweig, CERN-8182/Th.401 (1964), unpublished; G. Zweig, CERN-8419/Th.412 (1964), unpublished.

[86] Y. Ne'eman, Nucl. Phys. **26**, 222 (1961); M. Gell-Mann and Y. Ne'eman, *The Eightfold Way* (Benjamin, New York, 1964).

[87] M. Y. Han and Y. Nambu, Phys. Rev. **139**, 1006B (1965).

[88] E. D. Bloom *et al.*, Phys. Rev. Lett. **23**, 930 (1969); M. Breidenbach *et al.*, *ibid.* **23**, 935 (1969).

[89] R. P. Feynman, Phys. Rev. Lett. **23**, 1415 (1969).

[90] D. Gross and F. Wilczek, Phys. Rev. Lett. **30**, 1343 (1973); D. Politzer, *ibid.* **30**, 1346 (1973).

[91] M. Alguard *et al.*, Phys. Rev. Lett. **37**, 1258 (1976); *ibid.* **37**, 1261 (1976); *ibid.* **41**, 70 (1976).

[92] J. Ashman *et al.*, Phys. Lett. **B 206**, 364 (1988); Nucl. Phys. **B 328**, 1 (1989).

[93] P. L. Anthony *et al.*, Phys. Rev. Lett. **71**, 959 (1993).

[94] I. R. Afnan, F. Bissey, J. Gomez, A. T. Katramatou, W. Melnitchouk, G. G. Petratos and A. W. Thomas, Phys. Lett. **B 493**, 36 (2000); G. G. Petratos, I. R. Afnan, F. Bissey, J. Gomez, A. T. Katramatou, W. Melnitchouk and A. W. Thomas, [nucl-ex/0010011].

[95] S. C. Bhatt, J. S. Levinger and E. Harms, Phys. Lett. **40B**, 23 (1972); Nucl. Phys. **A 197**, 33 (1972).

[96] R. Machleidt, Nucl. Phys. **A 689**, 11 (2001).

[97] O. W. Greenberg, Phys. Rev. lett. **13**, 598 (1964).

[98] H. Fritzsch, M. Gell-Mann and H. Leutwyller, Phys. Lett. **47B**, 365 (1973).

[99] K. Ackerstaff *et al.*, Phys. Lett. **B 464**, 123 (1999).

[100] F. M. Steffens and A. W. Thomas, Phys. Rev. **C 55**, 900 (1997).

List of Publications

Published papers

- **Comments on "Parton distributions, d/u, and Higher Twist Effects at High x"**.
  Published in Phys. Rev. Lett. **84**, 5455 (2000).
- **Neutron structure functions and $A = 3$ mirror nuclei**.
  Published in Phys. Lett. **B 493**, 36 (2000).
- **Deep inelastic scattering on asymmetric nuclei**.
  Published in Phys. Lett. **B 493**, 288 (2000).
- **Structure functions for the three-nucleon system**.
  Published in Phys. Rev. **C 64**, 024004 (2001).

Contribution to conferences

- **Extracting nucleon spin structure functions from nuclear data**.
  Talk given to the "Circum-Pan-Pacific RIKEN Symposium On High-Energy Spin Physics (Pacific Spin 99)" , Wako, Japan, 4 - 6 Nov. 1999.
  Published in Riken. Rev. **28**, 90 (2001).
- **Measurements of the F_2^n/F_2^p and d/u ratios in deep inelastic electron scattering off ^{3}H and ^{3}He**.
  Invited talk at "Workshop on Nucleon Structure in High x-Bjorken Region (HiX2000)", Philadelphia, Pennsylvania, 30 Mar. - 1 Apr. 2000.
  Unpublished. [nucl-ex/0010011].

Submitted papers

- **Complete analysis of the spin structure function g_1 of ^{3}He**.
  Submitted to Phys. Rev. **C**. [hep-ph/0109069].